



저작자표시-비영리-변경금지 2.0 대한민국

이용자는 아래의 조건을 따르는 경우에 한하여 자유롭게

- 이 저작물을 복제, 배포, 전송, 전시, 공연 및 방송할 수 있습니다.

다음과 같은 조건을 따라야 합니다:



저작자표시. 귀하는 원저작자를 표시하여야 합니다.



비영리. 귀하는 이 저작물을 영리 목적으로 이용할 수 없습니다.



변경금지. 귀하는 이 저작물을 개작, 변형 또는 가공할 수 없습니다.

- 귀하는, 이 저작물의 재이용이나 배포의 경우, 이 저작물에 적용된 이용허락조건을 명확하게 나타내어야 합니다.
- 저작권자로부터 별도의 허가를 받으면 이러한 조건들은 적용되지 않습니다.

저작권법에 따른 이용자의 권리는 위의 내용에 의하여 영향을 받지 않습니다.

이것은 [이용허락규약\(Legal Code\)](#)을 이해하기 쉽게 요약한 것입니다.

[Disclaimer](#)

Ph.D. DISSERTATION OF NATURAL SCIENCE

**Natural Variation of Subsurface Gas
Concentration Reflected in the Vadose Zone
Wells: Implication for Predicting CO₂ Leakage**

**불포화 관정에서 관찰된 지하 환경 내 가스 농도의
자연적 변동 : CO₂ 누출 탐지와 예측에의 적용성 분석**

Won-Tak Joun

August 2020

School of Earth and Environmental Sciences

The Graduate School

Seoul National University

ABSTRACT

Author: Joun Won-Tak

Major: Hydrogeology

School of Earth and Environmental Sciences

The Graduate School, Seoul National University

The geologic carbon sequestration (GCS) has been suggested as one of the best methods to mitigate climate change and global warming by sequestering CO₂ at the reservoir and consequent reduction of CO₂ emission into the atmosphere. However, the potential risk of CO₂ leakage and the effective methods for responding to the CO₂ leakage have to be prepared to ensure the safety of the human. It is hard to respond to the CO₂ leakage near the GCS site because the escaped CO₂ takes a long time to reach the monitoring area and the influence on the aquifer system could be wide temporally and spatially. Thus, controlled CO₂ release tests have been conducted to understand the factors for identifying the CO₂ leakage and the influence of the escaped CO₂ on the shallow aquifer with a relatively shorter time, the K-COSEM (Korea-

CO₂ Storage Environmental Management) also performed the experiment by constructing more intensive CO₂ monitoring system.

To monitor the CO₂ gas concentration along a depth profile, multi-level wells were installed in the shallow unsaturated zone and the meteorological parameters such as temperature, relative humidity, wind speed, wind direction, and atmospheric pressures were also monitored. The results of the monitoring represented dynamic variations in CO₂ concentration according to day and night periods, even in the depth deeper than 5 m. It showed that the variation is related to the effects of intermittent weather changes. To clarify the controlling factors of the daily dynamic variation of CO₂ concentration in the vadose zone wells, four different methods were applied on the vadose zone wells. All the results supported the reason why the large-swing variations were represented naturally as follows: 1) during the day, CO₂ gas is coming out from the soil zone and high concentration is maintained; 2) during the night, the fresh air could invade through the vadose zone wells because the air of the atmosphere at the night is relatively heavier than during the day.

Reproducing the natural pattern of gas concentration in the vadose zone well was also attempted to explain the actual influence factors on the gas

concentrations through the numerical simulation. Unlike previous studies, the results of the numerical model represented that the fluctuating water table was an important factor even it has small variation and it is far from the source emission zone in the vadose zone well. Case 3 of numerical simulations well recreated a real-pattern of CO₂ gas concentrations and based on this case, a pulse-leaking scenario was predicted simply. This application could be useful for understanding and analyzing not only the results of artificial CO₂ injection field experiments but also the leak signal near the GCS site. In addition, the results from this study can be used as a fundamental knowledge to identify the leaking signal from the mixed CO₂ gas concentration.

Keyword: vadose zone CO₂, unsteady natural variation, recreating patterns of [CO₂], gas monitoring, leaking CO₂ signal.

Student Number: 2014-31020

This page intentionally left blank

TABLE OF CONTENTS

ABSTRACT i

TABLE OF CONTENTS v

LIST OF FIGURES xi

LIST OF TABLES xxi

CHAPTER 1. Introduction	1
1.1 Motivation	1
1.2 Background for the study	9
1.3 Purpose of the study	17
1.4 Organization	18
CHAPTER 2. Controlled CO₂ Release Test in the Shallow Aquifer	21
2.1 Introduction	21
2.2 Background and trends	26
2.3 Study site description	33
2.4 Material and methods	40

2.5 Performing field-scale experiments	50
2.6 Fluctuating gas concentration	87
2.7 Conclusion	88

CHAPTER 3. Understanding the Natural [CO₂] (g)

Variations in the Vadose Zone Well	91
3.1 Introduction	91
3.2 Materials and methods	93
3.3 Results and discussion.....	107
3.4 Conclusion.....	117

CHAPTER 4. Reproducing the Naturally Fluctuating

[CO₂] (g) in the Vadose Zone Well 121

4.1 Introduction 121

4.2 Materials and methods 124

4.3 Results of numerical modeling 143

4.4 Discussion 146

4.5 Verification 151

4.6 Conclusion 155

CHAPTER 5. Simple-application about Predicting

CO₂ Short-term Leakage through the Well 157

5.1 Introduction 157

5.2 Materials and methods	158
5.3 Results and remarks	159
CHAPTER 6. Conclusion	163
Bibliography	167
Abstract in Korean	197

This page intentionally left blank

LIST OF FIGURES

CHAPTER 1

- Figure 1-1** Increasing rate of CO₂ emissions from 1990 to 2017 depending on sectors including electricity and heat producers, industry, and transport (data source: International Energy Agency, (www.iea.org)) 6
- Figure 1-2** Climate change and global warming are affecting humanity and wildlife 7
- Figure 1-3** The conceptual diagram of CO₂ leakage from the storage to the shallow aquifer and vadose zone along the fault 8
- Figure 1-4** A schematic diagram of the subsurface environment. The vadose zone includes the root zone, perched zone, and intermediate zone. Phreatic zone can be called the aquifer, saturated zone with groundwater 11

CHAPTER 2

- Figure 2-1** A conceptual sketch for representing a potential CO₂ leakage pathways through the fracture zone or an artificial injected CO₂ at the shallow aquifer 25
- Figure 2-2** There are four kinds of wells and almost shallow depth wells (< 30 m) are gathered west side of testbed. Bed rock wells have drilling log information. The log data was obtained by performing S. P. T. (standard penetration test) at the time of the well installation 36
- Figure 2-3** The study site is located in North Chungcheong Province and a plottage of the study area is about 4.7 km²..... 37
- Figure 2-4** The geologic cross section was generalized based on the drilling log information..... 38
- Figure 2-5** Annual precipitation and mean air temperature of the study site from 2007 to 2017 (10 years) (<http://data.kma.go.kr>) 39
- Figure 2-6** (a) The distribution of monitoring wells installed in the shallow depth of the vadose zone and the aquifer at the west side of test bed, (b) The generalized geologic cross section at the shallow depth part of test bed from A to B 47
- Figure 2-7** The monitoring wells comprise nested types (A, B, C, and D) and single types (F and G). The red-color dots represent the location of NDIR sensors inside of monitoring wells 48

Figure 2-8 (a) Davis Instruments monitoring system for meteorological parameters, (b) CO₂ gas monitoring control boxes and well distribution, (c) Program interface for monitoring the meteorological parameters, (d) Program interface for CO₂ gas monitoring 49

Figure 2- Two tanks (5 m³ volume) were used for the field-scale experiment in the K-COSEM research site. A circulation pump and CO₂ dissolver were attached on the left tank for preparing the CO₂ infused water 56

Figure 2-10 Time series of CO₂ gas concentration from December 2016 to February 2018. Diamond symbol and seperated line represented the collected data with four differnt brown colors depending on the pipe line length of UMW 1 nest (5, 8, 11, and 14 m). Soild line shows the daily average values of the CO₂ gas concentraiton data with different colors such as red, blue, skyblue, and green. The grey line and shade shows the dat and period of two injection tests 62

Figure 2-11 Time series of CO₂ gas concentration from December 2016 to February 2018. Diamond symbol and seperated line represented the collected data with four differnt brown colors depending on the pipe line length of UMW 2 nest (5, 8, 11, and 14 m). Soild line shows the daily average values of the CO₂ gas concentraiton data with different colors such as red, blue, skyblue, and green. The grey line and shade shows the dat and period of two injection tests 63

Figure 2-12 Time series of CO₂ gas concentration from December 2016 to February 2018. Diamond symbol and seperated line represented the collected data with four differnt brown colors depending on the pipe line length of UMW 2 nest (5, 8, 11, and 14 m). Soild line shows the daily average values of

the CO₂ gas concentration data with different colors such as red, blue, skyblue, and green. The grey line and shade shows the date and period of two injection tests 64

Figure 2-13 Time series of CO₂ gas concentration from December 2016 to February 2018. Diamond symbol and separated line represented the collected data with four different brown colors depending on the pipe line length of UMW 4 nest (5, 8, 11, and 14 m). Solid line shows the daily average values of the CO₂ gas concentration data with different colors such as red, blue, skyblue, and green. The grey line and shade shows the date and period of two injection tests 65

Figure 2-14 Time series of meteorological parameters from December 2016 to February 2018 for (a) Barometric pressures, (b) Atmospheric temperature, (c) Air relative humidity, (d) Rainfall, (e) Wind velocity, and (f) Wind direction. The black and gray circles represented the observed data at the weather station and CO₂ monitoring well (UMW-1-1, 5 m) respectively. The red color line is the daily mean values for the black circle data. The orange color line shows the average values of obtained data from the UMW-1-1 well shown in Figure 2-7 66

Figure 2-15 Spatial distribution of EC values before, during, and after the second CO₂ injection test 68

Figure 2-16 (a) A plotting field for applying the gas composition on the process-based analysis method (depict a figure based on Romanak et al., 2014a), (b) the gas sampling times, (c) the results of gas monitoring and applied on the process-based analysis plot 70

Figure 2-17 Time series of CO₂ gas concentration from April to August 2018.

The area of gray shade is the assumption period if the CO₂ injection is conducted at the same period of second injection test in 2017. Diamond symbol and separated lines shows observed data of CO₂ gas concentration and solid line shows the daily average values as shown in the legend. Depending on well types (SMW, UMW, and BS) and conditions (open and closed), the results of CO₂ gas monitoring shows the different patterns ... 75

Figure 2-18 The results of real time CO₂ gas monitoring data in SMW-2-4 which has open top according to the depth such as 5, 8, 11, and 14 m. Only one pipe line was used to detect the CO₂ concentration in SMW-2-4. Solid lines shows the daily average of CO₂ gas concentrations. Gray color shade represents the assumption period of the injection performance not the real injection period..... 76

Figure 2-19 The results of real time CO₂ gas monitoring data in SMW-4-4 which has closed-top according to the depth such as 5, 8, 11, and 14 m. Only one pipe line was used to detect the CO₂ concentration in SMW-4-4. Solid lines shows the daily average of CO₂ gas concentrations. Gray color shade represents the assumption period of the injection performance not the real injection period..... 77

Figure 2-20 The results of real time CO₂ gas monitoring data in UMW-1-4 which has open-top according to the depth such as 5, 8, 11, and 14 m. Only one pipe line was used to detect the CO₂ concentration in UMW-1-4. Solid lines shows the daily average of CO₂ gas concentrations. Gray color shade represents the assumption period of the injection performance not the real injection period..... 78

Figure 2-21 The results of real time CO₂ gas monitoring data in UMW-4-4 which has closed-top according to the depth such as 5, 8, 11, and 14 m. Only one pipe line was used to detect the CO₂ concentration in UMW-4-4. Solid lines shows the daily average of CO₂ gas concentrations. Gray color shade represents the assumption period of the injection performance not the real injection period..... 79

Figure 2-22 The results of real time CO₂ gas monitoring data in BS-9 which has open-top according to the depth such as 5, 8, 11, and 14 m. Only one pipe line was used to detect the CO₂ concentration in BS-9. Solid lines shows the daily average of CO₂ gas concentrations. Gray color shade represents the assumption period of the injection performance not the real injection period..... 80

Figure 2-23 The results of real time CO₂ gas monitoring data in BS-5 which has closed-top according to the depth such as 5, 8, 11, and 14 m. Only one pipe line was used to detect the CO₂ concentration in BS-5. Solid lines shows the daily average of CO₂ gas concentrations. Gray color shade represents the assumption period of the injection performance not the real injection period..... 81

Figure 2-24 Time series of meteorological parameters from April to August 2018 for (a) Barometric pressures, (b) Atmospheric temperature, (c) Air relative humidity, (d) Rainfall, (e) Wind velocity, and (f) Wind direction. The black and gray circles represented the observed data at the weather station and CO₂ monitoring well (UMW-1-4, open-top) respectively. The red color line is the daily mean values for the black circle data. The orange color line shows the average values of obtained data from the UMW-1-4 well shown in Figure 2-17 85

Figure 2-25 Time series of meteorological parameters from April to August 2018 for (a) Barometric pressures, (b) Atmospheric temperature, (c) Air relative humidity, (d) Rainfall, (e) Wind velocity, and (f) Wind direction. The black and gray circles represented the observed data at the weather station and CO₂ monitoring well (UMW-4-4, closed-top) respectively. The red color line is the daily mean values for the black circle data. The orange color line shows the average values of obtained data from the UMW-4-4 well shown in Figure 2-18 86

CHAPTER 3

Figure 3-1 The monitoring data for four days from 20 to 24 June 2017..... 110

Figure 3-2 The process-based analysis was applied on real-time gas monitoring at the well for a day using 5 hr intervals 114

Figure 3-3 Results of $\delta^{13}\text{C-CO}_2$ isotopic and CO₂ gas concentration in the well from 23 to 26 September 2017 115

Figure 3-4 A conceptual diagram about the natural inhalation and exhalation through a well in a day 120

CHAPTER 4

Figure 4-1 The collected monitoring data from Dec 05, 2016 to Jun 09, 2017 (35 days)	127
Figure 4-2 Standard penetration test (SPT) was conducted at the study site	129
Figure 4-3 Drill log in BH-4 which is the nearest rock formation well with the gas monitoring wells (BS, SMW, and UMW series) and the results of SPT from 12 to 19.5 m	130
Figure 4-4 Drill log in BH-4 and the results of SPT from 19.5 to 39 m	131
Figure 4-5 The conceptual diagram for the numerical model domain (cylindrical)	139
Figure 4-6 The space discretization and the diffusive porosity of the model domain	140
Figure 4-7 The model grid and the initial source position	141
Figure 4-8 The results of numerical simulations for each case and the observed CO ₂ (g) monitoring data	148
Figure 4-9 Conceptual model of multi-phase CO ₂ and water behavior depending on water table fluctuation (Joun et al., 2017)	149
Figure 4-10 Schematic diagram for a possible flow pathway of gas fluid through the porous media	150

CHAPTER 5

Figure 5-1 Conceptual diagram for representing CO₂ pulse-leakage scenario through the monitoring well 161

Figure 5-2 Three kinds of results including two modeling and one observed data at the K-COSEM research site 162

LIST OF TABLES

CHAPTER 2

Table 2-1 The information of controlled CO ₂ release tests	52
Table 2-2 Statistics of CO ₂ concentration depending on the monitoring depths during the field test	60
Table 2-3 Statistics of meteorological parameters during the field test	61
Table 2-4 Statistics of CO ₂ concentration depending on the monitoring wells	74
Table 2-5 Statistics of meteorological parameters during extra field test ..	84

CHAPTER 3

Table 3-1 Input parameters for the analytical solution	106
--	-----

CHAPTER 4

Table 4-1 The soil composition and texture for each layer	134
Table 4-2 The values of van Genuchten parameters for each layer	135
Table 4-3 The physical and chemical properties of TCE and CO₂.....	142
Table 4-4 Results of evaluation for comparing Case 3 with observed data ..	154

CHAPTER 1 . Introduction

1.1 Motivation

There is a lot of attention to global warming and climate change. There are many important components of the greenhouse gases which gradually affect the increasing temperature of the Earth. One of the greenhouse gases which has a big issue is atmospheric carbon dioxide (CO₂) in the world. Although CO₂ has relatively small value (1) of warming index (WI) comparing the others such as SF₆ (23,900), CH₄ (21), N₂O (310), HFCs (140 to 11,700), and PFCs (6,500 to 92,000), since 1990, the emission volume of CO₂ gas has been increased (Figure 1-1) and that volume can't be ignored in

these days for considering the cause of the global warming and climate changes. In addition, since 2000, the rate of global atmospheric concentration of CO₂ has been increased 20 parts per million (ppm) per decade that is up to 10 times faster than any documented rate (Lüthi et al., 2008; Bereiter et al., 2015, IPCC, 2018) The consequent abnormal weather and damage to mankind is often reported by various broadcasting media (Figure 1-2). Mora et al. (2013) estimated that the surface temperature could exceed historical records in the near future based on simulating the global warming scenario with Earth System Models and that will be catastrophic changes for the human race such as the supplying water and food (Lobell and Gourджи, 2012; Zhang and Cai, 2013; Taylor et al., 2013), infectious vector-borne diseases (Epstein, 2002; Khasnis and Nettleman, 2005), heat stress (Sherwood and Huber, 2010), mental illness (Berry et al., 2010), and etc. According to the recent report which is written by an interdisciplinary group, the Lancet Countdown (USA), climate change was specifying that it will give people a dismal future. The report said the most serious problems would be global warming and air pollution, which would make people sicker and lose working hours (Duncombe, 2020). Now, it has become the must-do

fate of the human race to mitigate global warming by conducting any possible action until finding an effective technology.

Carbon capture and storage (CCS) is a widely accepted strategy within the scientific community and the general public to reduce the rate of global warming and climate change. The outline of this strategy has sequences such as capturing CO₂ gas from industry emission sources, transporting CO₂ to a storage site, and then sequestering CO₂ at a safety reservoir. Especially, the geologic carbon storage (GCS) that is injecting supercritical CO₂ into inland or coastal geologic reservoir with a depth of 0.8 km to 1.0 km has been suggested as a feasible technique (Metz et al., 2005; DOE, 2011). But a more important task in this strategy is that the CO₂ storage site should be free from the potential risks to human health and the environment. The best scenario is that the stored CO₂ remained in the reservoirs as long as possible. If not, however, previous researchers suggested that acceptable leakage-level rules (less than 0.1% of stored CO₂ volume per year, Song and Zhang (2012)) should be met. One of the potential risks is that the CO₂ could migrate from a reservoir to arrive in shallow groundwater zone. The escaped CO₂ will flow vertically because of the buoyancy and it will generally reach the aquifer system in gas and aqueous phases simultaneously because CO₂ can easily

dissolve into the groundwater partially or fully as natural characteristics according to the subsurface environmental condition such as temperature and pressure. Figure 1-3 shows one of the schematic scenarios how CO₂ can escape from the deep depth reservoir through a high permeable pathway such as faults or an open abandoned well. As shown in Figure 1-3, the escaped CO₂ could be dissolved in the groundwater and the other gas will be going out to the atmosphere. This is a critical point why the accidental leaking of CO₂ is a big problem for human. The dissolved CO₂ can change the geochemical conditions in the potable aquifer by dropping pH and the flow out of CO₂ gas into the atmosphere can affect the human inhalation (Gasparini et al., 2016). In this regard, installing an intensive monitoring network covering the shallow phreatic zone, the vadose zone near the CO₂ geological storage site is highly recommended.

Monitoring technology has been also developed along with the GCS strategy to ensure that stored CO₂ does not escape the reservoir and to come up with safety solutions for potential problems in case of an emergency. Unfortunately, however, it is not yet established or assessed which monitoring technology is optimal because it takes a long time period to detect CO₂ at the shallow aquifer and analysis it, which is coming from the

storage reservoir (generally over 800 m bsl (below surface level)). For this reason, Peter et al. (2011) state that specialized facilities for injecting CO₂ at the shallow aquifer are required due to the time scale challenge. Although the best experimental site for developing the leakage monitoring technique is where the place CO₂ is actually being injected, the alternative facilities including artificial CO₂ releasing pipelines have been installed around the world to understand the impact of CO₂ leakage on the shallow groundwater and atmospheric condition in a time when it is relatively shorter than detecting a real-leakage CO₂ at the CCS site. One of the important tasks in developing the monitoring technologies is to separate the leakage signal from the naturally varying CO₂ from the soil system with different conditions. In addition, because each country has a specific soil condition, it is also necessary importantly to establish a CO₂ leakage detection technique is suitable for each subsurface environmental condition including not only the saturated zone but also the vadose zone (Kim et al., 2018).

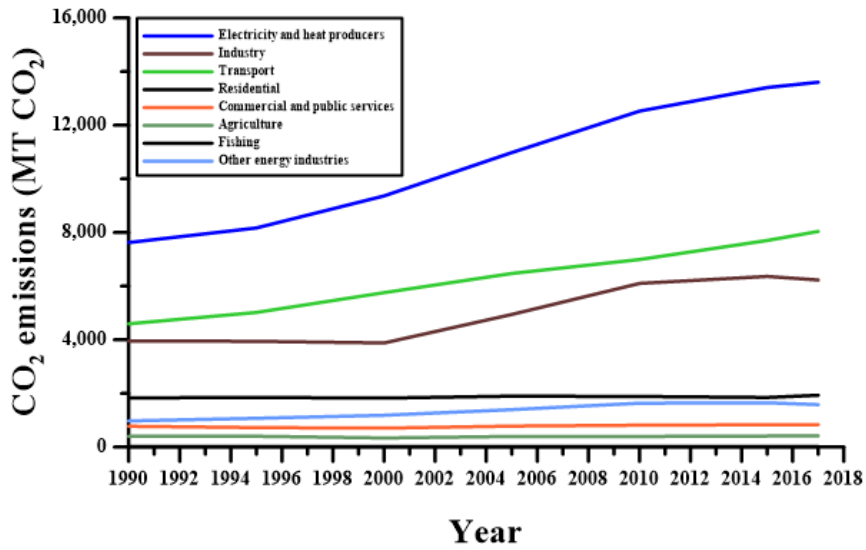


Figure 1 -1 Increasing rate of CO₂ emissions from 1990 to 2017 depending on sectors including electricity and heat producers, industry, and transport (data source: International Energy Agency, (www.iea.org)).



PIXABAY



UCSUSA.ORG



REUTERS TV

Figure 1-2 Climate change and global warming are affecting humanity and wildlife.

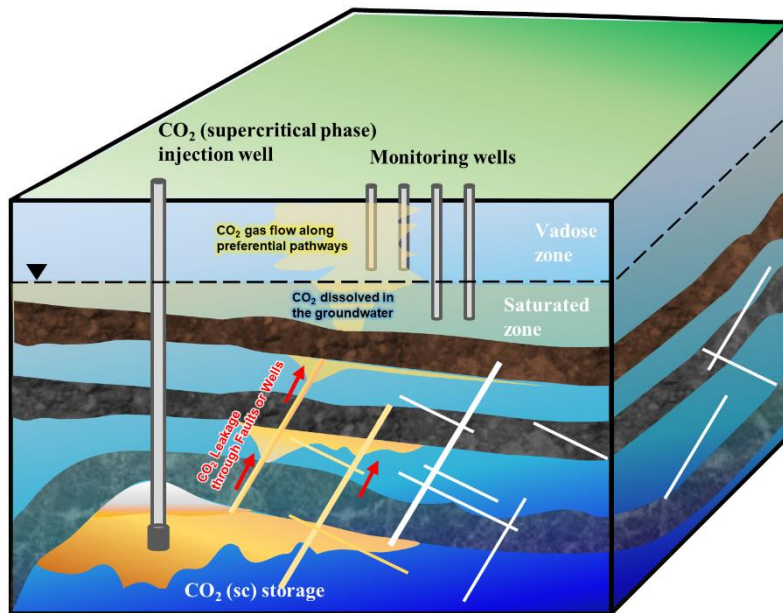


Figure 1-3 The conceptual diagram of CO₂ leakage from the storage to the shallow aquifer and vadose zone along the fault.

1.2 Background for the study

1.2.1 Vadose zone

The unsaturated zone is defined as the section between the ground surface and the regional water table (Stephens, 1996) and is an area that is considered important in the field of geological research (Figure 1-4). This section is also broadly called as vadose zone and in recent, according to grow a requirement of the comprehensive logic in the interdisciplinary fields for understanding the complex natural phenomena, the considered important section is gradually extended as the critical zone which is including the land surface, the water bodies, the pedosphere, the vadose zone, and the groundwater zone (Guo and Lin, 2016). Although throughout the 20th century, the vadose zone had been treated as a sub-research field for remediating the groundwater in waste sites, since 2000, the importance of vadose zone processes has been increased and direct gas sampling at the contaminated subsurface environment is the typical rule rather than the exception (Looney and Falta, 2000a). In case of DNAPLs (Dense non-Aqueous Phase Liquids) contaminated site, because the source can't reach the groundwater without penetrating from the ground to the vadose zone, the comprehensive research

is necessary to protect the groundwater by monitoring the groundwater in the aquifer and the gas in the vadose zone simultaneously. In addition, when the gas sampling and monitoring are performed by using open wells, it is more difficult to understand the relevant factors on gas concentrations temporally and spatially because the concentration of gas would be diluted by the induced airflow caused natural forces (Kuang et al., 2013) and the pressure-driven advective flux of gas would be generated by fluctuating atmospheric pressure or changing water table level (You and Zhan, 2013).

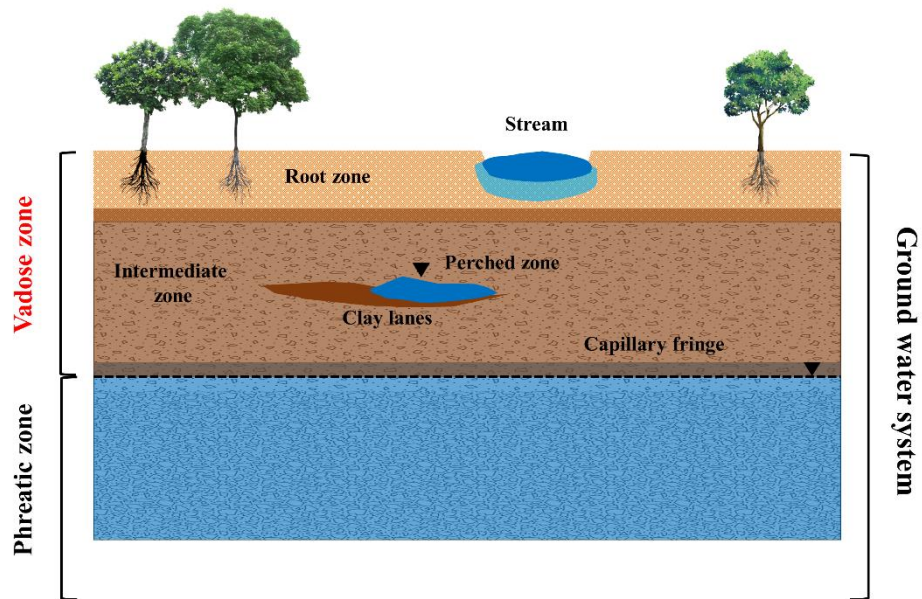


Figure 1 -4 A schematic diagram of the subsurface environment. The vadose zone includes the root zone, perched zone, and intermediate zone. Phreatic zone can be called the aquifer, saturated zone with groundwater.

1.2.2 Air flow through the vadose zone

Investigations of airflow and mass transport in the vadose zone have been consistently performed in many research fields to qualify the contaminants, to protect the fresh groundwater, to verify the safety of human health from the toxic gases, and to provide effective environmental remediation strategies using field or laboratory experimental data and analytical or numerical models (Kuang et al., 2013). Before analyzing the concentration of gas species sampled from the subsurface environment at each research field, it is an indispensable task to characterize properties of soil porous media and to estimate the main factor that is hindering the airflow and gas mass transport. Generally, the disturbance factors of airflow in the vadose zone are 1) the air permeability at the unsaturated zone, 2) water contents in soil, and 3) gas solubility in water vapor. These three factors are remarkable to increase the effectiveness of removing the air contaminated by Volatile Organic Components (VOCs) such as TCE, PCE, and BETX from the soil media when the soil vapor extraction (SVE) is performed at the vadose zone (Boulding and Ginn, 2004). But if the gas monitoring is for determining the signal of CO₂ leakage from the sequestration reservoir, these disturbance

factors are not enough to understand the profile of gas concentration. Because the CO₂ gas is naturally produced at the shallow subsurface environment (about 3 to 5 m sections from the ground surface) and the CO₂ monitoring on the CCS site is not for CO₂ gas elimination but for leakage signal separation from the naturally produced CO₂. Ultimately, the purpose of CO₂ monitoring is to obtain the warning signal as early as possible and to assure the safety or the capacity of CO₂ storage. Therefore, more detailed investigations are necessary to understand the profile of CO₂ gas concentration in open wells affected by natural forces such as infiltration, atmosphere pressure, temperature, wind, and etc.

There are various well designs and gas sample techniques to investigate gas concentrations in the vadose zone (VDI 3865-2, and ASTM D 5314-92). These methods have been advanced and recommended by European countries and the United States to apply the specific research site because the materials did not provide the application progress depending on all geologic characteristics. Especially, multi-depth soil-gas sampling is recommended in the case of DNAPL contaminated sites because this type of well is helpful to identify the source composition by sampling the VOC gases according to the depths. Generally, if the source location is more than 1 m

deep from the ground surface, the multi-level wells, called nest-type well, would be advised in the standard methods. In the case of CO₂ storage site, a monitoring system using the nest-type wells is an applicable technique at the vadose zone and at the saturated zone to cover the entire subsurface environment and to discover the leaking signal early. In addition, because CO₂ gas has the high solubility (1.019 vol. /vol. at 15°C and 1 bar) in water and the large density (1.81 kg/m³ at 25°C and 1 bar) then air (1.17 kg/m³ at 25°C and 1 bar) if the sequestered CO₂ escapes from the storage, leaking CO₂ will make the plumes in liquid phase and gas phase during flow to the atmosphere. The plume of CO₂ infused water tends to lay on the water table and the CO₂ gas could be partially trapped in the saturated pore or flow out by the buoyancy effect. More detailed explanations are in Oldenburg and Unger (2003). Thus, building up the monitoring system on those both environments using nest type well is a considerable challenge to increase the accuracy of detecting real-leak signals.

In standard methods such as ASTM D 5314-92, the example of well condition for gas sampling is represented with packing the top of well. Generally, for sampling the gas from the subsurface environment, sealing the top of monitoring well is encouraged to block the inflow air caused by the

pressure difference between atmosphere and monitoring well. However, even if the top of the well was cemented, the potential gas migration pathways would exist (Gasda et al., 2004) and those pathways could be linked with the atmosphere environment as an airflow pathway. In addition, to detect the signal of the CO₂ leakage event, open well is more appropriate than sealed well to cover the sampling area from the saturated zone to the vadose zone. Although whether sampling the water or the gas or both is determined according to the research fields or objectives, if the target species are volatile and have high solubility in groundwater, sampling at both side areas is encouraged to reduce the error range of concentrations in the gas phase.

1.2.3 A common interest in this study

CO₂ gas monitoring at the near-surface area is highly recommended for obtaining the guarantee of safety when CCS project is performed at the geologic storage reservoir because this area has not only the last boundary for detecting CO₂ that is leaking from the storage but also the closest zone to

affecting the surface-lives. In addition, long-term monitoring is essential because of the abnormal migration from the storage to the atmosphere spatially and temporally. Thus, it is necessary to conduct gas sampling periodically or continuously for recognizing when it was started, how long will the exposure time be, and how long will the influence radius be by CO₂ leakage.

Thus, the questions are:

If using the open well is inevitable, the gas sample without the consideration of fluctuating atmospheric pressure would provide good data? An observational error caused by meteorological parameters is ignorable? Even though the gas concentration ranges could be changed according to day and night, can we state that the data is the representative values at a research area because the sample is collected in a day (12 to 24hr)?

1.3 Purposes of the study

The objective of this study is to investigate fluctuating gas concentration in wells and to understand the monitored gas concentration patterns caused by natural effects using real-time monitoring data with multi-level installed wells and analytical and numerical models. The research has been performed with the following intentions:

1. To understand whether the CO₂ leaking sign can be identified by using real-time monitoring data and performing the controlled CO₂ release test and it will be influenced by the meteorological parameters.
2. To clarify the reason why the unsteady pattern of CO₂ gas concentration exists in the vadose zone well and propose a possible hypothesis of the natural mechanism using considerable evidence.
3. Reproduce a natural variation of CO₂ gas concentration in the vadose zone well using a new approaching method and an application and predict a possible leaking pattern of CO₂ gas concentration through the vadose zone well as a plus-leak event happens.

1.4 Organization

This dissertation is organized as follows:

Chapter 1 represented the motivation, the background, and the purpose of this study. In chapter 2, monitoring the variations of CO₂ concentrations at the four different levels of the unsaturated area is explored at the artificial CO₂ injection site, and suggestions are provided to understand the pattern of gas concentration data measured directly with real-time monitoring system at the field. In chapter 3, the evidence about the dynamical intrusion of the fresh air into vadose zone wells are provided by using new approaches in the open well installed in several-layer-composed unsaturated zones and insights are provided to recognize the major mechanism why the large-swing patterns are represented naturally at the vadose zone section of the monitoring well. In chapter 4, reproducing the natural pattern of gas concentrations in the vadose zone well is conducted by using the numerical model (STOMP), and the advanced method is applied to reproduce the natural pattern. In chapter 5, based on the results of numerical simulation from chapter 4, a simple-concept of leaking scenario is conducted and a possible pattern of CO₂ gas

concentration is proposed. Finally, this dissertation is ended with conclusions in chapter 6.

This page intentionally left blank

CHAPTER 2. Controlled CO₂ Release Test in the Shallow Aquifer

2.1 Introduction

Controlled CO₂ release tests and monitoring developments have been conducted in many countries to understand the quality change of the groundwater affected by the escaped CO₂ from the storage, to evaluate monitoring methodologies that provide evidence recognizing the changes at the subsurface environment. In addition, they tried to reveal which monitoring methods should be applied on and how many times of monitoring should be recommended, and eventually, to find out the specific parameters which are

suitable according to the soil condition at each country (Lee et al., 2016; Kim et al., 2018).

Typically, two kinds of experiment types have been used around the world to conduct a controlled CO₂ release test in shallow depths aquifer. One used the same well for CO₂ source injection that could be in gas/aqueous phase and groundwater monitoring by pumping the groundwater after the CO₂ injection (Yang et al., 2013; Mickler et al., 2013; Rillard et al., 2014) and the other separates the injecting and monitoring wells for the test (Zheng et al., 2012; Trautz et al., 2013; Cahill et al., 2014; Humez et al., 2014). Although both types of the test have pros and cons the latter test type tend to have more advantage to focus on evaluating the CO₂ infused water plume spatially and temporally.

Figure 2-1 shows a conceptual sketch of the CO₂ injection and monitoring system with the latter type experiment which separates the wells between the injection and the monitoring at the shallow aquifer. As represented in Figure 2-1, whether it is the escaped CO₂ through the fracture zone or the injected CO₂ artificially, the flow path or mechanism will be completely different depending on the gaseous phase or the dissolved phase of the invaded CO₂

into the shallow aquifer. In addition, in case of the dissolved phase of the invaded CO₂, because the CO₂ infused water will be heavier than the native groundwater, the plume of dissolved CO₂ groundwater could flow downward direction with the shape of fingering. For this reason, it is a tricky condition to evaluate the quality of the groundwater. For example, if A-well (Orange color letter A as showed in Figure 2-1) is used for CO₂ leakage monitoring, any specific characteristics won't be found because the screened interval is deeper than the main plume zone. If B (blue color letter) or D (green color letter)-well is used for CO₂ leakage monitoring, the concentration of CO₂ which is dissolved in the groundwater will be fluctuating because the fingered plume will pass through those wells. Lastly, if C (red color letter)-well is used for CO₂ leakage monitoring, the concentration of CO₂ dissolved water could be relatively constant with the other wells because this well pose at the middle of the plume and the fingered plume will be covered by other plumes. On the other hand, in the case of the gaseous phase, the escaped CO₂ (g) from the storage will invade into the vadose zone and, finally, it will seepage out through the ground surface. Because the dominant pathway is vertical, it is highly recommended that the intensive CO₂ gas monitoring system or well is installed near the injection well or the predicted main CO₂ leaking zone. The

monitoring in the vadose region has still remained as a challenging part because many uncertainties of gas migration exist in understanding the reciprocal influence of natural heterogeneity in sediment. In addition, in or ex-situ field experiments are tricky to construct the CO₂ monitoring network because there are no comprehensive rules or protocol contents for all geologic systems. Therefore, to get enough data for understanding the gaseous CO₂ plume migration is necessary by conducting further field experiments.

The aim of this chapter is to review the trend of previous studies that were about the controlled release test at the field condition and to introduce two ex-situ field-scale experiments that were conducted for short and long-term respectively and one in-situ field-scale experiment at the K-COSEM research site where the place is for intensive studies (Chapter 3 and 4). This chapter also represented the reason why a further artificial test was performed at the shallow aquifer and during this field-scale test, we discovered something unusual, which is not appropriate for CO₂ leakage monitoring, therefore, it will be led to intensive research into natural phenomena.

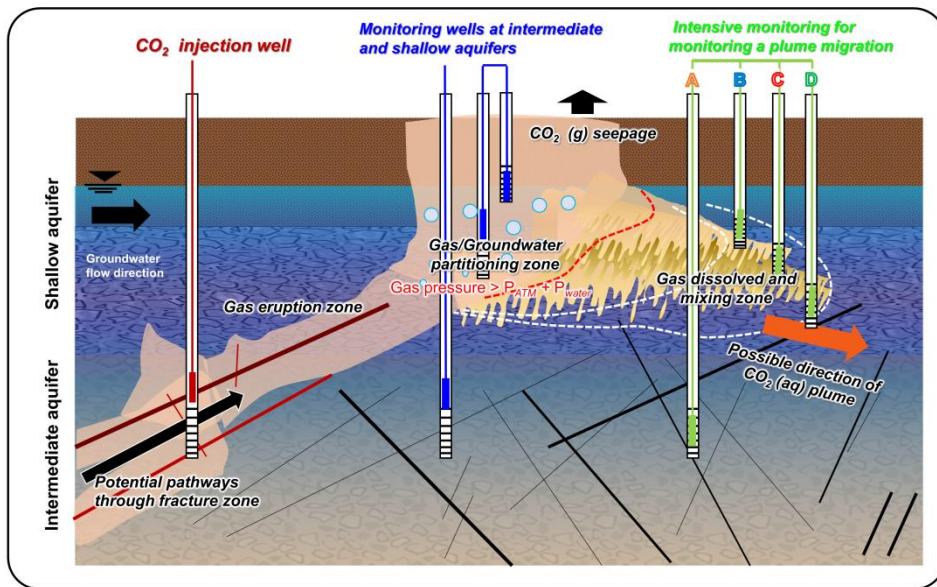


Figure 2-1 A conceptual sketch for representing a potential CO₂ leakage pathways through the fracture zone or an artificial injected CO₂ at the shallow aquifer.

2.2 Background and trends

To understand whether groundwater is affected by the CO₂ leakage from deep geologic carbon sequestration reservoir, to explain that the affected groundwater zone can be detected by the recent monitoring techniques, and to evaluate whether the fugitive CO₂ in shallow groundwater impacts on the health problems causing the potable water contaminated by induced heavy metals or mineral and inhalation problems according to the CO₂ concentration and exposure time, many controlled CO₂ injection tests have been conducted at the shallow aquifer system (Newell et al., 2014; Trautz et al., 2013; Lee et al., 2016). These previous studies with their purposes and their observed data can explain the specific mechanism of the leak CO₂ migration from the CO₂ storage to the shallow aquifer a little bit at the CCS site but more field experiments are still conducted around world because there still remained challenging parts of researches (e. g. the vadose zone monitoring that is an important area intended the final boundary to detect the CO₂ leakage and the closest region to humans. In addition, the observed data influenced by the meteorological parameters critically).

Finding the answer about which research field is a little less than the others and which points should be emphasized more for detecting the CO₂ leakage at the shallow aquifer is still necessary because in situ field conditions are complex to control the sample collection or the sample depth and difficult to decide the main source area that exposed by CO₂ continuously for a long time. Thus, in this chapter, look into the previous study trends and explain an advanced part of the controlled CO₂ release test at the K-COSEM project.

2.2.1 International trend

Many kinds of research and technology are being developed around advanced countries to reduce greenhouse gases such as CO₂, CH₄, SF₆, CFCs, etc. among those greenhouse gases, CO₂ (g) is picked as a representative component to mitigate climate change and following this reason, the varied project of carbon capture and storage as called CCS is also being progressed in the world from pilot-scale to the commercial-scale demonstration.

Because the subsurface environment has naturally and highly heterogeneous and anisotropy formation, the potential risk generated by the

escaped CO₂ from the storage reservoir is remained as a crucial problem during the project performing. In particular, once the escaped CO₂ is approached into the shallow aquifer and smearing into the atmosphere through the preferential flow path such as fault or fracture, it would give a potential impact on human inhalation problems depending on the exposure time or the concentration (Gasparini et al., 2016). Thus, if the CCS project is conducted, intensive monitoring schedules should be included in the master plan before the projected begin. However, it is difficult to find a major effect on the shallow aquifer at the commercial-scale CCS project site. Because in this scale, the CO₂ injecting location is so deep and it will take so long time to detect CO₂ gas which impacts the shallow aquifer. In addition, it is limited to understand or evaluate the subsurface environment because if the leaking event happens, CO₂ (g) will randomly migrate to soil zone, human living area, shallow aquifer environment temporally, spatially, and broadly. For those reasons as previously stated, evaluating the subsurface environment and developing CO₂ detection technology by artificially injecting CO₂ into the shallow subsurface environment should be performed with the CCS project simultaneously.

This kind of facilities are called as “Controlled release field experiment” and it is still conducted at many countries such as USA, Canada, Europe, Australia, etc.. There are much research was performed for understanding the effect on the aquatic environment at the aquifer and some representative researches are introduced briefly in this section as follows:

1) ZERT (Zero Emissions Research and Technology)

The facilities of this project are located in Bozeman, Montana, USA. The purpose of this study was to detect the plume migration made by CO₂ in the shallow groundwater and the soil layer. The horizontal pipeline was buried under 2.5 m subsurface ground for conducting this researches and the length of this pipe was 70 m. the main studies were identifying the distribution of CO₂ concentrations when the artificial CO₂ release was performed. In addition, following this action, they would like to check the CO₂ flux through the ground surface and this CO₂ concentration could be detected at the atmosphere (Spangler et al., 2010; Lewicki et al., 2007; 2009; Strazisar et al., 2009; Wells et al., 2010).

2) CO₂FieldLab Project

The study site is located in the Svelvik region, Norway. The research team surveyed the geologic formation by drilling the sample cores to 330 m. the baseline surveys including the groundwater quality, the geochemical analysis, and the soil gas analysis were conducted and the inclined borehole was installed through 20 m below ground surface and CO₂ injecting experiment was performed after all baseline surveys were finished (Bakk et al., 2012). Multi-level monitoring wells were installed to sample the soil gas and the groundwater and these well were used before, during, and after the CO₂ injection test for understanding the geochemical change affected by the injected CO₂. The continuous monitoring system was also constructed and the environmental factors were monitored spatially and temporally including temperature, ORP, EC, and DO. Using those monitored factors, Gal et al. (2013) was developed the technique for detecting the CO₂ leakage and Humez et al. (2014) verified the mechanism of the critical impact on the potable groundwater quality.

3) EIT facility near Wittstock

The artificial CO₂ injection test was conducted at Brandenburg, Germany and injecting depth was 18 m bgs. There were three injecting wells and the total amount of injected CO₂ was 400,000 L for 10 days. The monitoring period was 204 days to detect changing the quality of the groundwater derived from the artificial CO₂ injection. The monitoring parameters were methane, cations, anions, TIC/TOC, and LNAPL/DNAPL (Peter et al., 2012).

4) Plant Daniel

In this study, the monitoring well, injection wells, and pumping well were constructed based on the results of the pumping, slug, and hydraulic interaction tests. To characterize the geologic formation, geophysical methods (e. g., gamma-ray test) were applied on the well which had 30.5 m depth. After the controlled CO₂ release test, they focused on the mineralogical and biological changes in the subsurface environment and pH, EC, Alkalinity, etc. were also monitored continuously for comparing ion changes before, during, and after the test (Trautz et al., 2013).

5) RISCS (Research into Impacts and Safety in Carbon Storage) project

This project had the goal of developing regulations and guidelines to manage the carbon storage site and to provide the safety rules of the management in those kinds of sites in Europe. Thus, ASGARD (Artificial Soil Gassing and Response Detection) facility was constructed in the UK (Smith et al., 2013) and the researches of the impact on the plants, the biomass, or the subsurface environments affected by CO₂ (g) concentration explosion. This project was more focused on the unsaturated zone than the saturated zone to evaluate the ecological change with the controlled CO₂ release tests.

2.2.2 Domestic trend

To gain the annual plan of reducing greenhouse gases and to meet the emission scale allocated to the country, CO₂ sequestrating and storage project has been conducted under the national control and commend. The project of Korea CCS 2020 has conducted the research to construct the model of the stratospheric structure by drilling 1,200 m depth and analyzing the core

samples. Moreover, in other projects, the preliminary step project has performed the research on the relevant technologies for actual injection and storage capacity of the reservoir for a million ton-CO₂ injection scale. However, although it is necessary to evaluate and predict the critical impact on the shallow depth aquifer influenced by the escaped CO₂ from the storage to the atmosphere, only limited researches have been performed. Thus, the relevant ministries are necessary to solve those challenging problems for preparing regulatory and institutional guidelines for determining the environmental impacts by conducting CCS projects.

2.3 Study site description

The study site is located in North Chungcheong Province, Korea. The site plottage is about 5488.8 m² and the surface area shape is rectangle. The short side distance and the long side distance are about 30 m and 140 m respectively and the region is placed diagonally from south-west to north-east direction. Based on the study region, Chiljangcheon (stream) is on the left hands side and Jungbu express way is on the right hands side. (Figure 2-

2). The test bed has a gentle hill and a range in altitude from 91 to 96 m above sea level (a. s. l.) with an average slope of 3.0° and maximum slope of 45.3° (MLTMA and KWRC, 2009). The geological features are composed of gneissose biotite granite (51 % in surface cover) and Quaternary alluvium layer (48 % in surface cover). A weathered zone has more than 10 m in thickness. As hydrogeological features, the rock basement consists of Jurassic and Triassic intrusive igneous rock and overlying unconsolidated sediments. Groundwater level is located in the unconsolidated sediments at a depth of approximately 17 m from the ground surface. Ten wells (BS-01 to BS-10, pipe length is 30 m) which has continuously screened interval from 3 to 30 m below ground surface (bgs) were installed and four boreholes, each containing four nested wells screened at different depths (total pipe length is 5, 8, 11, and 14 m) were drilled in the vadose zone. Each well has a 1 m screen at the bottom of the borehole (UMW-01 to UMW-16) Figure 2-3 and 2-4 represents the monitoring well distribution and generalized geologic cross-section image at the study site. From 2007 to 2017, the maximum and minimum of the annual mean temperature of this region were 4.5°C and 18.5°C , respectively and their mean was around 11.5°C . The annual average precipitation during the same period was 1164.7 mm. The maximum and

minimum of annual precipitations were 1395.5 mm in 2012 and 733.5 mm in 2008, respectively (Figure 2-5). According to this data, the wet season is to be from June to September and the dry season is to be from October to February. Because 50 ~ 81 % of rainfall event belongs to the wet season, this region has the monsoon weather (Lee and Lee, 2000).

The hydraulic conductivity was estimated as $4.0\text{E-}06$ m/s to $2.0\text{E-}05$ m/s before the artificial CO_2 injection test and this range was derived from the push-draft-full test using two conservative tracers (Cl^- and SF_6). This area can't assume a representative value of the physical property for hydraulic conductivity as a monolithic because of the heterogeneous distribution of weathered material (Kim et al., 2018). The results of the electrical resistivity survey also represented the heterogeneous permeability distribution (Lee et al., 2017). Based on those results, the results of numerical simulation predicted that the initial-injected CO_2 plume could flow along a high permeability zone around the injection borehole.

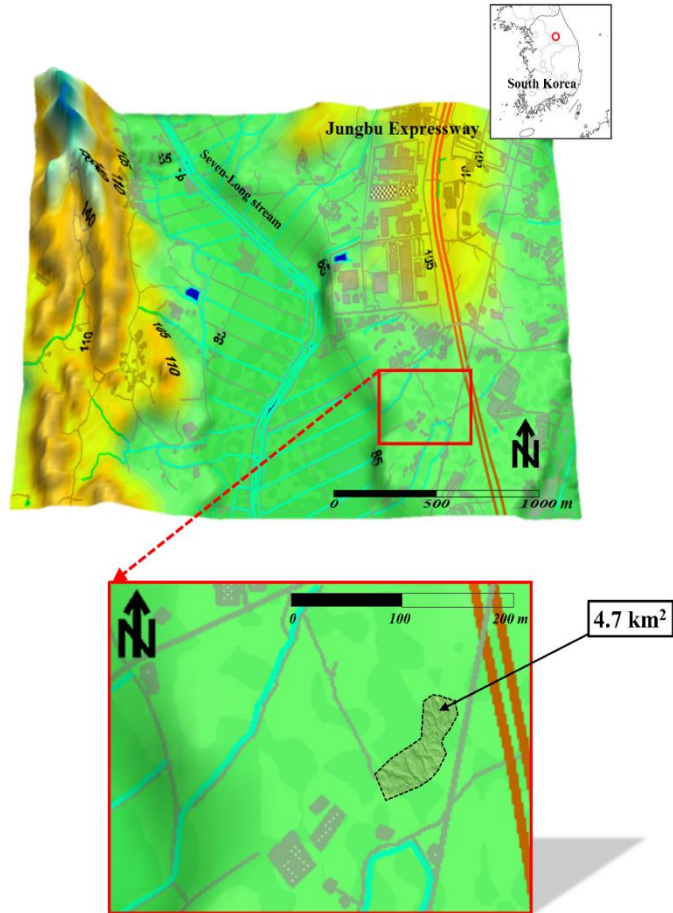


Figure 2-2 There are four kinds of wells and almost shallow depth wells (< 30 m) are gathered west side of testbed. Bed rock wells have drilling log information. The log data was obtained by performing S. P. T. (standard penetration test) at the time of the well installation.

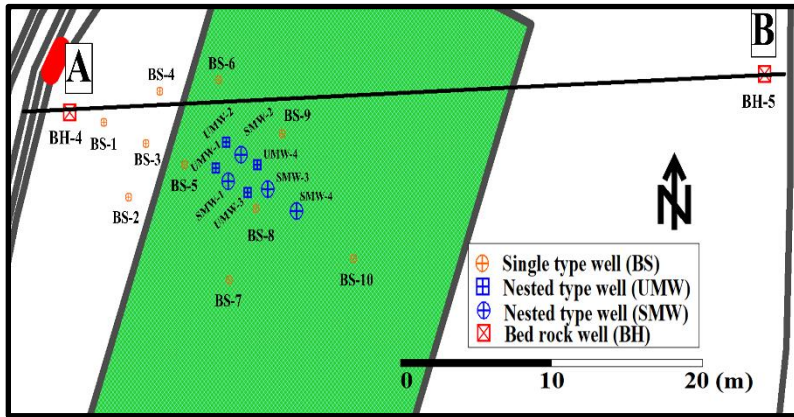


Figure 2-3 The study site is located in North Chungcheong Province and a plottage of the study area is about 4.7 km².

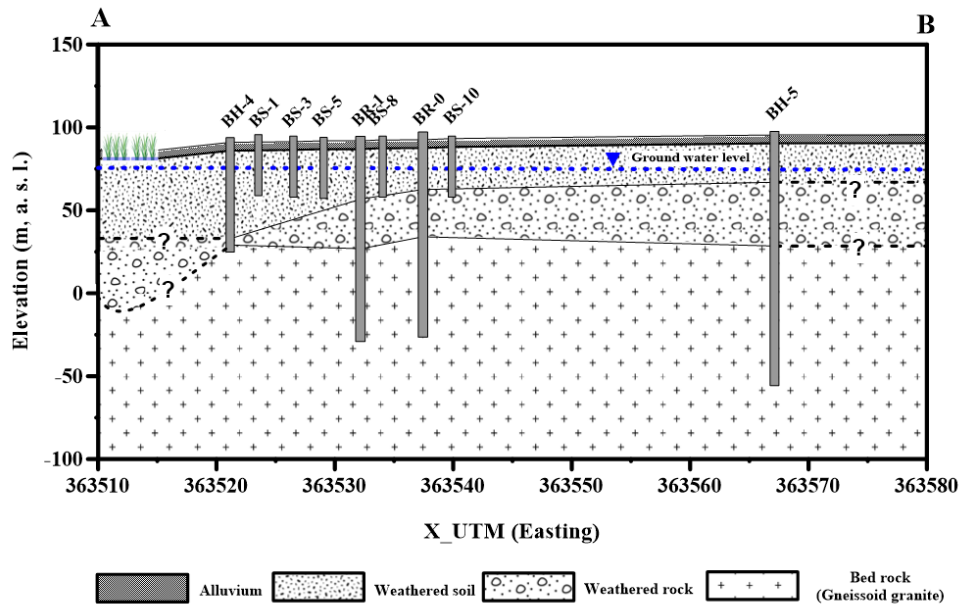


Figure 2-4 The geologic cross section was generalized based on the drilling log information.

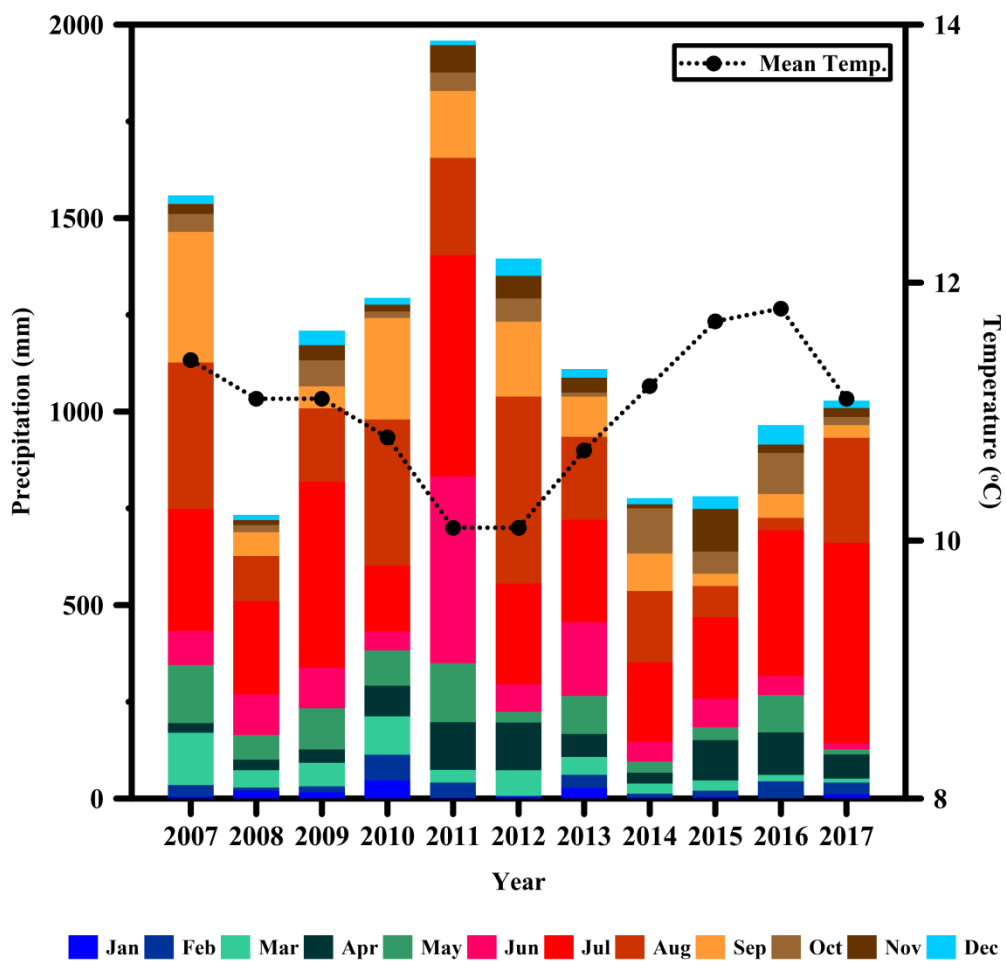


Figure 2-5 Annual precipitation and mean air temperature of the study site from 2007 to 2017 (10 years) (<http://data.kma.go.kr>).

2.4 Materials and methods

2.4.1 Monitoring wells

Figure 2-6 represents (a) the monitoring well distribution for injecting CO₂ gas into a shallow depth of aquifer and monitoring the concentrations with real-time recording system in the groundwater and the vadose zone. The ground surface amplitude gradually increases about 2.2 m (above sea level) from BS-01 to BS-10. On the contrary to the surface elevation gradient, the groundwater level drops from BS-01 to BS-10 as shown in Figure 2-6 b. The mean level of the groundwater was about 17.77 m (bgs, below ground surface) in the study site. To protect the gas monitoring sensor and to avoid the effect of water level rise on gas monitoring data as stated in Joun et al. (2016), at the first time, we thought that the total penetrating depth of the well pipes should not be exceeded over 14 m as for exclusive use of vadose zone monitoring. However, because we need to discuss later the covering the regional area of the study site and understanding that the pattern of gas concentration is varied depending on well types, decided that more wells were included for gas monitoring even though these were not for vadose zone only. We selected three kinds of monitoring well. First, the SMW series is

composed of four different lengths of the pipeline (18, 22, 26, and 30 m). The screened interval is only 2 m from the bottom of the pipe (16 to 18, 20 to 22, 24 to 26, and 28 to 30 m) and the remnant length of pipe is the casing which is the non-permeable interval (0 to 16, 0 to 20, 0 to 24 and 0 to 28 m). Second, the UMW series which have also four kinds of lengths pipeline (5, 8, 11, and 14 m). The screened interval is 1 m from the bottom of the pipe (4 to 5, 7 to 8, 10 to 11, and 13 to 14 m) and the remnant interval of the pipeline is also impermeable. Third, the BS series has only one length pipe and the total length is 30 m. To avoid the contamination of the groundwater or the vadose zone by incoming a material from the outside area, 3 m interval from the topsoil ground was not screened and grouted by bentonite and cement. All remnant intervals are screened. These three kinds of series monitoring well can be separated as nest type and single type as shown in Figure 2-7.

2.4.2 CO₂ gas monitoring at the vadose zone wells

In this study, to characterize and analyze the natural pattern of gas concentration in the vadose zone well, 24 NDIR modules that can detect CO₂ gas concentrations were applied on 6 pipelines. CO₂ gas is a useful source to use implying the representative pattern of gas species in the vadose zone well because CO₂ gas exists with the high concentration naturally (1000 to 100,000 ppm, Clark and Fritz, 1997) and the variations affected by external factors is easily detected using the simple sensing system such as NDIR (Non-dispersive infrared absorption) without any air extraction which could affect the concentration of a target gas by increasing or decreasing the air pressures in the soil pore. The long-term field experiment and monitoring were conducted under two condition as following cases: the First case is CO₂ gas monitoring with all open-top condition from Dec 2016 to Feb 2018 by inserting the sensors for each pipeline that has four different lengths according to the targeted depth using UMW series; and the second case is CO₂ gas monitoring with coupling closed and open-top depending on the well types

from Apr to Sep 2018 using three different types of wells (SMW, BS, and UMW) as shown in Figure 2-7.

2.4.3 Meteorological parameters

Because the CO₂ gas concentration in the vadose zone is sensitively responded by a natural force such as the wind velocity, the variation of an atmosphere pressure, temperature, rainfall, and humidity, one of the meteorological parameters should be monitored with gas concentrations in the subsurface environments simultaneously. Previous researchers have considered one or more meteorological parameters to understand the natural phenomena for each their studies purpose (Massman and Farank 2006; Risk et al., 2002; Schloemer et al., 2013; Garcia-Anton et al., 2014; Pla et al., 2016). Kuang et al. (2013) also emphasized the importance of natural effects such as water infiltration, fluctuating water table, topographic effect, and atmospheric pressure variation on subsurface airflow by synthesizing the published literature. Although the meteorological parameters data near the location of study site could be obtained fundamentally from the web site of Korea

Meteorological Administration (<https://data.kma.go.kr>), a regional weather station was constructed on 2.5 m above the ground surface to record the raw data without exterior hindrances and to investigate the detail correlation between the variations of gas concentration in the vadose zone well and meteorological parameters daily, weekly, monthly, and annually. The weather station (Vantage Pro2™ 6152C, Davis Instruments, Hayward, CA, USA) had capabilities for measuring air temperature (°C), relative humidity (%), wind velocity (m/sec) and direction (deg. from due north), precipitation (mm). To measure barometric pressures at the atmosphere and vadose zone well, pressure loggers (Model 3001 Barologger Edge, Solinst, Canada Ltd.) were installed inside and outside of vadose zone wells. All data was recorded with 10 min interval simultaneously and the recording time-stamped in Coordinated Universal Time (UTC). The weather station and CO₂ monitoring network were operated at the same time and the same study area. Figure 2-8 shows the pictures of those monitoring stations and each program interface.

2.4.4 A method for identifying CO₂ origin

Romanak et al. (2012, 2013, and 2014a) have introduced one of the simple methods for understanding the origin source by detecting the concentration in the soil gas such as O₂, CO₂, and N₂ and plotting these concentrations at the diagram consisted of two lines (Figure 2-16). One line indicates biologic respiration (BR), and the other represents methane oxidation (MO). These two lines can be derived from chemical formulas such as (CH₂O + O₂ → CO₂ + H₂O) for BR line and (CH₄ + 2O₂ → CO₂ + 2H₂O) for MO line. They called this method as Process-based analysis. Romanak et al. (2014a) represented the source identification successfully by applying this method on three different known types of CO₂ sources in Kerr Farm, ZERT, and Mt. Etna volcano. Base on two lines, the possible source can be analyzed as CO₂ dissolution, exogenous addition of CO₂, biological respiration, and oxidation of methane. In this study, to understand the source origin of detected CO₂ gas concentration before, during, and after field experiment, one-time gas monitoring was performed on 12 April, 27 April, 14 July, 21 July, 09 August, and 10 September 2017 at the SMW series. As like the previous researches, these results provided the information of source origin and a possible clue to

understand the leak signals were covered by the real-time multi-depth CO₂ monitoring system.

2.4.5 EC monitoring

Electrical conductivity (EC) is a representative parameter as the core indicator to demonstrate the CO₂ leakage at the test sites such as ZERT (zero-emission research and technology, USA), CO₂FieldLab (Norway), Brandenburg (Germany), Vrøgum (Denmark), and Escatawpa (USA) (Kharaka et al., 2010; Peter et al., 2012; Cahill and Jakobsen, 2013; Trautz et al., 2013; Humez et al., 2014). EC value in the background of the groundwater is changed depending on increasing and decreasing the dissolved ion in water because the CO₂ infused water has low pH (acidic liquid) and it changes the condition of the aquifer by eluting the geologic ions from the sediment. In this study, 20 times EC measurements were conducted before, during, and after the second injection test. The results of EC measurement was utilized to determine the direction of CO₂ infused water plume and the coverage area of the monitoring network.

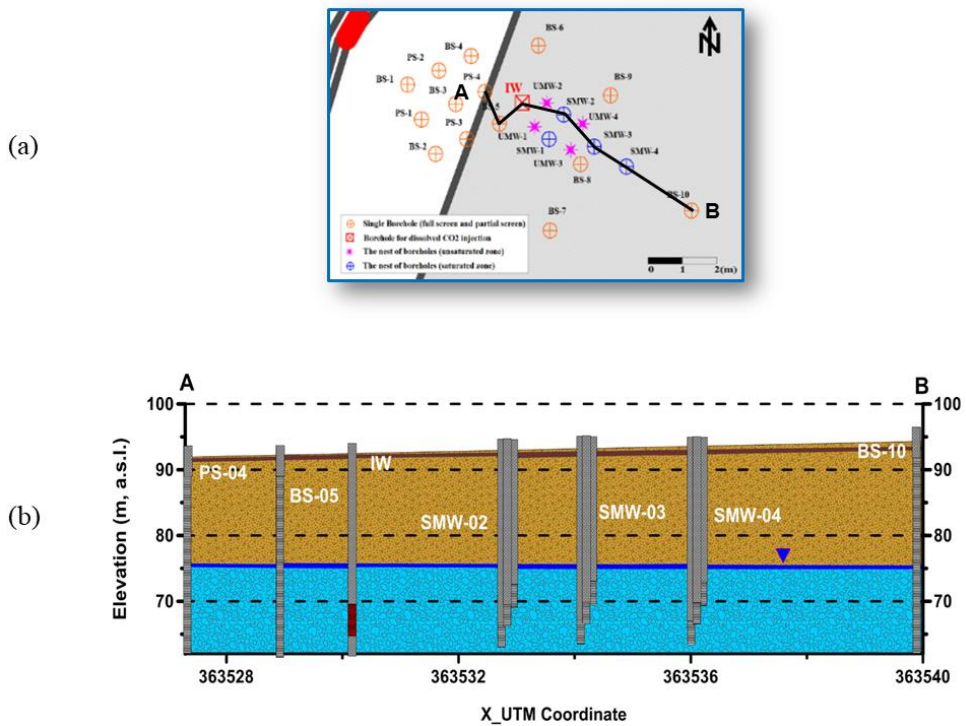


Figure 2-6 (a) The distribution of monitoring wells installed in the shallow depth of the vadose zone and the aquifer at the west side of test bed, (b) The generalized geologic cross section at the shallow depth part of test bed from A to B.

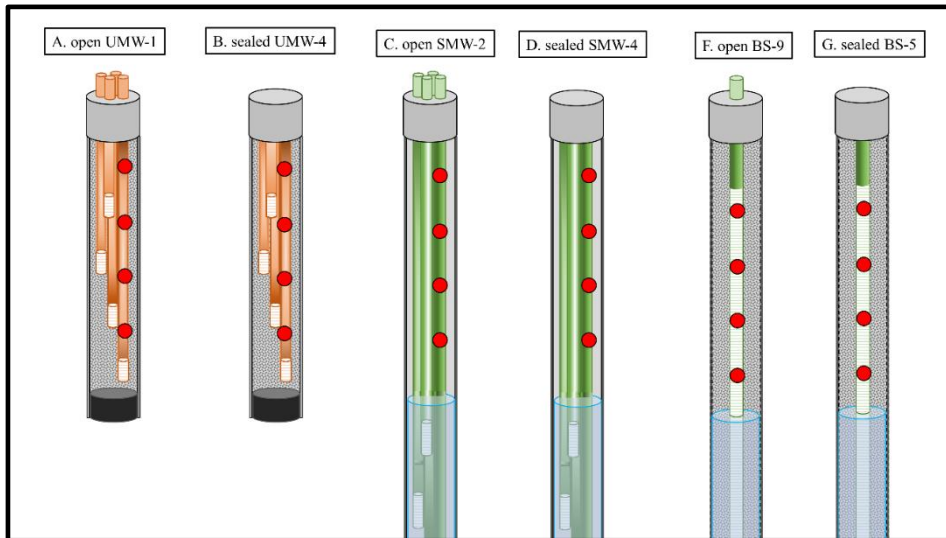


Figure 2 -7 The monitoring wells comprise nested types (A, B, C, and D) and single types (F and G). The red-color dots represent the location of NDIR sensors inside of monitoring wells.

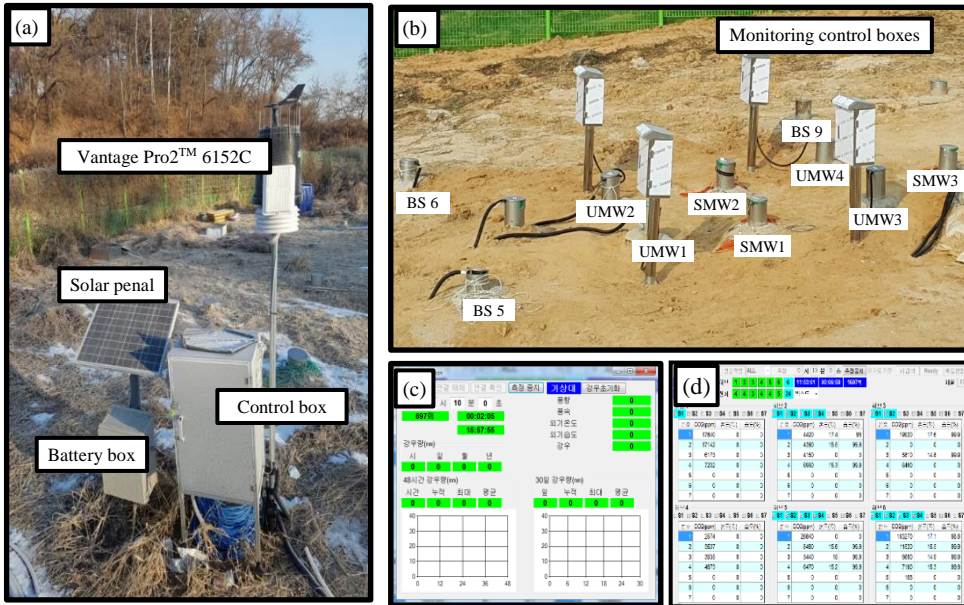


Figure 2-8 (a) Davis Instruments monitoring system for meteorological parameters, (b) CO₂ gas monitoring control boxes and well distribution, (c) Program interface for monitoring the meteorological parameters, (d) Program interface for CO₂ gas monitoring.

2.5 Performing field-scale experiments

The purpose of this study area is for understanding the environmental change if the sequestered CO₂ is escaped from the reservoir and to develop the technique for identifying the CO₂ leak signal easily, promptly, and economically. To prepare possible CO₂ leak event in case approaching the shallow depth aquifer (0 to 50 m bgs, below ground surface), two artificial CO₂ injection experiments were conducted with each different day and each purpose. The first injection test was performed on 29 Nov 2016 (winter season). The 1st test injection type was the pulse. The injection period was only 7.5 hours and the total amount of injected CO₂ was 13.5 kg in the water (about 7.5 m³). The injected CO₂ phase was not gas but aqueous which can be called CO₂ fully-saturated water at 1 atm (Ju et al., 2019). The average water temperature was 5.07 °C during the period of 1st injection test. Before conducting the injection test, the CO₂ gas infused water was prepared. The used water was the groundwater that was pumped from background wells. the Second injection test was conducted from 27 Jun to 24 July 2017 (summer season). The injection type in the 2nd test was continuous. The injection period was 26.8 days (85.7 times longer than 1st injection test) and the total amount

was 247.4 kg (in water 136.1 m³). The mean water temperature was 21.75 °C during the 2nd injection test period. The first injection test was performed under the natural gradient condition ($I = 0.02$) and the second injection test was conducted under the forced gradient condition ($I = 0.2$). Table 2-1 shows information about those artificial CO₂ injection tests and more detailed descriptions and figures can be found in the published literature (Lee et al., 2017). Here, only important parts of the experimental process are briefly discussed as following the next sections about the experiments.

Table 2 -1 The information of controlled CO₂ release tests.

Parameters	Values	
	Natural gradient	Forced gradient
injection type	pulse	continuous
injection period	29 Nov (winter) 0.3125 d (7.5 hr)	27 Jun ~ 24 Jul (summer) 26.8 d
monitoring period	30 Nov ~ 23 Mar 113 days	16 Jun ~ 12 Sep 90 days
total injection (m ³)	7.5	136.1
injection rate (m ³ /d)	24	5.08
gradient (I)	0.02	0.2
T_CO ₂ (kg)*	13.9	247.4

*Calculated values based on Henry's constant (Carroll et al., 1991) depending on the temperature of experiment conditions (avg. 5.07 °C and avg. 21.75 °C respectively during the CO₂ infused water injection).

2.5.1 Short-term CO₂ infused water injection

In this case of field experiment, the controlled CO₂ release test was supposed to be a prototype drill for preparing an advanced main test later. Thus, the research group considered that the volume of injected CO₂ into the shallow aquifer would be too small to detect the changing parameter by using the main physical indicators such as pH, EC, DO, etc. clearly. However, this test could be an important task because from this short-term CO₂ infused water injection test, the research group can decide how the monitoring system would be performed, what parameters should be gained, and how many times and much time interval of gas or groundwater samples should be conducted for effective data collections. As shown in figure 2-9, the experimental set composed of two tanks, a circulation pump, and CO₂ dissolver. The Left-hand-side tank is for making the CO₂ infused water and the right-hand-side tank is for pushing the remained water inside of the injection well. CO₂ infused water was 5 m³ and pushing water was 2.5 m³. Both of water was pumped out from the same aquifer system where CO₂ infused water is injected. The injecting rate of CO₂ infused water was 16.34

L/min and the total injected CO₂ was 16.9 kg. The injection was conducted for 7.5 hours (2016-11-29) using a controllable quantitative pump (MP1 model, GRUNDFOS, Denmark) by locating in the screened interval (21 to 24 m below ground surface) of the injection well (IW) with an isolating packer which can be blowing at the inside of well.

During the injection period, the groundwater levels absolutely were increased by the volume of CO₂ infused water and the trend of GW level increasing around the injection well not have the same time and magnitude. Thus, these results mean that this study area was the place where the sediment at the target depth has strongly heterogeneity characteristics. The main impact of CO₂-infused water on around the monitoring well was initiated about 4 days later. Ju et al. (2019) represented all monitored parameters including the noble gases. They stated that although this case of the controlled CO₂ release test (short-term injection) does not show the clear indicator which can represent the CO₂ leakage impacted on the groundwater system with physical parameters such EC, pH, DO, T, etc., the clear signal of CO₂ leak event could be achieved if noble gases (Helium, Krypton, etc.) was mixed with the CO₂ infused water. Because this test was performed under the natural hydraulic gradient (0.02), we considered that the plume of

injected CO₂ was supposed to flow from the high potential energy level of groundwater to the low potential energy level of groundwater. But as mentioned previously, because this study area has complex geological sediment even at the shallow depth (20 to 30 m bgs), the order of the observed wells being initially measured was also showed randomly. Thus, the real closed pathway of the plume of CO₂ infused water was no revealed using the observed data from this test. Based on those results, we decided that the artificial forced hydraulic gradient will be better than the natural gradient to collect the reasonable data with the main CO₂ injection test later (long-term CO₂ infused water injection test). A more detailed description of the mass balance of CO₂ and other information of this short-term CO₂ injection test can be found in Ju et al. (2019).

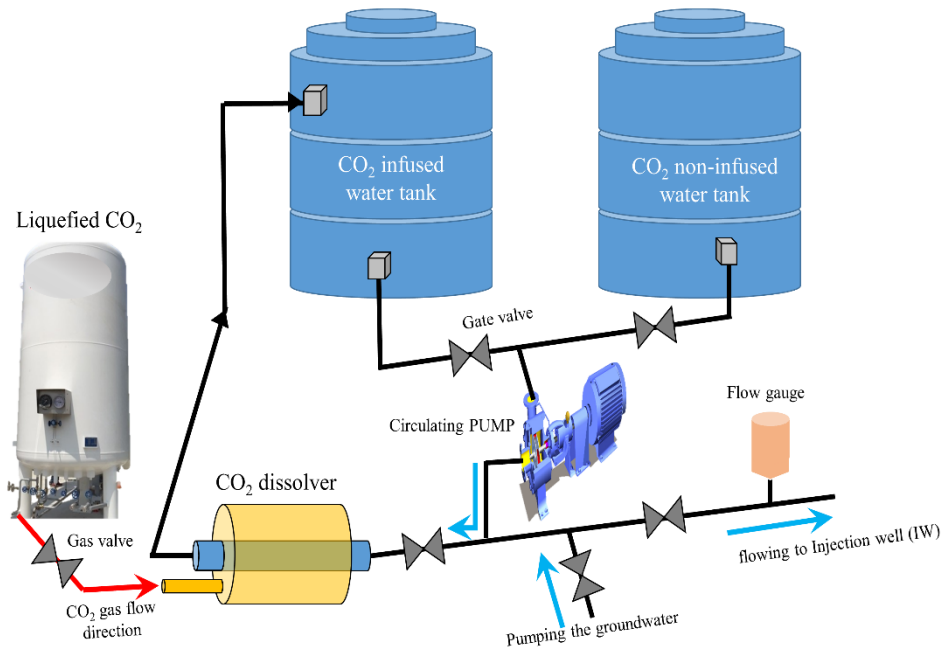


Figure 2-9 Two tanks (5 m³ volume) were used for the field-scale experiment in the K-COSEM research site. A circulation pump and CO₂ dissolver were attached on the left tank for preparing the CO₂ infused water.

2.5.2 Long-term CO₂ infused water injection

A real-time monitoring of CO₂ gas concentrations is shown in Figures for each well numbers. Figure 2-10, -11, -12, and -13 represents the monitoring results of UMW 1, 2, 3, and 4 nests depending on the target depth respectively. As previously mentioned at the explanation of well specification, the screening interval poses at the bottom of each pipe and this monitoring pipe condition can block the other sources which could smear and be mixed among different depth sources in the one pipe. Space exists among those four pipes and it can give clear data for the target depth such as 5, 8, 11, and 14 m separately. Over 45,000 ppm (vol. /vol.) of maximum CO₂ gas concentration is marked with red color in Table 2-2. The highest level of CO₂ gas concentration was 75,680, 56,520, 53,264, and 40,390 ppm (vol. /vol.) at 5 m of UMW 1, 14 m of UMW 2, 5 m of UMW 3 and 5 m of UMW 4 respectively. As shown in Figure 2-10, -11, and -12, the constant high level of CO₂ gas concentrations remained at 5 m during the summer season (Jun, July, and August). These levels of gas concentrations were included in the range of naturally produced CO₂ in the soil media (Clark and Fritz, 1997). However,

because the second injection test was conducted during the summer season, those CO₂ monitoring results can't represent the pure natural productions but some abnormal data contained at that time. Unfortunately, because the background data of CO₂ gas concentration in soil gas was not obtained at the other summer season of years in this study area, these figures were confused to determine whether the leak signal was detected from 27 to June to 24 July 2017 which is the period of the second CO₂ injection test. As shown daily average lines in those Figures, the pattern was very unstable across the years and it seems to be affected by external influences naturally. Besides, although some sharp peak was observed during and after 2nd test and those peaks could show the CO₂ leaking event, it can be ignored that these pattern supposed to observe the natural CO₂ production for the other summer season of years. Unlike other UMW nests, in UMW-2 the maximum concentration was detected at 11 and 14 m pipelines. It could be one of the clues for the CO₂ leaking event was monitored during this summer season but need to more information which can explain these shape patterns of CO₂ gas concentration data. Meteorological parameters were also monitored as shown in Figure 2-14 to understand the natural interference on the gas concentration in the monitoring wells and the statistics are summarized in Table 2-3. By

comparing the highest level of CO₂ gas concentration with the same time series of meteorological parameters in Figure 2-14, we try to explain that the pattern of soil CO₂ gas concentration was increasing and decreasing with some of the meteorological parameters. The increases in soil CO₂ gas concentration at the beginning of the summer season (June-July) were observed simultaneously with decreases in atmospheric pressure or wind velocity (Figure 2-14(a), (e)). During the rainy season with high rainfall frequencies and high air humidity (Figure 2-14(c), (d)), the low CO₂ gas concentration was expected because the rainwater can carry down the CO₂ gas concentration by infiltrating from the ground surface to the subsurface environment (Kuang et al., 2013) but the data not represented the distinct pattern. To clarify the observed data and its correlation with the meteorological parameters, the statistical analysis should be conducted.

Table 2-2 Statistics of CO₂ concentration depending on the monitoring depths during the field test.

Well	Depth, m / No.	Data	Average	SD	Min.	Max.
UMW-1	5 / 1	7,249	16,854	13,191	329	75,680
	8 / 2	7,250	6,050	2,992	362	30,330
	11 / 3	7,250	4,914	2,428	283	32,640
	14 / 4	7,248	5,372	2,554	332	30,090
UMW-2	5 / 1	7,251	9,970	8,812	478	34,350
	8 / 2	5,404	6,555	2,663	404	23,560
	11 / 3	7,251	5,630	3,338	351	48,390
	14 / 4	6,404	4,982	2,906	308	56,520
UMW-3	5 / 1	3,414	16,697	10,930	1,476	53,264
	8 / 2	7,251	8,672	3,355	949	36,160
	11 / 3	7,250	6,152	1,658	695	16,530
	14 / 4	7,251	6,411	1,282	666	18,190
UMW-4	5 / 1	7,243	9,345	7,980	290	40,390
	8 / 2	7,248	7,370	2,634	360	14,400
	11 / 3	7,250	5,428	2,180	350	23,620
	14 / 4	7,251	6,087	1,794	342	11,420

Table 2-3 Statistics of meteorological parameters during the field test.

Parameters	Unit	Data	Average	SD	Min.	Max.
Pressure	hPa	10,918	1,004.45	7.75	980.10	1,022.50
Temp.	°C	9,646	8.06	11.75	-17.69	35.73
Rainfall	mm day ⁻¹	9,661	70.69	19.14	14.70	97.60
Relative Humidity	%	2,087	5.06	12.11	0.20	98.40
Wind velocity	m s ⁻¹	5,121	2.19	1.92	0.10	15.30
Wind direction	°North	5,111	201.81	81.39	0.10	358.30

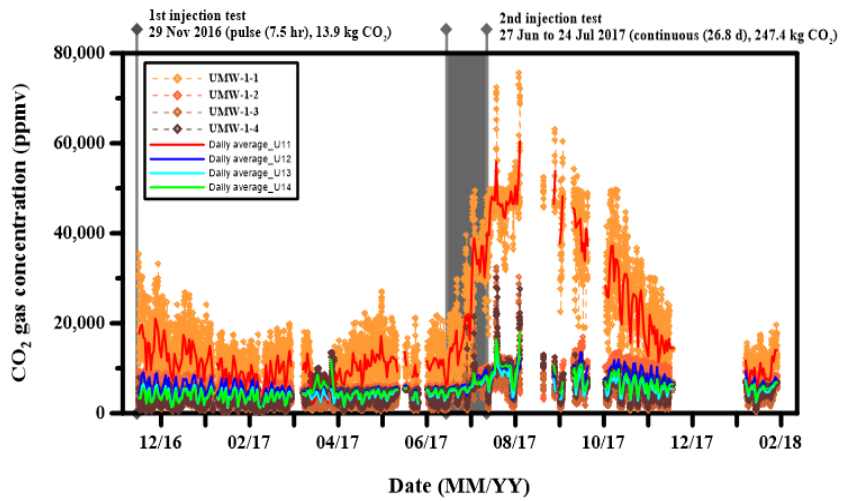


Figure 2-10 Time series of CO₂ gas concentration from December 2016 to February 2018. Diamond symbol and separated line represented the collected data with four different brown colors depending on the pipe line length of UMW 1 nest (5, 8, 11, and 14 m). Solid line shows the daily average values of the CO₂ gas concentration data with different colors such as red, blue, skyblue, and green. The grey line and shade shows the date and period of two injection tests.

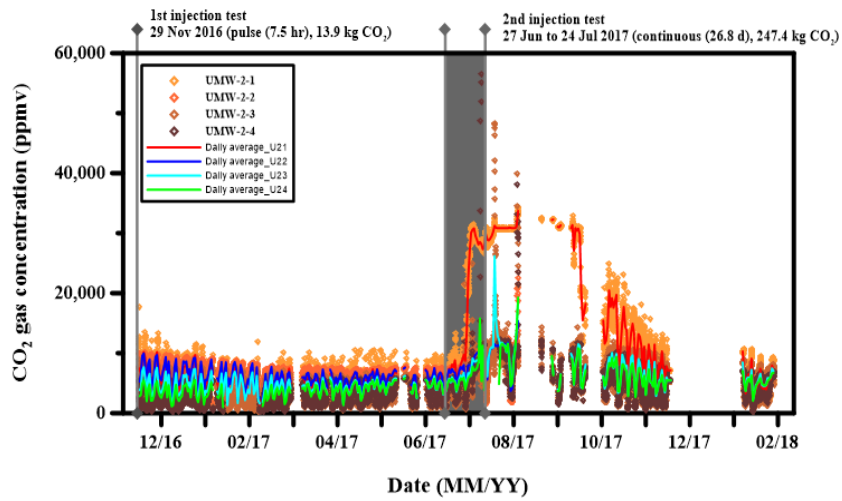


Figure 2 -11 Time series of CO₂ gas concentration from December 2016 to February 2018. Diamond symbol and separated line represented the collected data with four different brown colors depending on the pipe line length of UMW 2 nest (5, 8, 11, and 14 m). Solid line shows the daily average values of the CO₂ gas concentration data with different colors such as red, blue, skyblue, and green. The grey line and shade shows the date and period of two injection tests.

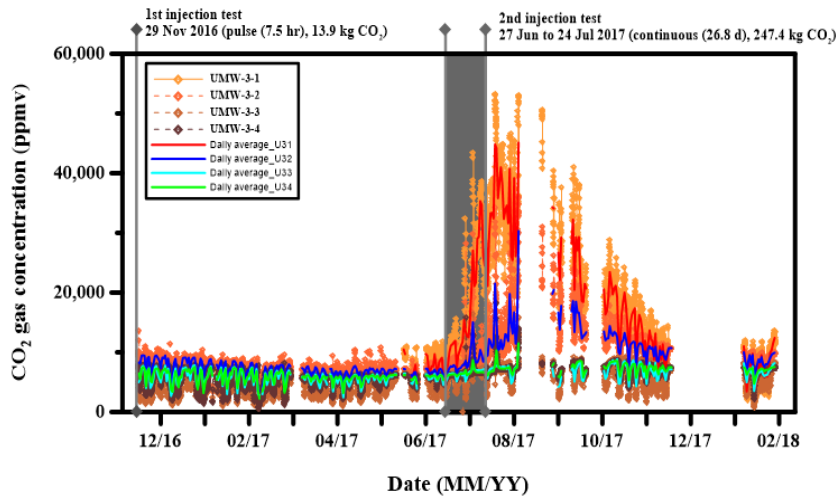


Figure 2 -12 Time series of CO₂ gas concentration from December 2016 to February 2018. Diamond symbol and separated line represented the collected data with four different brown colors depending on the pipe line length of UMW 2 nest (5, 8, 11, and 14 m). Solid line shows the daily average values of the CO₂ gas concentration data with different colors such as red, blue, skyblue, and green. The grey line and shade shows the date and period of two injection tests.

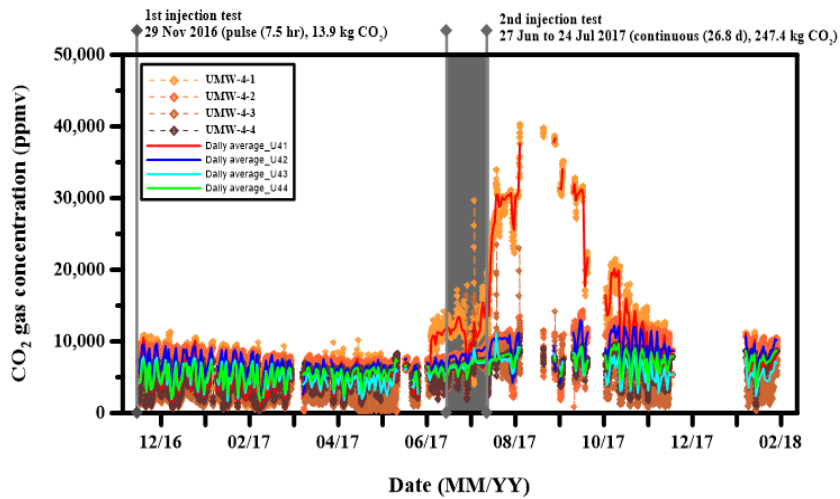


Figure 2 -13 Time series of CO₂ gas concentration from December 2016 to February 2018. Diamond symbol and separated line represented the collected data with four different brown colors depending on the pipe line length of UMW 4 nest (5, 8, 11, and 14 m). Solid line shows the daily average values of the CO₂ gas concentration data with different colors such as red, blue, skyblue, and green. The grey line and shade shows the date and period of two injection tests.

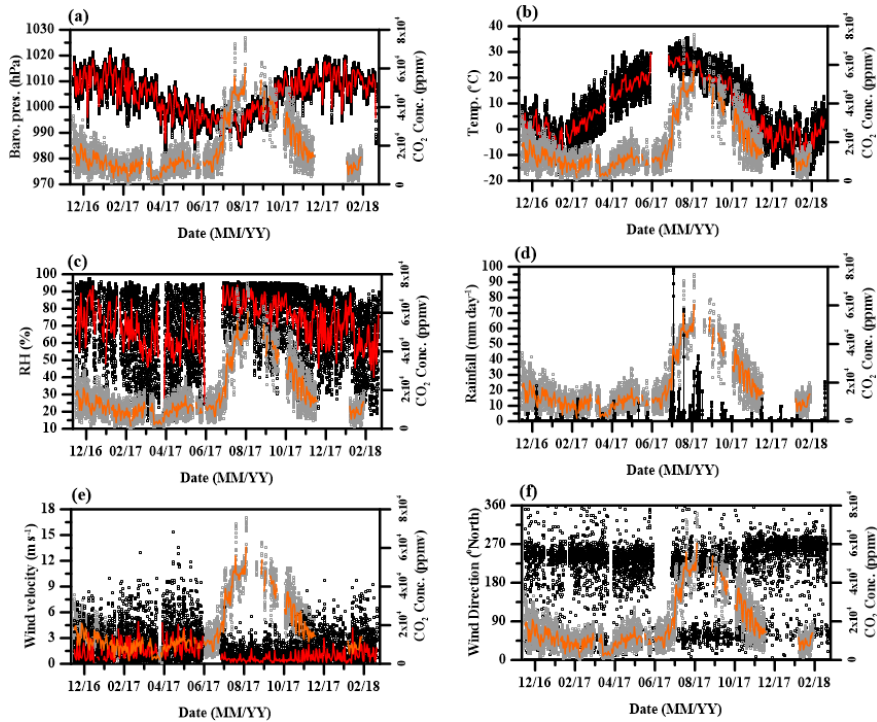


Figure 2 -14 Time series of meteorological parameters from December 2016 to February 2018 for (a) Barometric pressures, (b) Atmospheric temperature, (c) Air relative humidity, (d) Rainfall, (e) Wind velocity, and (f) Wind direction. The black and gray circles represented the observed data at the weather station and CO₂ monitoring well (UMW-1-1, 5 m) respectively. The red color line is the daily mean values for the black circle data. The orange color line shows the average values of obtained data from the UMW-1-1 well shown in Figure 2-7.

The results of the EC measurement is shown in Figure 2-15. The contribution of EC values can easily represent the plume size and flow direction. Kharaka et al. (2010) show EC values were increased after CO₂ injection from 600 to 1100 or 1800 $\mu\text{S}/\text{cm}$ and it suggests that EC parameter could be utilized for understanding the plume migration when the CO₂ injection experiment is performed. As shown in Cahill and Jakobsen (2013), the results of this study also represented the clarified plume shape and it was migrated following the groundwater flow direction which was built up artificially (Table 2-1, I=0.2). The time when the CO₂ infused water plume was formed was matched before, during, and after the second injection experiment.

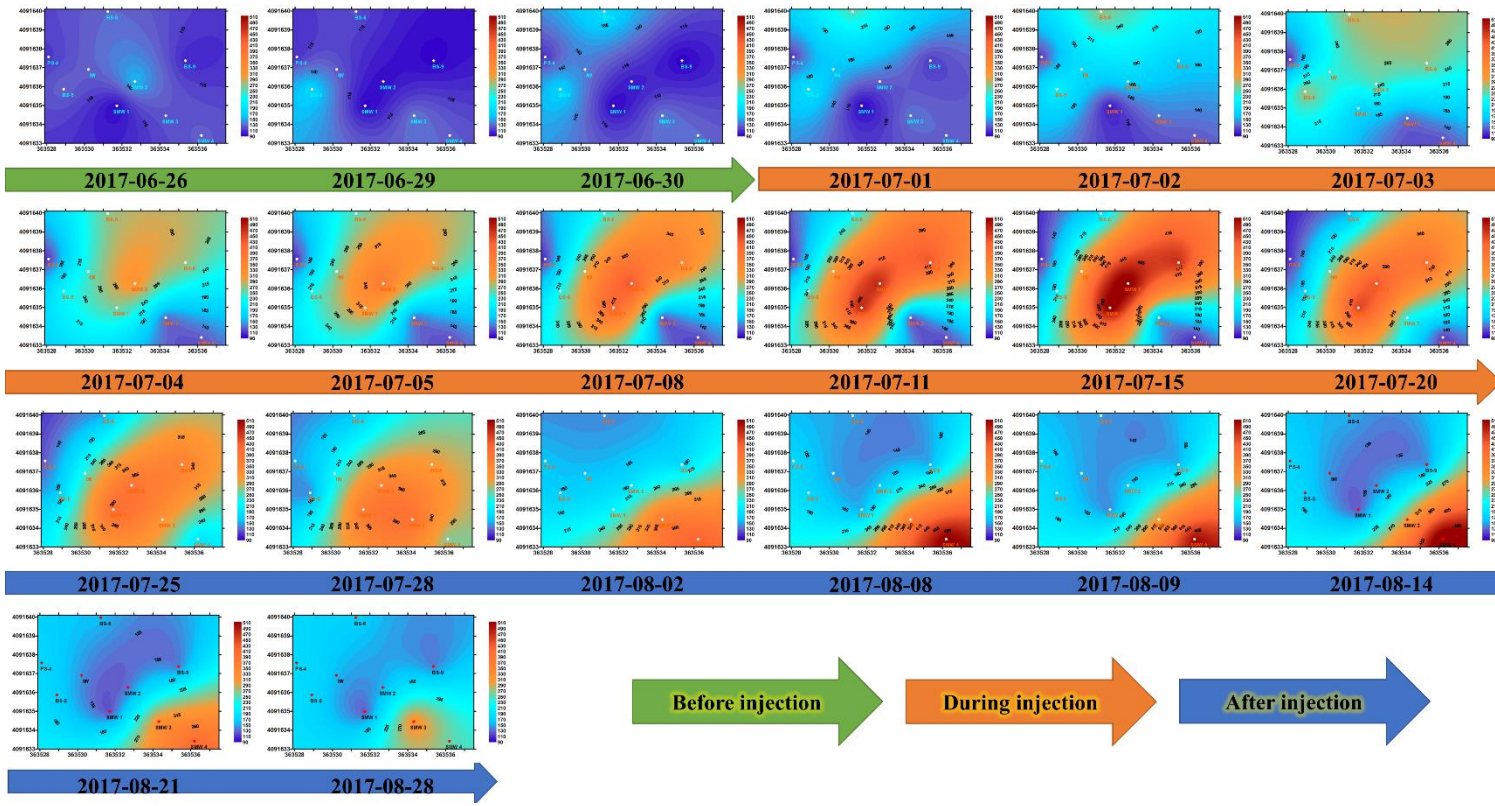


Figure 2-15 Spatial distribution of EC values before, during, and after the second CO₂ injection test.

Artificially injected CO₂ degasses during the CO₂ infused water plume migration. As mentioned in 2.4.1 section, because the natural production was confused to determine whether the injected CO₂ gas was migrated from the groundwater to the atmosphere or not, the composition of gases such as CO₂, and O₂ was measured at the SMW nest using a portable GC called GA 5000 (Geotech instrument). Based on previous researches (Romanak et al., 2012; 2013; 2014a), the results of those gas concentrations are represented in Figure 2-16. Before CO₂ injection, the source origin of CO₂ gas was derived from the biomass respiration or the methane oxidation. On the contrary to this, during and after CO₂ injection, the source origin was changed by being plotted at the exogenous addition of the CO₂ area. It means that the degassed CO₂ from the CO₂ infused water plume was detected during and after the second field test. Also, depending on the plume positions, the plotted well number was changed spatially and temporally.

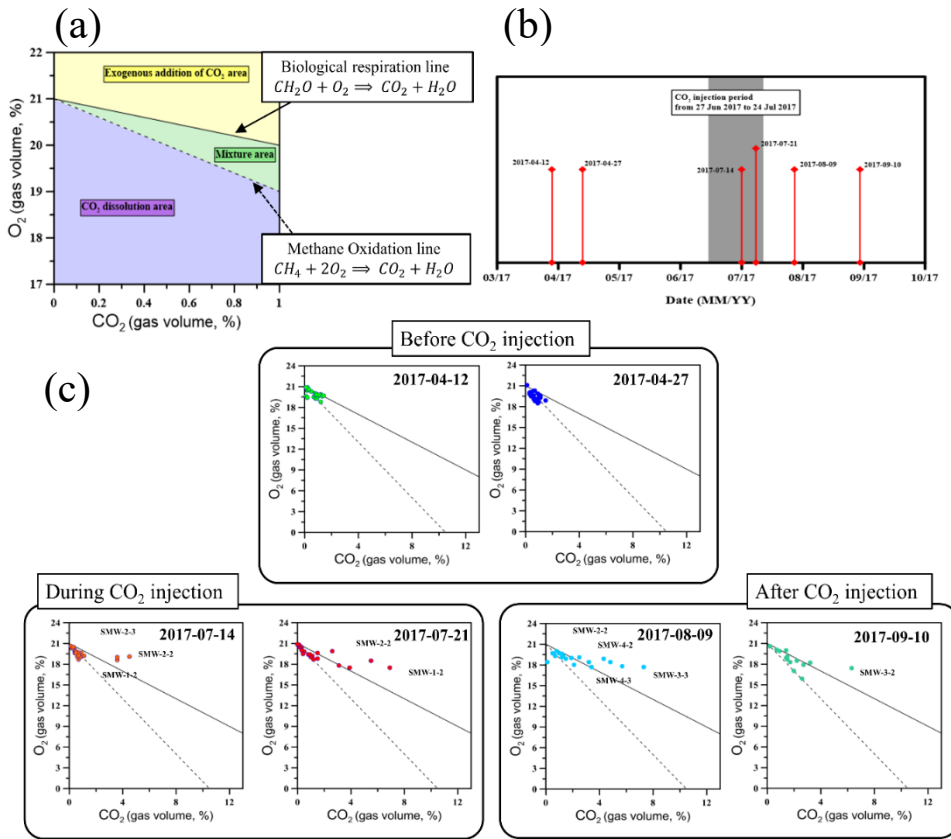


Figure 2-16 (a) A plotting field for applying the gas composition on the process-based analysis method (depict a figure based on Romanak et al., 2014a), (b) The gas sampling times, (c) The results of gas monitoring and applied on the process-based analysis plot.

To compare the pattern of CO₂ gas concentration between the summer season in 2017 and in 2018, the other field experiment was conducted from 27 April to 30 August 2018. Although unlike in the summer season of 2017, different well types (SMW, UMW, and BS series) and monitoring conditions (open and closed top) were used for monitoring CO₂ gas concentration in 2018, it was enough to find the characteristics of natural pattern and the highest level of CO₂ gas concentration which produced by biomass respiration or methane oxidation. By inserting the assumed injection performance period as gray color shade in Figure 2-17, we could compare between previous and extra field experiments within the same period from 27 June to 24 July 2017 and 2018 respectively. The results for all type wells represent the increased and high level CO₂ gas concentrations except open-top BS well during the assumed injection period. The highest level of CO₂ gas concentration was not exceeded over 52,000 ppm (vol. /vol.) as shown in Table 2-4. If all CO₂ gas which was from the groundwater by the second injection experiment disappear, it can be assumed that all level and pattern in the results of second monitoring was derived by the naturally produced CO₂ gas. Although it is impassible whether the CO₂ leakage event was detected or

not by comparing between 2017 and 2018, one thing is clear that even the gas sampling is performed at the same site, the results of gas concentration could be varied depending on well type and condition. The pattern of gas concentration in the monitoring well also would be affected by the external (meteorological parameters) and internal (fluctuating water table) condition. Figure 2-18, -19, -20, -21, -22, and -23 shows the results of CO₂ gas monitoring in detail depending on well types and well conditions. Almost gas concentrations in open-top wells were lower than closed-top wells and in closed-top wells, a constant level of gas concentration was detected during the monitoring period at 11 m depth (BS and SMW) and 14 m depth (BS, SMW, and UMW). These results represent that the CO₂ gas exists within the specific ranges from 10,000 to 52,000 ppm (vol. /vol.) in this study area. However, all monitoring results had fluctuated patterns each depth. Especially, Figure 2-20 and 2-22 shows the large swing patterns daily or in a short term period. The results of open-top SMW well had the large swing patterns at 5 m depth. Those patterns suggested that the low level of CO₂ was smeared with the advective flow as like flushing out the air from inside the monitoring well

to the atmosphere. The detailed researches about this natural phenomenon will be described in the next chapter.

Table 2-4 Statistics of CO₂ concentratoin depending on the monitoring wells.

Well	Depth, m	Data	Average	SD	Min.	Max.
2.5.3 MW open (2-4)	5	2,981	22,532	9,818	1,080	51,600
	8	2,981	31,687	11,533	14,866	51,047
	11	2,981	17,416	5,250	10,147	26,612
	14	2,981	17,897	4,161	12,200	25,086
2.5.4 MW closed (4-4)	5	2,981	27,343	10,221	10,023	51,003
	8	2,981	18,164	6,695	9,900	37,000
	11	2,981	15,668	3,826	10,490	26,400
	14	2,981	14,167	2,212	10,960	20,660
2.5.5 S open (9)	5	2,981	2,872	3,115	65	9,769
	8	2,981	3,766	3,462	293	10,899
	11	2,981	4,060	2,538	133	9,541
	14	2,981	5,146	2,408	354	9,360
2.5.6 S closed (5)	5	2,981	25,268	8,274	5,810	49,910
	8	2,981	14,834	3,765	6,100	24,620
	11	2,981	9,158	1,487	5,700	11,800
	14	2,981	8,765	1,610	5,510	11,800
UMW open (1-4)	5	2,981	4,507	4,429	240	49,010
	8	2,981	4,791	4,329	280	51,680
	11	2,981	5,048	3,997	208	47,232
	14	2,981	5,908	2,669	320	22,937
UMW closed (4-4)	5	2,981	30,695	8,736	5,410	50,390
	8	2,981	27,383	9,648	5,630	51,730
	11	2,981	17,031	6,908	5,260	30,170
	14	2,981	9,154	984	7,500	12,180

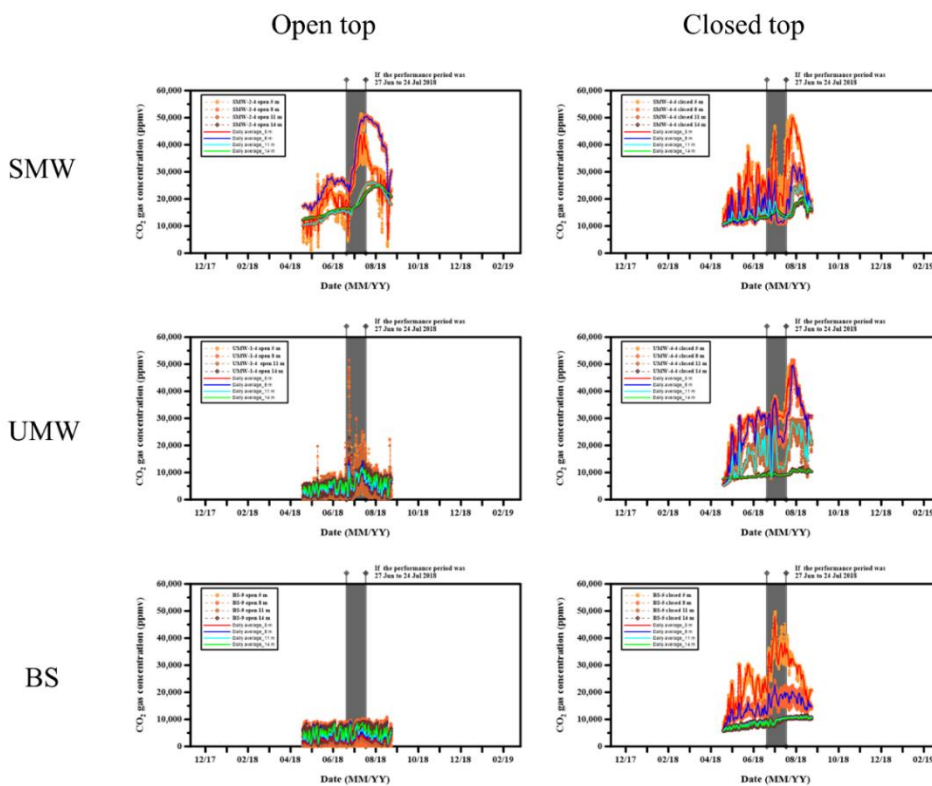


Figure 2 -17 Time series of CO₂ gas concentration from April to August 2018. The area of gray shade is the assumption period if the CO₂ injection is conducted at the same period of second injection test in 2017. Diamond symbol and separated lines shows observed data of CO₂ gas concentration and solid line shows the daily average values as shown in the legend. Depending on well types (SMW, UMW, and BS) and conditions (open and closed), the results of CO₂ gas monitoring shows the different patterns.

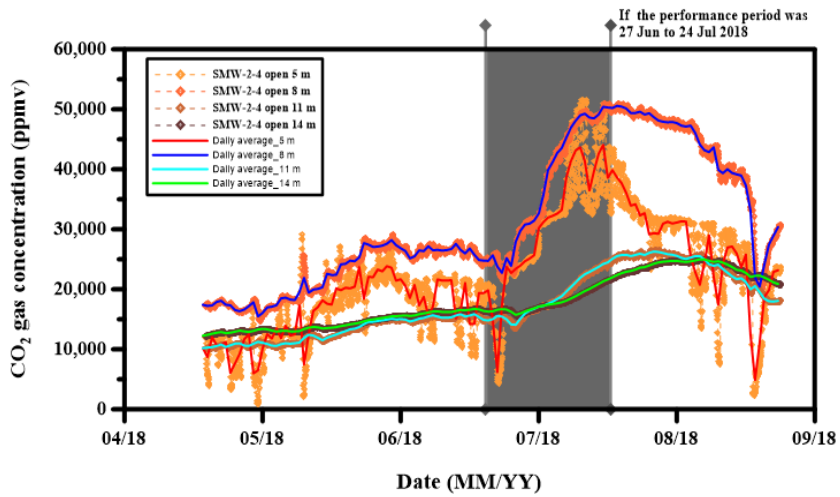


Figure 2 -18 The results of real time CO₂ gas monitoring data in SMW-2-4 which has open top according to the depth such as 5, 8, 11, and 14 m. Only one pipe line was used to detect the CO₂ concentration in SMW-2-4. Solid lines shows the daily average of CO₂ gas concentrations. Gray color shade represents the assumption period of the injection performance not the real injection period.

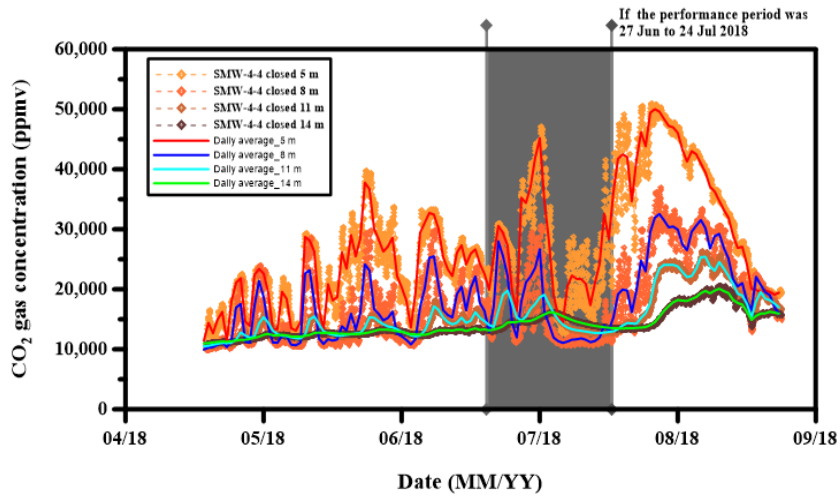


Figure 2 -19 The results of real time CO₂ gas monitoring data in SMW-4-4 which has closed-top according to the depth such as 5, 8, 11, and 14 m. Only one pipe line was used to detect the CO₂ concentration in SMW-4-4. Solid lines shows the daily average of CO₂ gas concentrations. Gray color shade represents the assumption period of the injection performance not the real injection period.

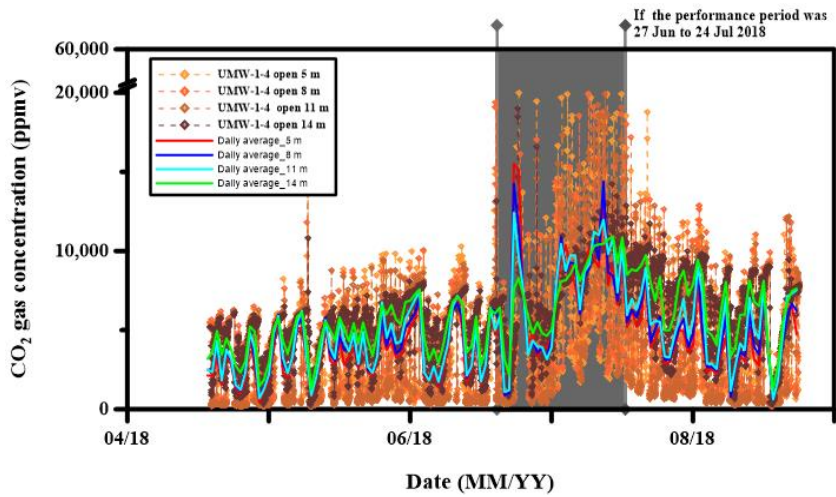


Figure 2 -20 The results of real time CO₂ gas monitoring data in UMW-1-4 which has open-top according to the depth such as 5, 8, 11, and 14 m. Only one pipe line was used to detect the CO₂ concentration in UMW-1-4. Solid lines shows the daily average of CO₂ gas concentrations. Gray color shade represents the assumption period of the injection performance not the real injection period.

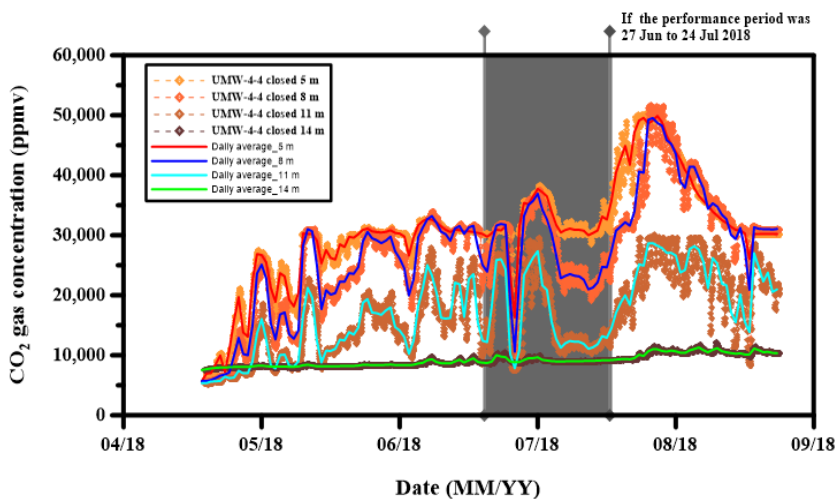


Figure 2 -21 The results of real time CO₂ gas monitoring data in UMW-4-4 which has closed-top according to the depth such as 5, 8, 11, and 14 m. Only one pipe line was used to detect the CO₂ concentration in UMW-4-4. Solid lines shows the daily average of CO₂ gas concentrations. Gray color shade represents the assumption period of the injection performance not the real injection period.

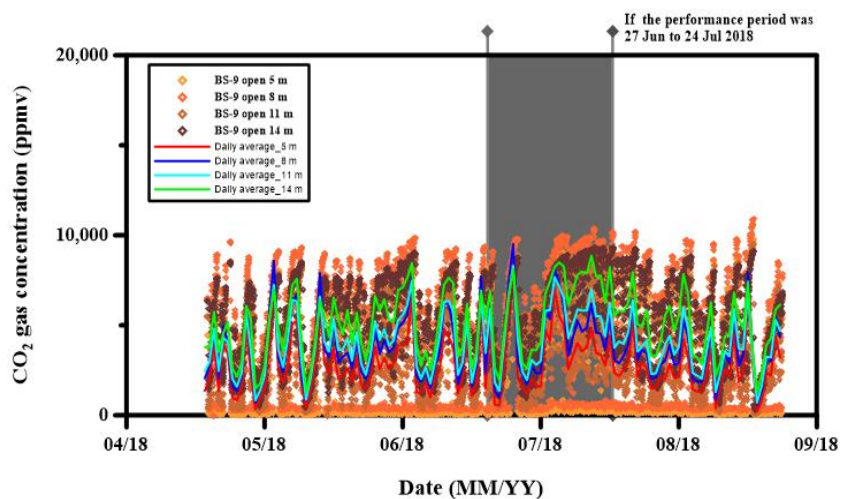


Figure 2 -22 The results of real time CO₂ gas monitoring data in BS-9 which has open-top according to the depth such as 5, 8, 11, and 14 m. Only one pipe line was used to detect the CO₂ concentration in BS-9. Solid lines shows the daily average of CO₂ gas concentrations. Gray color shade represents the assumption period of the injection performance not the real injection period.

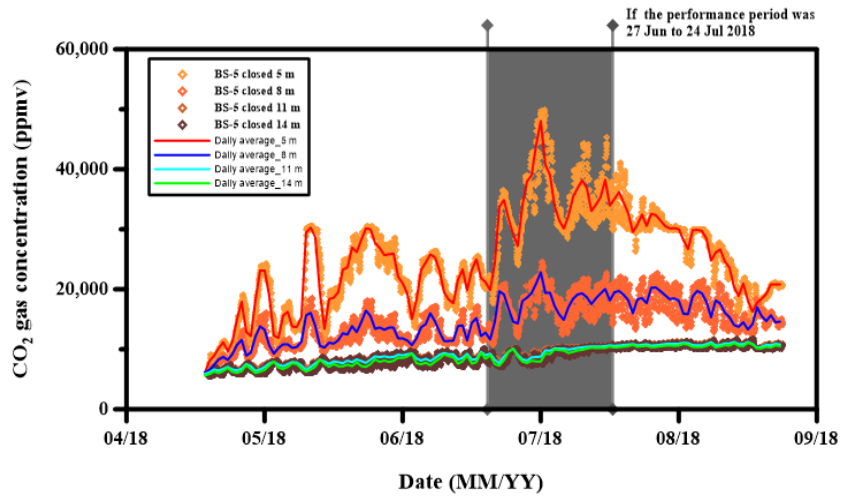


Figure 2 -23 The results of real time CO₂ gas monitoring data in BS-5 which has closed-top according to the depth such as 5, 8, 11, and 14 m. Only one pipe line was used to detect the CO₂ concentration in BS-5. Solid lines shows the daily average of CO₂ gas concentrations. Gray color shade represents the assumption period of the injection performance not the real injection period.

A time series of meteorological parameters and one of the typical pattern of CO₂ gas concentration is shown in Figure 2-24 for open-top well and in Figure 2-25 for a closed top well. The statistics of meteorological parameters are summarized in Table 2-5. By comparing the meteorological effect on the pattern and trend of CO₂ gas concentration in the subsurface environment with mentioned in section 2.4.1 seasonal variation of CO₂ gas concentration, we recognized that the trend and pattern in the seasonal pattern are completely different as we show the data in a short term as months or days as detail. In the open well, the correlation between barometric pressure and CO₂ gas concentration was represented negatively, on the contrary to this, in the closed well, the correlation between barometric pressure and CO₂ gas concentration was shown positively. During the rainfall event occur, the specific pattern was not detected at the open-top well. However, at the closed-top well, the CO₂ gas concentration was decreased with a lag time. In the summer season, the CO₂ gas concentration might be not following the barometric pressure pattern because the CO₂ gas would be produced with a huge amount by supplying an appropriate temperature and humidity into the soil media. These results suggest that the barometric pressure and rainfall event could be provided an

answer to why the patterns of CO₂ gas concentrations in the monitoring wells have fluctuated naturally.

Table 2 -5 Statistics of meteorological parameters during extra field test.

Parameters	Unit	Data	Average	SD	Min.	Max.
Pressure	hPa	3,000	997.45	4.78	977.01	1013.51
Temp.	°C	2,667	22.73	6.32	4.18	38.84
Rainfall	mm day ⁻¹	626	9.94	14.85	0.2	87.60
Relative Humidity	%	2,667	76.35	14.60	28.10	94.70
Wind velocity	m s ⁻¹	1,105	2.09	1.70	0.05	12.60
Wind direction	° North	1,104	198.63	83.13	7.20	359.80

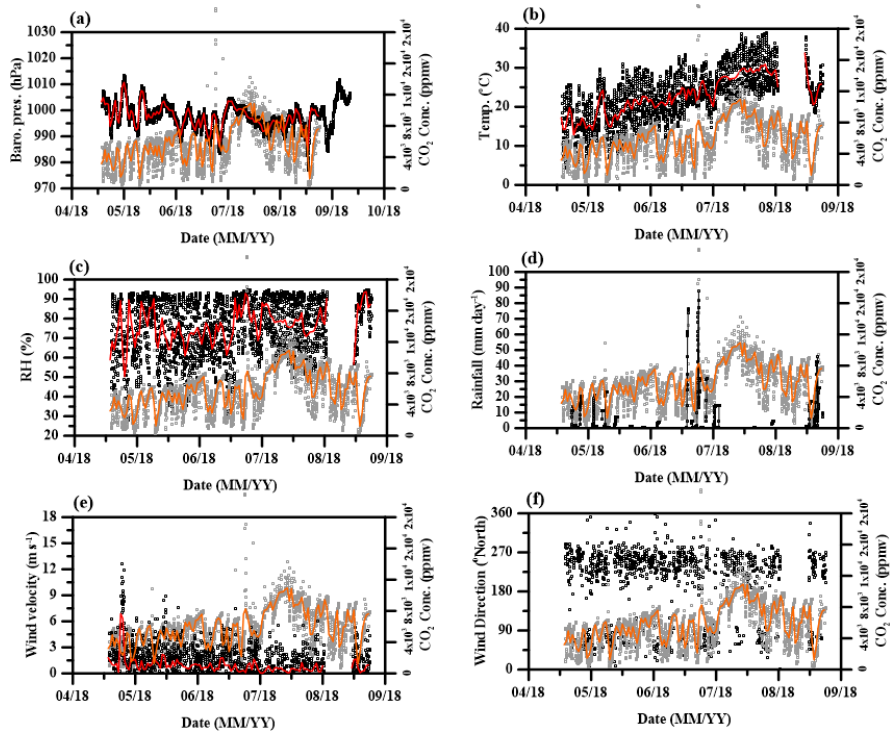


Figure 2-24 Time series of meteorological parameters from April to August 2018 for (a) Barometric pressures, (b) Atmospheric temperature, (c) Air relative humidity, (d) Rainfall, (e) Wind velocity, and (f) Wind direction. The black and gray circles represented the observed data at the weather station and CO₂ monitoring well (UMW-1-4, open-top) respectively. The red color line is the daily mean values for the black circle data. The orange color line shows the average values of obtained data from the UMW-1-4 well shown in Figure 2-17.

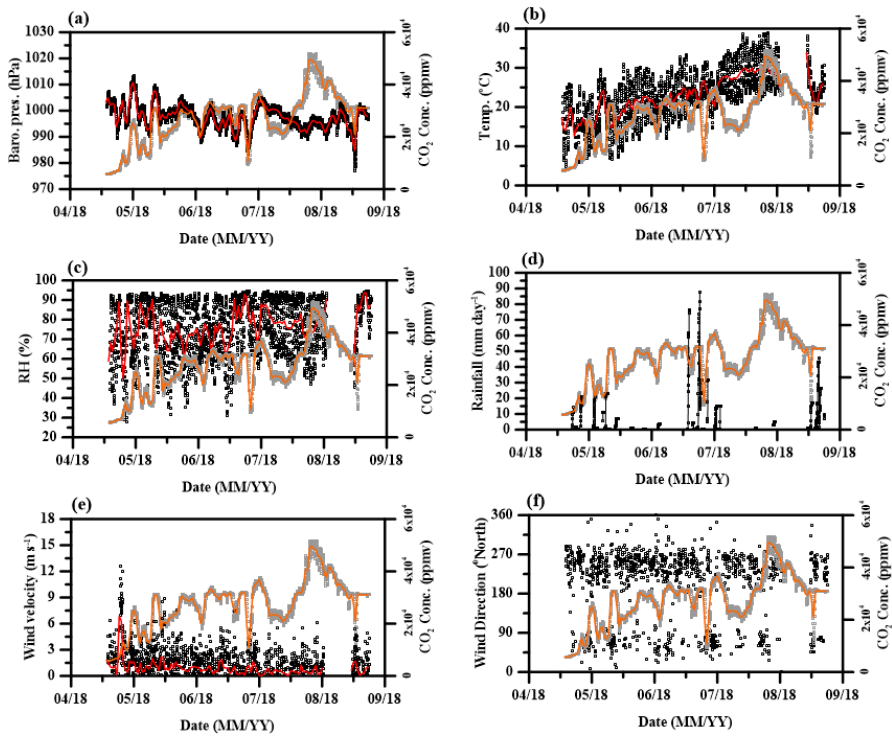


Figure 2-25 Time series of meteorological parameters from April to August 2018 for (a) Barometric pressures, (b) Atmospheric temperature, (c) Air relative humidity, (d) Rainfall, (e) Wind velocity, and (f) Wind direction. The black and gray circles represented the observed data at the weather station and CO₂ monitoring well (UMW-4-4, closed-top) respectively. The red color line is the daily mean values for the black circle data. The orange color line shows the average values of obtained data from the UMW-4-4 well shown in Figure 2-18.

2.6 Fluctuating gas concentrations

Real-time monitoring of CO₂ (g) concentration at the vadose zone well was one of the good applications to identify the signal of CO₂ leakage through the shallow aquifer and to understand the mechanism of the gas migration through the subsurface environment. However, because the naturally produced CO₂ can be one of the sources and it can be overlapped on the real leaking CO₂ (g), it should find out the clue to separate between two source what emits from different origin sources. In addition, there is a more confidential problem with the results of CO₂ (g) monitoring at the vadose zone wells. CO₂ (g) signal steadily and periodically represented a fluctuating pattern even the level of the CO₂ (g) concentration was dropping as much as the atmosphere and then increasing to over 50,000 ppm. Especially, the lowest concentration was monitored at night and the highest concentration was observed at the day. The reason why these phenomena occur is a challenging problem and some researches that find rules should be suggested to solve it when the controlled CO₂ release test is conducted at the shallow depth aquifer.

Moreover, it would be an important basic research process that must be taken into consideration when the gas sampling and analysis are applied to this test.

2.7 Conclusion

A real-time monitoring method was applied on the controlled CO₂ release test by using three kinds of well types such as SMW, UMW, and BS series. The directly measured CO₂ gas concentration had an unexpected large swing during the main and extra monitoring periods. These patterns of CO₂ gas concentration supposed to be affected by natural forces dependently. Especially, the barometric pressure was a major trigger on the natural aeration inside the vadose zone wells. Although the open- and closed-top well were compared to understand exact patterns which are not hindered by the barometric pressures, the patterns of gas concentration were always affected by barometric pressure at not only open-top wells but also closed-top wells. The results of CO₂ gas concentration patterns suggested that natural phenomena by natural force should be clarified to use the real-time

monitoring data and to understand the signals that mixed two sources including the naturally produced CO₂ and the degassed CO₂ from the CO₂ infused water.

This page intentionally left blank

CHAPTER 3 . Understanding the Natural [CO₂] (g) Variations in the Vadose Zone Well

3.1 Introduction

To reduce the increasing rate of temperature in the earth, several researchers have suggested that CO₂ gas capture and storage from the atmosphere to the geologic storage is appropriated method (Benson and Cole, 2008) and many previous studies have developed several techniques to detect and analysis the leaking problem by simulating the CO₂ leakage event artificially in the real geologic formations (Kharaka et al., 2010; Peter et al., 2012; Cahill and Jakobsen, 2013; Trautz et al., 2013; Humez et al., 2014).

However, the challenge of long-term storage in the geologic reservoir is still remained a crucial problem, and researchers always faced it after the CO₂ injection. To determine that the leaking volume is less than the proposed values (0.1% storage volume per year (Harvey et al., 2012; Song and Zhang, 2012) and to understand the CO₂ leaking signal when the gas monitoring is conducted at the near-surface area, multi-depth real-time gas monitoring is a good application because it could provide the evidence to solve the problem, quickly respond it, and prepare to reduce the impact on the subsurface and surface environment.

The time series of CO₂ gas concentration depending on the target depths and the well conditions was detected seasonally and monthly before, during, and after the injection experiments in the study site. Although the reasonable pattern due to separating two signals of CO₂ concentration produced by the natural process or from the CO₂ infused water artificially, we recognized that the barometric pressures are a major natural force on the pattern of gas concentration. Therefore, in this chapter, we would like to more focus on the daily cycle of CO₂ gas concentration data and try to understand why the

natural pattern of CO₂ gas concentration in the vadose zone wells had a large swing regularly.

◆ Some depicted figures, graphs, and tables in this chapter 3 were cited from the published article, Joun et al. (2019).

3.2 Materials and methods

3.2.1 Methods discussion

The available solutions for understanding the natural pattern of gas in the vadose zone were discussed and arranged as follows,

1. Sealing the top of wells to disconnect between the atmosphere air and the vadose zone wells.
2. Comparing the monitoring data for each depth: sequential signals would be detected according to inhale and exhale mode in the wells.

3. Deviations of Helium (He) gas concentration: The He concentration in the atmosphere is quite constant with 5,240 ppb (Glückauf and Paneth, 1946)
4. $\delta^{13}\text{C}$ -CO₂ isotope monitoring: the $\delta^{13}\text{C}$ -CO₂ isotope in the air (-7.00 ‰ to -10.00 ‰, Klusman, 1993) is relatively heavier than the $\delta^{13}\text{C}$ -CO₂ isotope in the soil (-30 ‰ to -10 ‰, Clark and Fritz, 1997).
5. The process-based analysis: this is a simple method to understand the origin of CO₂ (Romanak et al., 2014a).

We applied all the above methods on the study area except the monitoring He gas because in our knowledge, at that time, there are no instruments to directly measure the He gas concentration with high resolution in the real time scale at the field.

3.2.2 Meteorological parameters monitoring

The intensive monitoring was conducted from June to October 2017 including meteorological parameters. To record and analyze the data directly, the field laboratory was constructed near the monitoring well and the weather station as shown in Figure 2-8. All communication lines were covered by the protection plastic tube and buried in 50 cm depth from the ground surface. For monitoring air temperature, air relative humidity, wind velocity, wind direction, and precipitation, the weather station was located above the ground surface with 2 to 3 m height. To collect the barometric pressures in the atmosphere and the wells, Barologger (Model 3001, Solinst, Canada Ltd.) was installed. The recording interval was set up with 10-min for all sensors and loggers. The starting time was synchronized to record all data simultaneously.

3.2.3 CO₂ concentration in the vadose zone wells

Basically, the method for monitoring CO₂ gas concentration in the vadose zone wells is the same technique with the previous explanation in the method section of Chapter 1. But the new monitoring well, BS-09 was selected for detecting the CO₂ gas concentration depending on the depths such as 5, 8, 11, and 14 m from 20 to 24 June. In addition, to verify the concentration detected by the NDIR modules, a portable gas analyzer (GA 5000, Geotech Ltd., England) was installed at 5 m of BS-9 well. The pumping rate was 128 mL/min with attaching a 4 mm (inner diameter) polyurethane tube. The preliminary test to determine whether the airflow derived by instrument pump affected the gas concentration or not was performed before the main test. The results of the preliminary test show that under a low pumping rate (<150 mL/min), the level of gas concentration in the vadose zone well was constant. The continuous logging over a 10 min interval was performed and the pump switch is just on during the gas monitoring time. The output data represents Methane

(CH₄), Carbon dioxide (CO₂), and Oxygen (O₂) on the LED screen of the instrument and the remaining volume will be almost Nitrogen (N₂). The detailed information about GA5000 presents on the web site (<http://www.geotechuk.com>).

3.2.4 Application of process-based analysis

The process-based analysis is already presented at the methodology part of chapter 1 and shows two-line made by two chemical formulas such as biologic respiration (BR line) and methane oxidation (MO line) as shown in Figure 2-16. The previous application was that the gas monitoring was conducted at one point and one time a day. In addition, the time was not considered whether the nighttime or the daytime. In this study, instead of this application which basically was used by Romanak et al. (2014a), we performed continuous gas monitoring O₂ and CO₂ simultaneously and the temporal analysis by plotting these data for a day. The results of this

monitoring are separated with 5-hour intervals depending on a key characteristic of the gas concentrations and compositions. For instance, [CO₂] and [O₂] were increasing or decreasing together and [O₂] was increasing or decreasing when [CO₂] was constant. These separated data could be determined as following assumptions: If the measured data are plotted above the biologic respiration line with the low [CO₂] (about 300 to 400 ppm (vol. /vol.)), the gas including [CO₂] would have been sampled at a time when the well was inhaling surface air. On the contrary, if the data are plotted along or between the two lines (BR and MO lines) the gas would have been sampled at a time when the well was exhaling soil gas as shown in Figure 2-16 and 3-2.

3.2.5 $\delta^{13}\text{C}$ -CO₂ isotope monitoring

Using a Picarro G2101-i CO₂ $\delta^{13}\text{C}$ analyzer (G2101-i, Picarro Inc., Sunnyvale, CA), the carbon-isotopic composition of CO₂ gas in well BS-09 was monitored continuously. The measuring conditions included cavity

temperature and pressure of the Picarro CO₂ isotope analyzer was maintained at 45 °C and 140 torr (1 torr = 1 mmHg = 133.3224 Pa) respectively during the experiment. Measuring the carbon compositions was performed for four days from 16:00 on 22 September to 10:00 on 26 September 2017. Using a diaphragm pump at 5 L/min, gases including CO₂ gas in the well (BS-09) were pumped out of the 7.0 m depth. To connect directly between the outlet of the pump and the inlet of the Picarro CO₂ isotope analyzer, 3 mm (outer diameter) polyurethane tube was used. The amount of volume which is pumping out from the well introduced into the Picarro CO₂ isotope analyzer and other volume was controlled by using a three-way connector between the diaphragm pump and the Picarro CO₂ isotope analyzer. To avoid subsurface water vapor from being smeared into the Picarro CO₂ isotope analyzer, two impingers (100-mL vol.) were connected between the diaphragm pump and the Picarro CO₂ isotope analyzer. Carbon isotopic composition of the CO₂ gas was expressed using delta (δ) notation relative to the Vienna Pee Dee Belemnite (VPDB) scale as follows:

$$\delta^{13}\text{C} (\text{‰}) = [(\text{13C}/\text{12C})_{\text{sample}}/(\text{13C}/\text{12C})_{\text{VPDB}} - 1] \times 1000$$

Measured data were averaged over 5 min intervals and applied to evaluate variations of $\delta^{13}\text{C}$. Ultimately, the data was utilized for determining the atmospheric CO_2 contribution to total CO_2 in the borehole over time.

3.2.6 Gas flux calculation

We obtained reasonable ranges of gas flux that were 0.07 to 0.48 liters per minute (LPM) during inhale to borehole and 0.05 to 0.38 LPM during exhale to the atmosphere. These values were calculated by using a vertical profile of CO_2 gas concentrations detected at 5 and 8 m of BS-09 borehole respectively from 13 to 30 June 2017. However, those two ranges of gas flux could not explain the volumetric gas migration entirely but represented the diffusive flow of CO_2 gas mass to the borehole naturally. Besides, the time of inhale and exhale generation cannot exactly be counted by just

using the vertical profile of CO₂ gas concentration such as increasing start time, decreasing start time at each depth (5 and 8 m).

To measure the small volumetric flux of gas, an appropriate and sensitive instrument is necessary. Unfortunately, we not possessed the instrument during gas concentration monitoring. However, if the main derived force that influenced the migration of gas mass (diffusive transport) was the pressure variations, even the magnitude of gas flux was very small, the volumetric flux of gas might be calculated by following the application of analytical solution (Neeper, 2003). Also, the measured gas fluxes based on the vertical CO₂ gas profile could explain the volumetric gas fluxes through the borehole. Because Neeper (2001, 2002, and 2003) not only demonstrates a basic theory and mechanism of gas fluxes through borehole but also provides simple algorism coded by FORTRAN format, the readers who understand the theory and code can obtain the gas flux data on the basis of pressure variations in the air of atmosphere and borehole.

In this study, using the analytical solutions shows in Rossabi and Falta (2002), the volumetric gas fluxes and the subsurface pressures were

predicted. There are two kinds of code. One is for calculating the subsurface pressure derived by the atmospheric pressure and the other is for calculating the volumetric gas flux by using the differences between the atmosphere and the subsurface pressures. As stated by Rossabi and Falta (2002), to apply this analytical solution to the real-subsurface environment and to determine the characteristics of the study site, sensitivity analysis should be conducted with the varied range of values for each input parameter and then determine which values are fitted. However, because we obtain all parameters from the study site as represented in Table 3-1, we not conducted the sensitivity analysis yet. Target depth (z) was 5 m and vadose zone thickness (d) was determined as 17.77 m (mean values) by using groundwater level data (4,321 level values) and surface elevation (GPS, 92.44 m, a. s. l. (above sea level)). The soil texture data from 3 to 18 m was applied on RETC program (<https://www.pc-progress.com>) to obtain a permeability for each layer and then mean vertical and radial permeability (k_z, k_r) were calculated as $3.24E-12 \text{ m}^2$ and $4.34E-12 \text{ m}^2$ respectively by following Equations (3) and (4),

$$k_z = \sum_{i=1}^n \frac{k_i b_i}{b} \quad (3)$$

$$k_r = \frac{b}{\sum_{i=1}^n \frac{b_i}{k_i}} \quad (4)$$

where k_i is the permeability of the i th layer (m^2) and b_i is the thickness of the i th layer (m). It is assumed that each layer is homogeneous and the permeability is equivalent vertically and horizontally.

Rossabi and Falta (2002) used the method of images to account for the water table boundary to calculate the subsurface pressures and proposed the good agreement image well numbers was eleven for deriving suitable results. A single-image well can be represented as follows:

$$(P_z - P_{\text{mean}})_a = (P_{\text{atm}} - P_{\text{mean}})_0 \left[\text{erfc} \left(\frac{z}{2\sqrt{\epsilon_m t}} \right) + \text{erfc} \left(\frac{2d-z}{2\sqrt{\epsilon_m t}} \right) \right] +$$

$$\sum_{i=1}^a ((P_{\text{atm}} - P_{\text{mean}})_i) - ((P_{\text{atm}} -$$

$$P_{\text{mean}})_{i-1})) \left\{ \operatorname{erfc} \left[\frac{z}{2\sqrt{\varepsilon_m(t-t_i)}} \right] + \operatorname{erfc} \left[\frac{2d-z}{2\sqrt{\varepsilon_m(t-t_i)}} \right] \right\}, \quad t_a < t < t_{a+1} \quad (1)$$

for where P_z , P_{atm} , and P_{mean} are the pressure of subsurface at z m depth, the atmosphere, and the annual mean value, respectively. z is the target depth to predict the pressures each time, d is the distance between the ground surface and the water table, $\varepsilon_m = \frac{k_z P_{\text{mean}}}{\theta S_g \mu_g}$, k_z is the vertical permeability, θ is the porosity, S_g is the gas saturation, μ_g is the gas viscosity, t is the time, and the subscripts a, i , and 0 (initial) are the time steps.

The code for gas flux through a well incorporated thickness of the vadose zone, permeability, viscosity, pressures, borehole radius, moisture content, average pressure, and porosity as follows:

$$\begin{aligned}
Q_n(t) = 2\pi b \frac{k_r}{\mu_g} & \left[(P_{\text{atm}} - P_z)_0 \left(\frac{2}{\ln(2.25\alpha t)} \right) \right. \\
& + \sum_{i=1}^b ((P_{\text{atm}} - P_z)_i \\
& \left. - (P_{\text{atm}} - P_z)_{i-1}) \left(\frac{2}{\ln(2.25\alpha(t - t_i))} \right) \right], \\
t_b < t < t_{b+1} & \quad (2)
\end{aligned}$$

where $\alpha = \frac{k_r P_{\text{mean}}}{\theta S_g \mu_g r_w^2}$, k_r is the radial permeability, and r_w is the well radius.

Table 3-1 Input parameters for the analytical solution.

Input parameters	Values
Target depth (z)	5 m
Vadose zone thickness (d)	17.77 m
Vertical / radial permeability (k_z, k_r)	3.24E-12 / 4.34E-12 m ²
Viscosity (μ_g)	1.83E-5 kg/m sec
Porosity (θ)	0.37
Gas saturation (S_g)	0.33
Average pressure (P_{mean})	99,701 Pa
Borehole radius (r_w)	2.54E-2 m
Surface pressure (P_{atm})	text file*

*Monitoring data (4,321 data with 10 min interval).

3.3 Results and discussions

3.3.1 The large swing patterns in CO₂(g) monitoring data

Figure 3-1 represents the results of CO₂ gas concentration and the relation between the pattern of CO₂ gas concentration and each meteorological parameter which is the potentially influential factor. This figure includes wind speed (m/sec), temperature (°C), humidity (%), actual atmospheric pressure (Pa), calculated subsurface pressure (Pa), calculated volumetric flux (LPM), pressure differences (Pa) between barometric pressure and subsurface pressure, CO₂ gas concentration for each depth by measuring NDIR (ppm, vol. /vol.), and GA5000 (%), and N₂ ratio (-) in the monitoring well (BS-09).

We could assume that the ex- or in-hale, so called the air circulation, would be produced through boreholes. The profile of CO₂ concentration represented a gradual decreasing or increasing from one to another. When the decreasing trend was shown in the profiles, the dropping sequence was 5, 8, 11, and 14 m and the reverse sequence was observed when the CO₂ concentration was

increasing. The CO₂ concentration was measured with two different instruments. One was NDIR sensors and the other was portable GC (GA 5000). Two results detected at the same position (5 m) show similar patterns and the almost same magnitude of CO₂ concentration ($R^2 = 0.99$) was detected at the same time. The surface wind has been used for understanding the ventilation of gas in the fractures because the wind could generate the air circulation in a subsurface environment (Lewicki et al., 2003; Nachshon et al., 2012; Sánchez-Cañete et al., 2016). However, in our study, the wind was not the factor, which made a turbulence flow or the fresh air intrusion in boreholes because the study depth was deeper than the previous studies. Risk et al. (2002) stated that a soil temperature that is the main affectation to product CO₂ gases could elucidate CO₂ profiles in a few centimeter topsoil zone (0 to 100 cm). However, the temperature response could not explain all reasons why those unsteady patterns were continuously monitored because of the deep soil zone a.k.a. target depths (5 to 14 m) have isothermal conditions (14 to 15 °C) comprised of topsoil area. The calculated volumetric flux could suggest the clue of air circulation in the borehole. However, because those small magnitudes of flux will make a slow mass transport (diffusive flow),

the rapid fluctuating CO₂ profile (advective flow) could not occur if the pressures was the main factor about the air circulation in boreholes.

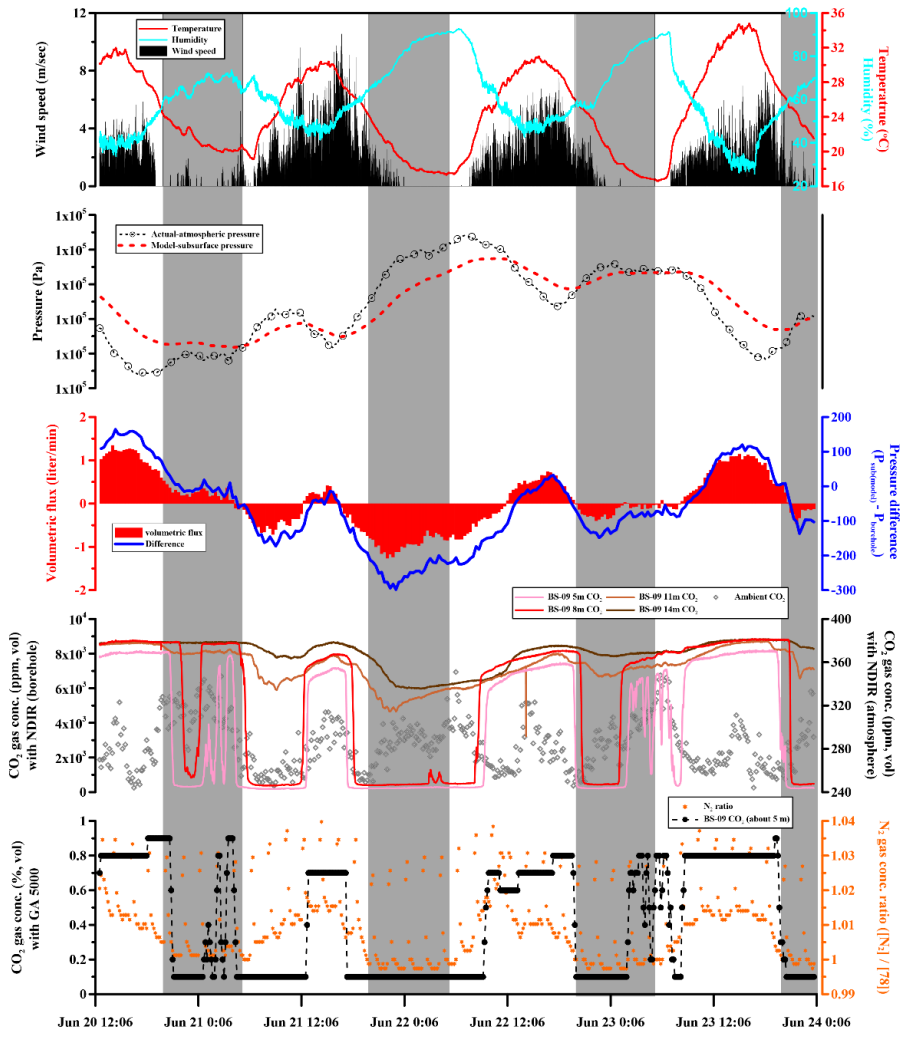


Figure 3-1 The monitoring data for four days from 20 to 24 June 2017.

3.3.2 Evidences of natural purging phenomena

The natural variation including pressures, temperatures, and wind can cause the flow to or out the boreholes. However, not always those forces have been used for demonstrating the unsteady natural patterns of gas concentration in boreholes. In this study, profiling the CO₂ concentration in boreholes provided the rule of sequences depending on increasing or decreasing gas concentration. The dropping sequences suggested that the fresh air was coming into boreholes. Besides, the rising sequences mean that the high-level CO₂ gas was inducing and storing from the bottom (Water table) to the top of the borehole. Following those profiles, we assume that the CO₂ gas purging and compiling without the responses of pressures, wind, or temperature could emerge. Plotting the ratio of Nitrogen between the air in the borehole and in the atmosphere (78 %) also represented that the fresh air was coming into the boreholes and the CO₂ concentrations were changed rapidly because of the low CO₂ concentration (350 ~ 400 ppm) in the air of the atmosphere. The more ratios were closed to one, the more occupied the

volume of fresh air is in the borehole. The process-based analysis introduced by Romanak et al. (2014a) was applied to the continuous monitoring for investigating the natural purging phenomena. Following the line derived from chemical formulas such as biological respiration ($\text{CH}_2\text{O} + \text{O}_2 \rightarrow \text{CO}_2 + \text{H}_2\text{O}$) and methane oxidation ($\text{CH}_4 + 2\text{O}_2 \rightarrow \text{CO}_2 + 2\text{H}_2\text{O}$), the origins of CO_2 gas could be identified in real-time as shown in Figure 3-2. 24hr data was divided by a 5hr period from the beginning. Each period displayed the different colors and the black allows mean the time sequences. The results of the continuous process based analysis represented the time when the natural purging was generated in boreholes. During the daytime (08:00 to 18:00), the origin of CO_2 was from methane oxidation or mixed with biological respiration thus the observed data was plotted along with the BR or MO line. In contrast, at the nighttime (18:00 to 08:00), because the exogenous air infiltrated the inside of the boreholes, the position of data was outside the BR line and the concentration value was low. To reconfirm the natural purging phenomena, we performed an additional investigation about $\delta^{13}\text{C}-\text{CO}_2$ isotopic signal by using Picarro instrument as shown Figure 3-3. As stated in Garcia-Anton et al. (2014), the negative relationship was presented between

CO₂ gas concentration and $\delta^{13}\text{C-CO}_2$ isotopic signal. Because the $\delta^{13}\text{C-CO}_2$ isotope in the atmosphere (-8 ‰) is heavier than the $\delta^{13}\text{C-CO}_2$ produced by biological respiration (-25 ‰) or methane oxidation, two kinds of continuous signals provided the unimpeachable evidence about the natural purging phenomena.

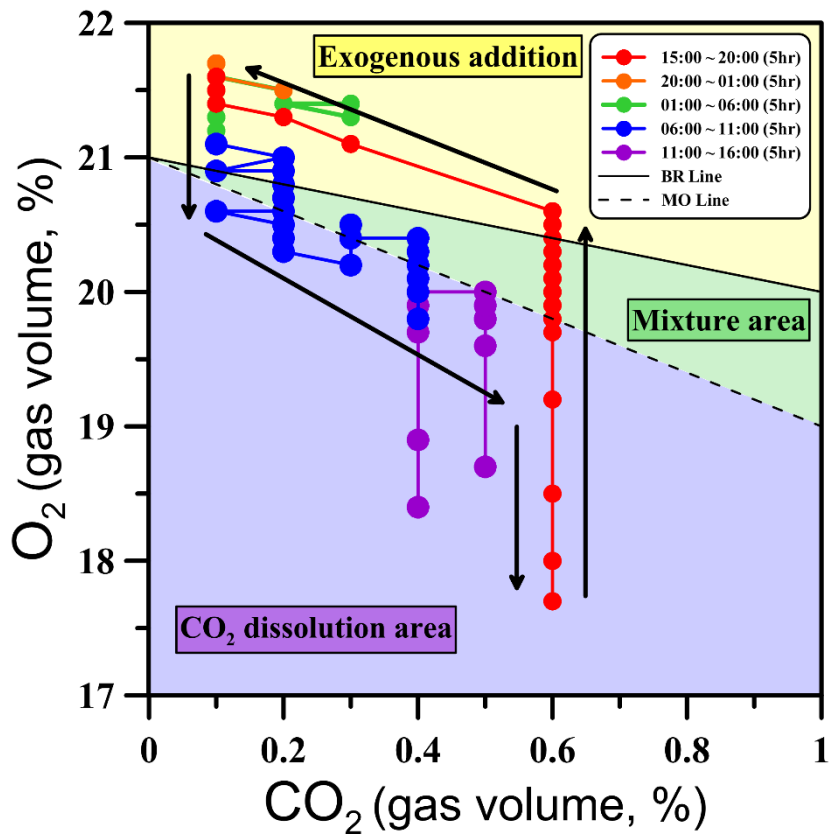


Figure 3-2 The process-based analysis was applied on real-time gas monitoring at the well for a day using 5 hr intervals.

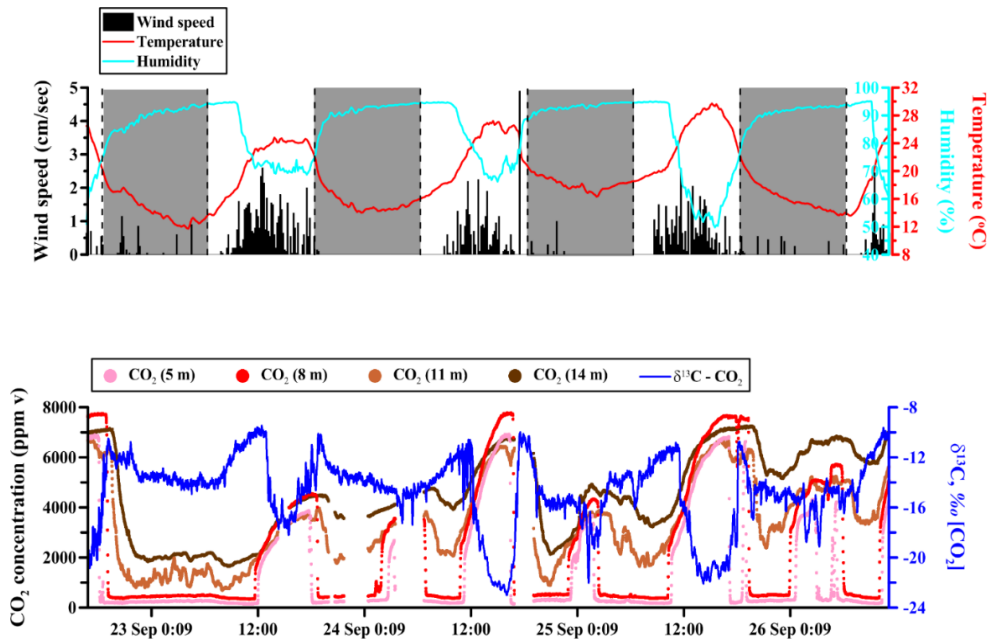


Figure 3-3 Results of $\delta^{13}\text{C}-\text{CO}_2$ isotopic and CO_2 gas concentration in the well from 23 to 26 September 2017.

3.3.3 Remark about real-time monitoring

To install the real-time monitoring system at the subsurface environment, the researchers should handle several problems included excessive moisture content in the soil layers, unknown range of CO₂ gas concentration in the subsurface environment of the study area, and monitoring interval and recording time providing the reasonable data. To protect the sensors from the water vapor, the NDIR module was covered by a water-proof solution (silicone modified conformal coating) and especially hand-made case (SOHA Tech). These arrangements give a long duration for NDIR modules. For the first time, we didn't recognize the CO₂ concentration at the subsurface environment of study site. Thus, we used the low-level range (0 to 3000 ppm (vol. /vol.)) of the NDIR module in the preliminary test and the results of monitoring represented the flat plot with the maximum level of that NDIR module. To gain accurate and constant data, a researcher should know the maximum and the minimum level of gas concentration at the target soil layer. The monitoring interval is also important to operate the real-time monitoring

because the time has to cover the patterns that are the key characteristics to understand the purpose of research.

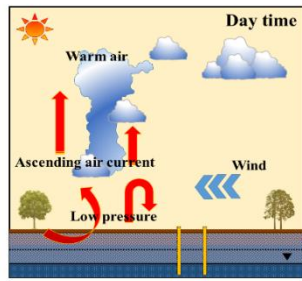
Romanak et al. (2014b) stated that a continuous smart data collection (time-sequential) is required to apply a process-based analysis on an industrial scale. However, the commercially-available sensors, especially the O₂ sensor, need to be improved for reducing the error of measurement if it is conducted for a long time (this comment received from Katherine Romanak when attended at the GHGT-14, Australia). At the same time, a generalized filtering technology should be developed to be used for any commercial sensors.

3.4 Conclusion

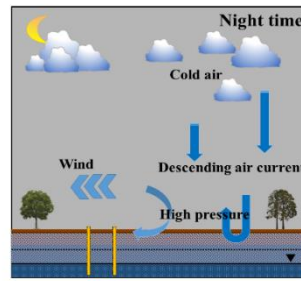
Gas circulation in the open borehole could be a critical problem if gas sampling and analysis were conducted to investigate the research area without the consideration of natural purging phenomena. The results proposed that although there is no strong relationship between gas concentration and

pressure, temperature, or wind, the dramatically changed pattern of gas concentration in borehole could emerge. This study cannot determine the main factor being able to explain the natural purging phenomena but evidence suggested that the quick swing pattern of gas concentration in borehole was caused by the air intrusion from the atmosphere. This evidence included: (1) $[CO_2]$ was decreasing from shallow to deep depth (5 to 14 m) and $[CO_2]$ was increasing from deep to shallow depth (14 to 5 m); (2) N_2 ratio approaches one because of atmospheric air intrusion; (3) the results of the process-based analysis indicated that an exogenous air with low $[CO_2]$ occupied the partial volume in a borehole; (4) the negative relation between $\delta^{13}C-CO_2$ and $[CO_2]$ was presented and the isotope value was changed according to the dominant sources such as atmosphere, biological production, etc. The study confirms that a continuous and vertical $[CO_2]$ profiling can be used to concretely assess the results of gas concentration affected by physical parameters directly and the air circulation in borehole could occur without pressures or wind by the dense air intrusion into the well. In addition, the researcher who has a problem with the unexpected signal of gas concentration may accomplish the answer

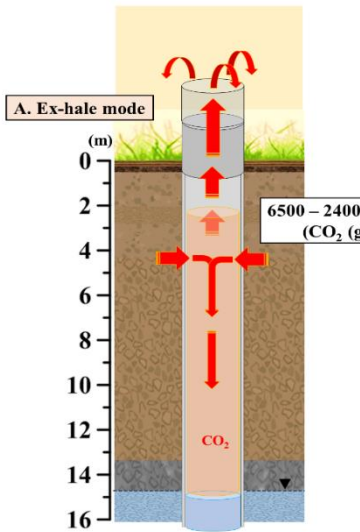
by applying a potential existence of the natural purging phenomena as shown in Figure 3-4.



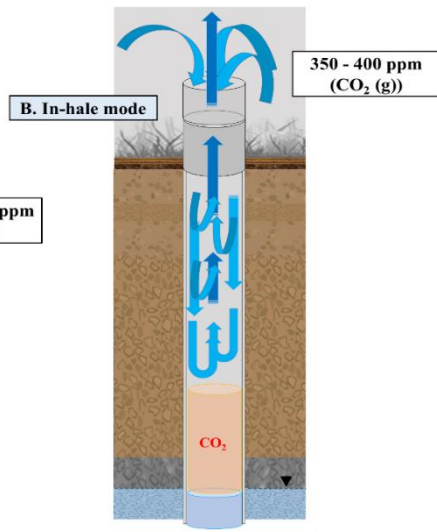
Atmospheric pressure is **low**



Atmospheric pressure is **high**



High concentration CO₂ gas is smeared in wells continuously



High concentration CO₂ gas is flushed out

Figure 3-4 A conceptual diagram about the natural inhalation and exhalation through a well in a day.

CHAPTER 4. Reproducing the Naturally Fluctuating [CO₂] (g) in the Vadose Zone Well

4.1 Introduction

The natural aeration along with a macro- or a micro-scale network in the subsurface environment have been considered reasonably in several study sites such as the landfill site that could emit the methane gas, the vadose zone contaminated by DNAPLs (Dense Non-Aqueous Phase Liquids), the natural ventilation in the cave, and the carbon storage site that has the potential risk by escaping the sequestered CO₂ (Christophersen and Kjeldsen, 2001; Kuang et al., 2013; Joun et al., 2016; Pla et al., 2016). However, the researches for

understanding the pattern of gas concentration which is affected by natural forces such as the atmospheric pressures, precipitation, temperature, and wind speed are still necessary. Kuang et al. (2013) stated that numerous studies have been performed to understand the natural force of atmospheric pressure on the gas transportation but more investigation is necessary because the natural mechanism of gas migration from the crack, the fracture, and the open well to the atmosphere has not been fully solved yet (Joun et al., 2019).

To understand the natural phenomenon of air exchange in shallow or deep soil zone through open wells, the analytical solutions have been proposed by several researchers (Rossabi and Falta, 2002; Neeper, 2003). Rossabi and Falta (2002) suggested the first analytical solution for the natural aeration derived by ASTM fluctuating surface pressures with an open well. Neeper (2003) calculated the airflow in open wells by applying the harmonic analysis on atmospheric pressure changes. The latest investigation by You et al. (2011) introduced the semi-analytical solution for calculating a gas flow rate through an open well and the decomposition method, which composed of two steps. First, deduction of subsurface pressure without an open well; second,

calculating horizontal airflow to and from an open well by using the subsurface pressures data obtained from the first step (You et al., 2011). Most studies for predicting subsurface pressure by using analytical solutions have assumed that the water table is to be fixed (Farrell et al., 1966; Nilson et al., 1991; Rojstaczer and Tunks 1995; Rossabi and Falta, 2002; You et al., 2011). However, Abbas (2011) stated that a fluctuating water table boundary condition rather than a static boundary has a notable effect on the subsurface pressure responded by the differences from the atmospheric pressures. Although these solutions could explain trends of increasing or decreasing the gas concentration patterns indirectly, it is hard to expect to predict the real-pattern of gas concentrations affected by atmospheric pressure fluctuations and gas mass transport into and out of open wells.

In this study, based on the introduced skill in Joun et al. (2016), we would like to introduce the feasible solution to reproduce the natural pattern of the gas concentrations in the open well and then utilize it to investigate the future studies such as identifying the real leaking signal pattern from the CO₂ sequestered reservoir, calculating the depth of the aeration zone depending

on the atmospheric pressure, and introducing the criterion of major gas flow mechanism in the vadose zone well such as the diffusion, the advection, and mixed both mechanisms.

◆ Some depicted figures, graphs, and tables in chapter 4 were cited from the published article, Joun and Lee (2020).

4.2 Materials and methods

4.2.1 Data collection from the study site

The monitoring data from Dec 05, 2016, to Jan 09, 2017 (35 days) was applied to this study. The result of monitoring is represented in Figure 4-1. Although the first pilot test (pulse type) in the saturated zone EIT facility was conducted on 29 Nov 2016, the results of CO₂ gas monitoring at the near-surface zone represented that the natural pattern of CO₂ gas concentration was not affected by injecting the CO₂ saturated water into groundwater (injection

well had a screened interval from 22 to 27 m, bgs) because the injected CO₂ mass was small (13.9 kg) for developing the reachable aqueous plume in a short time to arrive monitoring well and the CO₂ degassing rates were not enough to make the vertical gas fluxes. In addition, because the remarkable change of HCO₃⁻ concentration commenced after 24 Jan 2017, using the collected CO₂ (g) data could be possible to investigate the natural variation of gas concentration in vadose zone wells. A meteorological tower (Vantage Pro2™ 6152C, Davis Instruments, Hayward, CA, USA) was built on the ground surface of study site due to monitoring standard parameters such as temperature, wind, humidity, etc.. The variations of barometric pressure and groundwater level were measured by using Barologgers and Levellogger (Model 3001, Solinst, Canada Ltd.) respectively. All the aboveground parameters were observed with the 10-minute interval and stored automatically.

To obtain CO₂ gas concentration data without volume evacuation at the target depths (5 m), the real-time monitoring system using NDIR sensors (250NDS, SOHA Tech Co., Ltd., Korea) was applied on the vadose zone

section of an open well. Not all monitoring wells were fully customizable for conducting the gas sampling needs at the vadose zone because these wells were opened and connected with the atmosphere. If the purpose of the artificial injection test in this field is only for gas transport in the vadose zone, we should seal the top of monitoring wells to avoid the interferences of natural forces such as wind, pressures, rainfall, and temperature. However, we have utilized these monitoring wells not only for gas monitoring but for groundwater monitoring thus, the wells were supposed to staying open-top conditions. Generally, the gas sampling would be conducted by extracting the soil air from an unsaturated porous media to move and analysis them at the laboratory. However, in this study, to avoid the pressure dropping effect on the gas concentrations by extracting the soil air from the porous media and to obtain the real-time data of CO₂ concentration directly, NDIR sensors were installed in the vadose zone wells. The sensors measured CO₂ concentration every 60 seconds and store 10-minute averages. The sensors have $\pm 3\%$ accuracy around the measurement values and a precision of 60 ppm.

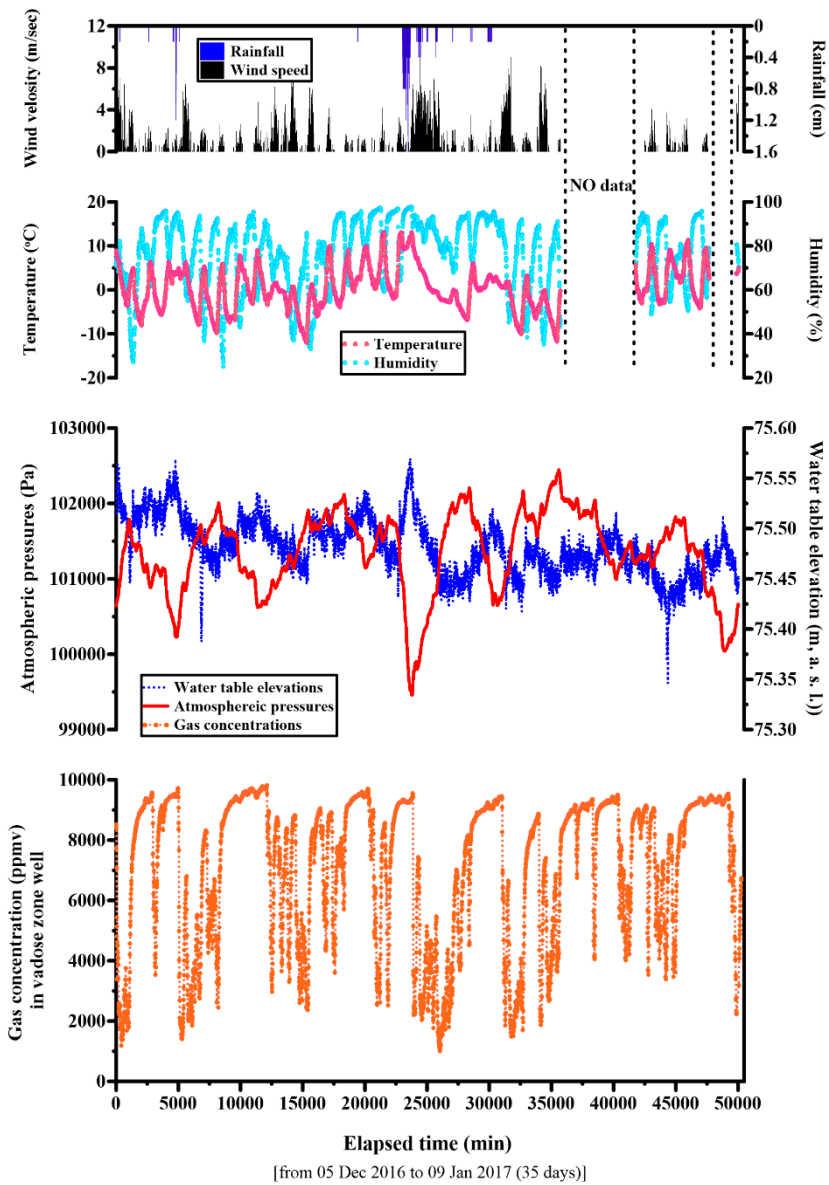


Figure 4-1 The collected monitoring data from Dec 05, 2016 to Jun 09, 2017 (35 days).

4.2.2 Core sampling and standard penetration test (SPT)

This test is a universal method for investigating the subsurface soil sample at the testbed. The rode (OD 5.1 cm, ID 3.5 cm, and length 81 cm) attached a split spoon sampler is inserted into the borehole and the hammer of 63.7 kg is dropping with 75 cm height. In that time, the number of strikes (N values) is counted for the rode is being penetrated into the borehole by 30 cm. In the case of sandy soil, the shear strength or compressibility of sand can be determined from the N values, and using these N values, a bearing power can be estimated.

Twenty specimens were obtained from the study site by performing the standard penetration test (SPT, ASTM D 1586-11 (2011)) for each layer (1.5 m thickness) from 0 to 30 m (bgs) as represented in Figure 4-2. Figure 4-3 and Figure 4-4 show one of the results from this test (SPT).

The view of boring apparatus



Standard penetration test



Soil samples



S. P. T. samples



Figure 4-2 Standard penetration test (SPT) was conducted at the study site.

시 추 주 상 도 DRILL LOG

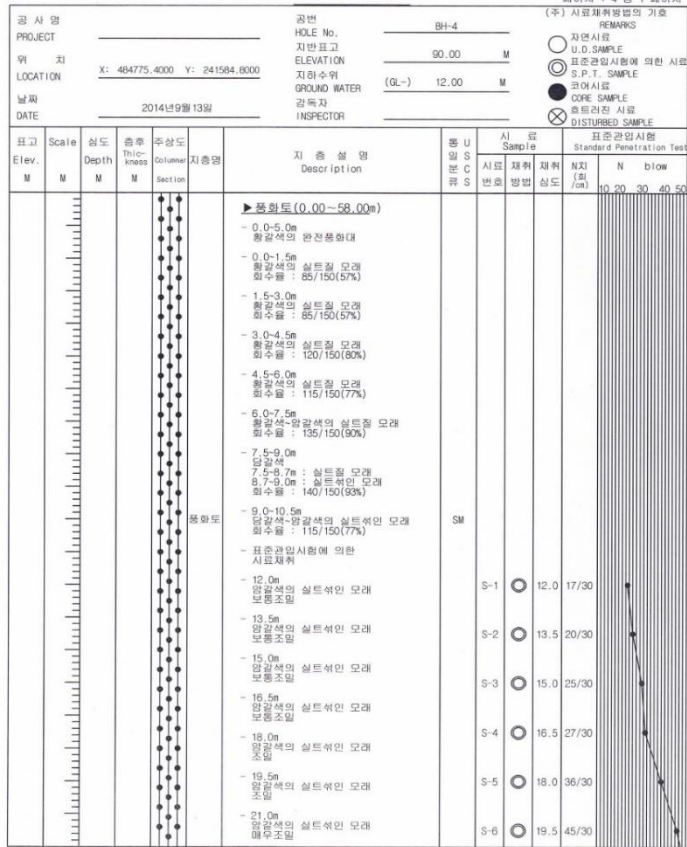


Figure 4-3 Drill log in BH-4 which is the nearest rock formation well with the gas monitoring wells (BS, SMW, and UMW series) and the results of SPT from 12 to 19.5 m.

시 추 주 상 도 DRILL LOG

공 사 명 PROJECT		공 번 HOLE No.		표 이 치 : 4 중 2 배 이 치 (주) 시료 채취 방법의 기호										
위 치 LOCATION		지 반 표 고 ELEVATION		REMARKS										
날 짜 DATE		지 아 수 위 GROUND WATER		<input type="checkbox"/> 자연 시료 <input type="checkbox"/> U.D. SAMPLE <input type="checkbox"/> 표준 관입 시험에 의한 시료 <input type="checkbox"/> S.P.T. SAMPLE <input type="checkbox"/> 코어 시료 <input type="checkbox"/> CORE SAMPLE <input type="checkbox"/> 흐트러진 시료 <input type="checkbox"/> DISTURBED SAMPLE										
X: 484775.4000 Y: 241584.8000		90.00 M												
2014년 9월 13일		(GL-) 12.00 M												
		감 독 자 INSPECTOR												
표 고 Elev. M	Scale M	심 도 Depth M	중 추 Thick- ness Columnar	주 상 도 Columnar Section	지 층 설 명 Description	종 류 U S C S	시 료 Sample		표 준 관 입 시 험 Standard Penetration Test					
							시 료 번호	채 취 방 법	채 취 심 도 (cm)	N (blow /cm)	N blow			
									10	20	30	40	50	
					원갈색의 실트석인 모래		S-7	○	21.0	50/28				
					- 24.0m 원갈색의 실트석인 모래 매우 조밀									
					- 25.5m 원갈색의 실트석인 모래 매우 조밀		S-8	○	22.5	50/20				
					- 27.0m 원갈색의 실트석인 모래 매우 조밀		S-9	○	24.0	50/17				
					- 28.5m 원갈색의 실트석인 모래 매우 조밀		S-10	○	25.5	50/12				
					- 30.0m 원갈색의 실트석인 모래 매우 조밀		S-11	○	27.0	50/8				
					- 31.5m 원갈색의 실트석인 모래 매우 조밀		S-12	○	28.5	50/7				
					- 33.0m 원갈색의 실트석인 모래 매우 조밀		S-13	○	30.0	50/7				
					- 34.5m 원갈색의 실트석인 모래 매우 조밀	SM								
					- 36.0m 원갈색의 실트석인 모래 매우 조밀		S-14	○	31.5	50/6				
					- 37.5m 원갈색의 실트석인 모래 매우 조밀		S-15	○	33.0	50/5				
					- 39.0m 원갈색의 실트석인 모래 매우 조밀		S-16	○	34.5	50/6				
					- 40.5m 원갈색의 실트석인 모래 매우 조밀		S-17	○	36.0	50/5				
					- 42.0~43.0m 원갈색의 실트석인 모래 함수율 : 80/100(80%)		S-18	○	37.5	50/5				
					- 43.0~46.0m 원갈색의 실트석인 모래 함수율 : 300/300(100%)		S-19	○	39.0	50/6				
					- 46.0~49.0m 원갈색의 실트석인 모래									
					- 22.5m									

Figure 4-4 Drill log in BH-4 and the results of SPT from 19.5 to 39 m.

4.2.3 Soil sample analysis for deriving the input values of the numerical model

Bring the core samples to an indoor laboratory, soil texture analysis was performed. The procedure of the laboratory experiment was following USDA NRCS soil survey laboratory methods manual (2004). The results of soil texture compositions are represented in Table 4-1. The results on soil texture analysis provide the information of soil compositions including silt, clay, and sand. Based on the soil composition data, categories were determined as loamy sand and sandy soil for each layer (Fetter, 2018). Investigated layers can separate only two types of soil categories. However, we used each layer property, although these were almost similar values, to reproduce the real pattern of observed gas concentrations in the study site. Using this Table, the significant values that determine the gas transport in the porous media were derived by using the coupled two models (van Genuchten and Mualem) in the RETC program (van Genuchten et al., 1991). The model results are represented in Table 4-2. Based on Table 4-2, the numerical model domain could make more being close to a real vadose zone condition and would

provide reasonable results of gas concentration when fluctuating atmospheric pressure or water table level will be applied on boundaries of the model domain.

Table 4-1 The soil composition and texture for each layer.

Labels on each layers	Depth (m, bgs)	Clay (%)*	Silt (%)*	Sand (%)*	Texture
L20	0~1.5	0.261	19.460	80.315	loamy sand
L19	1.5~3.0	0.167	18.960	80.890	loamy sand
L18	3.0~4.5	0.199	21.210	78.553	loamy sand
L17	4.5~6.0	0.172	14.630	85.210	sandy soil
L16	6.0~7.5	0.187	14.520	85.280	sandy soil
L15	7.5~9.0	0.243	12.650	87.111	sandy soil
L14	9.0~10.5	0.157	10.700	89.100	sandy soil
L13	10.5~12.0	0.146	12.530	87.340	sandy soil
L12	12.0~13.5	0.066	8.386	91.520	sandy soil
L11	13.5~15.0	0.067	8.417	91.530	sandy soil
L10	15.0~16.5	0.059	6.709	93.210	sandy soil
L9	16.5~18.0	0.029	4.897	95.080	sandy soil
L8	18.0~19.5	0.094	7.451	92.480	sandy soil
L7	19.5~21.0	0.075	6.665	93.210	sandy soil
L6	21.0~22.5	0.061	6.716	93.200	sandy soil
L5	22.5~24.0	0.079	6.215	93.720	sandy soil
L4	24.0~25.5	0.056	4.875	95.080	sandy soil
L3	25.5~27.0	0.050	5.562	94.400	sandy soil
L2	27.0~28.5	0.037	5.202	94.740	sandy soil
L1	28.5~30.0	0.026	5.624	94.320	sandy soil

*All data is mean value from routine laboratory experiments (over 3 times) following USDA NRCS soil survey laboratory methods manual (2004).

Table 4-2 The values of van Genuchten parameters for each layer.

Labels on each layer	θ_r	θ_s	α	n	K_s
L20	0.0306	0.3984	0.0507	1.7898	130.57
L19	0.0309	0.3981	0.0507	1.8257	136.57
L18	0.0291	0.4000	0.0512	1.7019	118.50
L17	0.0351	0.3938	0.0475	2.1655	201.22
L16	0.0353	0.3937	0.0473	2.1728	202.80
L15	0.0374	0.3917	0.0454	2.3663	251.70
L14	0.0396	0.3898	0.0435	2.6209	330.86
L13	0.0375	0.3918	0.0454	2.3960	260.09
L12	0.0423	0.3875	0.0412	2.9741	469.79
L11	0.0422	0.3876	0.0413	2.9730	469.29
L10	0.0442	0.3856	0.0397	3.2427	599.05
L9	0.0462	0.3836	0.0381	3.5553	775.00
L8	0.0434	0.3865	0.0403	3.1197	537.77
L7	0.0443	0.3855	0.0396	3.2436	599.93
L6	0.0442	0.3856	0.0397	3.2410	598.22
L5	0.0448	0.3851	0.0392	3.3230	642.05
L4	0.0462	0.3835	0.0381	3.5531	774.48
L3	0.0455	0.3843	0.0387	3.4384	706.02
L2	0.0459	0.3839	0.0384	3.4989	741.32
L1	0.0454	0.3844	0.0387	3.4294	700.39

The values shown in Table 4-1 were put on van Genuchten model in RETC program (van Genuchten et al., 1991) to derive the van Genuchten parameters. Where, θ_r is the residual water content ($L^3 \cdot L^{-3}$, $cm^3 \cdot cm^{-3}$); θ_s is the saturated water content ($L^3 \cdot L^{-3}$, $cm^3 \cdot cm^{-3}$); α is the inverse of the air entry suction (L^{-1} , cm^{-1}); n is the pore-size distribution (-); and K_s is the saturated conductivity ($L \cdot T^{-1}$, $cm \cdot day^{-1}$).

4.2.4 Numerical simulation (STOMP model)

The Subsurface Transport Over Multiple Phases (STOMP) model is a feasible tool to simulate the multi-phase mass flow and transport in the vadose zone (Ostrom et al., 2005; Gee et al., 2007; Yabusaki et al., 2008; Joun et al., 2016). STOMP-WOA (Water-Oil-Air) mode was applied to this study because of two reasons. First, this mode solves the three kinds of mass coupled equations (etc. air, water, and volatile component) and provides the useful boundary condition option named “fluctuating Water Table” by using the monitored pressures time-dependently at the study site (White and Ostrom, 2000). Second, because the migration of CO₂ gas through the unsaturated porous media is similar with the transport of vapor (VOCs) in the vadose zone (Zhang et al., 2004), if not requiring exact concentrations of CO₂ gas essentially, it is enough to reflect the unsteady natural pressure variations on the patterns of gas concentrations in open wells and to utilize explaining the [CO₂] signal which is mixed several sources by simulating leaking scenario numerically.

The model domain has a cylindrical composition with two vertical sections, which are unsaturated and saturated porous media with a radius of 28 m and at an angle of 60 degrees (meaningless value). 20 layers are piled up and each layer has 1.5 m thickness (Total 30 m) as shown in Figure 4-5. Using Table 4-2, input values for saturation function and physical properties were decided and van Genuchten saturation function was coupled with Mualem relative permeability model. The domain grids consist of 50 for horizontal direction and 60 for the vertical direction. The grids at the left-hand side of the domain are denser (0.025 m) due to applying two inches well (2.54 cm diameter and 30 m long pipe) on the west boundary and the length of grid cells is increased gradually as shown in Figure 4-5. The diffusive porosity is also represented in Figure 4-6. The initial source plume exists near the ground surface (3 to 5 m bgs) and the well is located at the left side of the model domain as shown in Figure 4-7. Because the distribution of CO₂ (g) exists everywhere of the soil environment if the condition of the soil has the appropriate humidity and temperature for the respiration (Clark and Fritz, 1997), the initial source setting as shown in Figure 4-7 is a reasonable assumption of a source which CO₂ (g) can be migrated from soil to the monitoring well. The chemical and

physical properties of the substitute source (TCE vapor) are not same with CO₂ gas (Table 4-3), but those have some similarity to fate and transport through the porous media because those (VOCs, 1.21 ~ 2.50 kg/m³; CO₂, 1.81 kg/m³) is heavier than the air (1.17 kg/m³). Thus, both of them flow downward direction at the vadose zone generally and it is called the density-driven transportation (Falta et al., 1989; Zhang et al., 2004).

The initial elevation of the water table poses about 13 m (bgs) and the initial gas pressure is 100,993.67 Pa. Those values are from the first recorded values of observed data files in this study site using the submersible Levellogger and the Barologger respectively. Based on this foundation set, the different boundary conditions were used for each case. In case 1, the variation of atmospheric pressure applied on the top of the model domain and the groundwater level was fixed; in case 2, the atmospheric pressure stayed in an initial condition and fluctuating water table condition was applied on the bottom and right boundary of the domain; and in case 3, both of case was simultaneously applied on top, bottom, and right boundaries of domain respectively.

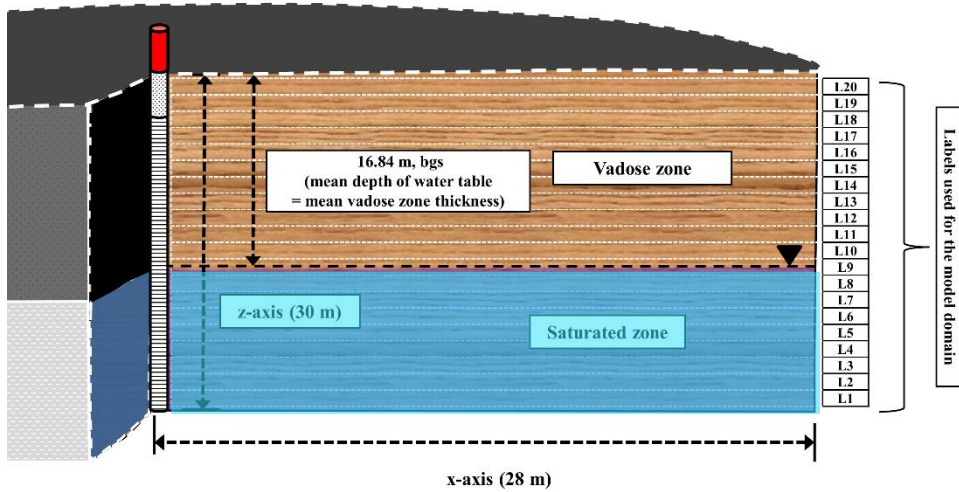


Figure 4-5 The conceptual diagram for the numerical model domain (cylindrical).

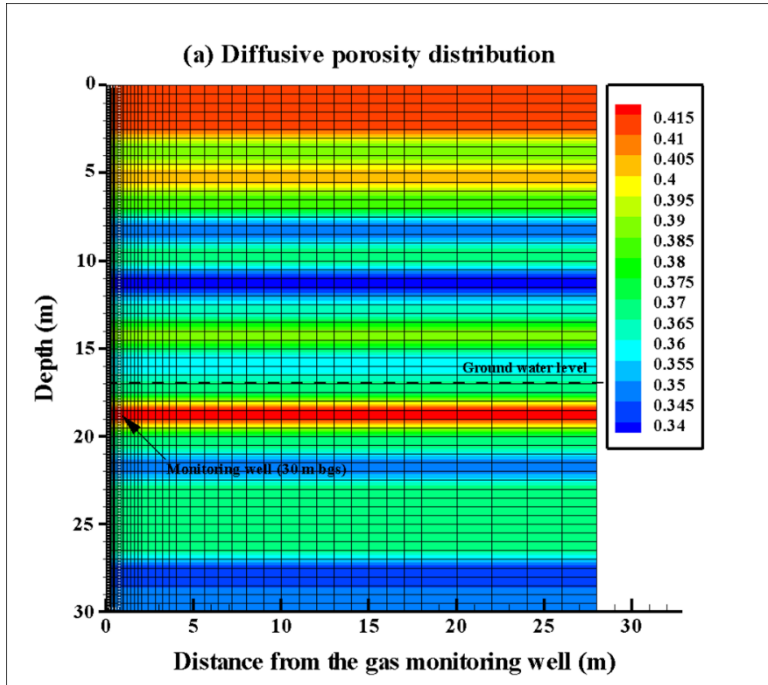


Figure 4-6 The space discretization and the diffusive porosity of the model domain.

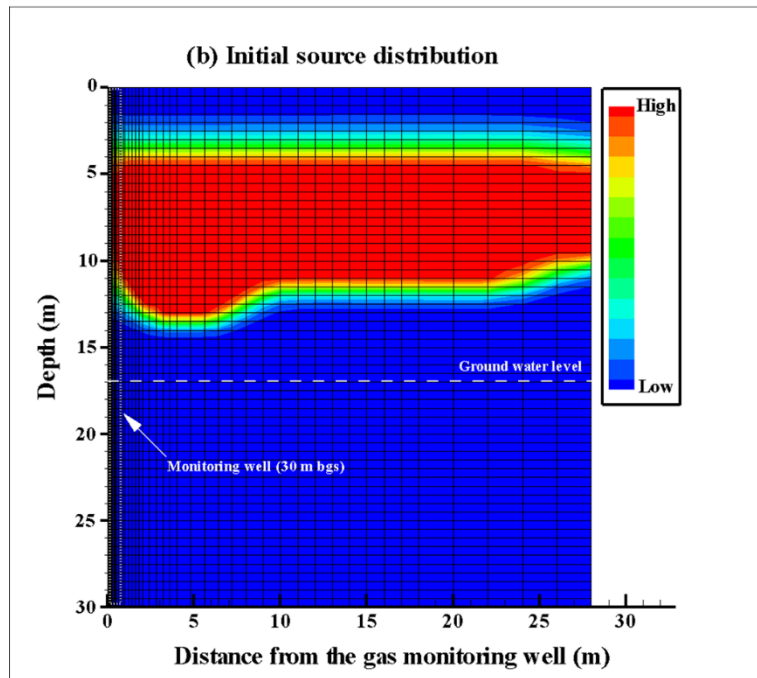


Figure 4-7 The model grid and the initial source position.

Table 4-3 The physical and chemical properties of TCE and CO₂.

Properties	C ₂ HCl ₃ (TCE, Trichloroethylene)	CO ₂ (Carbon dioxide)
Molecule weight (g/mole)	131.4	44.01
Freezing point Temp. (K)	186.8	194.7
Normal boiling point (K)	360.4	216.6
Critical Temp. (K)	572.0	304.0
Critical Pressure (MPa)	5.05	7.38
Critical molar volume (cm ³ /mole)	256.0	93.9
Critical compressibility (-)	0.265	0.274
Pitzner acentric factor (-)	0.213	0.239
Dipole moment (debye)	0.9	0.0
Isobaric molar specific heat constants		
a	3.017E+01	1.980E+01
b	2.287E-01	7.344E-02
c	-2.229E-04	-5.602E-05
d	8.244E-08	1.715E-08
Saturated vapor pressure function		
a	-7.3819	-6.95626
b	1.9482	1.19695
c	-3.0329	-3.12614
d	-5.3453	2.99448
Liquid density (kg/m ³)	1460	1440 (liquid); 1.977 (in gas at 1 bar, 273.15 K)
Liquid viscosity (Pa s)	4.9E-04	77.25 (at 195.2 K)
Henry's constant (Pa)	6.85E+07	2.15E+07
Solubility in water (g/L)	1.28	1.45

All values were adapted from Reid et al., 1987; Mackay et al., 1997; and Joun et al., 2016

4.3 Results of numerical modeling

Figure 4-8 shows the results of numerical modeling depending on the boundary condition for each case. The varied boundary condition of the model domain was determined using the observed data as Pascal pressure about the atmosphere, borehole, and groundwater level. Each result was normalized to be compared to each other. The results of case 1 which is following the general concept of the analytical model. Thus, only atmosphere pressures were applied on the top of the model domain using the monitoring data of the barometric pressure at the study site. We expected that some similar pattern with the observed data of gas concentration would appear in the model results of case 1 but only 5 peaking pattern was shown (Figure 4-8 first graph). By calculating the gas mass transport using the numerical model, we recognized that the barometric effect is a considerable factor for analyzing the natural pattern of gas concentration in the vadose zone well (Kuang et al., 2013) but another reasonable factor should be necessary to match up the natural pattern. As stated in Joun et al. (2016), the migration of gas fluid might be critically affected by the water table fluctuation. Although the variation of

water table level was smaller than the presented data in Joun et al. (2016), because, in the multi-phase simulation, a correlation among these phases is very complex (Figure 4-9), applying small fluctuating water table on the boundary is better than the constant water table or the fixed water table boundary conditions. The results of case 2 show the relative constant magnitude of gas concentration as shown in Figure 4-8 (second graph). This result is also not the representative results to explain the natural pattern of gas concentration in the vadose zone well. As shown in Joun et al. (2016), it should be handled that the gas flow is generated in the porous media. Finally, we applied both variations on the top and the bottom boundary of the model domain respectively using our self-improved technique. As represented in Figure 4-8 (third graph), the model results showed an almost similar pattern of gas concentration with the observed data. In contrast with the other cases, the results of Case 3 represented the fluctuating gas concentrations. Some studies for calculating the gas fluxes through the monitoring well using an analytical solution conceptualized that the small variation of the groundwater level is ignorable (Rossabi and Falta, 2002; Neeper, 2003) and it could be a reason that the small changes at the deep depth over 50 m bgs could be a small

influence on the gas transport near the ground surface at the noncoastal site because it is far from the water table motion and the frequencies are also little then at the coastal site (Parker, 2003; Tillman and Smith, 2005). You et al. (2011) stated that the effect of fluctuating the groundwater might be important for understanding the gas flow in the shallow aquifer system. However, they also not handled the influence of the variation of groundwater in their studies. In that sense, this study is proved that in the case of numerical simulation, the hypothesis in the previous studies cannot be acceptable. The reason why the only Case 3 could reproduce the natural pattern of gas concentration in the vadose zone well can be explained with Figure 4-10. The gas flow is highly influenced by the water contents in the limited volume of the pore as represented in Figure 4-10. If the groundwater level is changing periodically, the water contents in the pore volume would be also changed and according to this phenomenon, the possible pathway of gas fluid will be absolutely changed with time. This natural mechanism can be described theoretically because three parameters including capillary pressure, saturation, and relative permeability are always correlatively affected to another factor. It means that the researcher should consider not only changing the barometric pressure but

also the groundwater level changes for calculating a reproduced natural pattern of gas concentrations in the vadose zone well.

4.4 Discussion

The rainfall event could be one of the critical factors to hinder the gas migration in the porous media and some previous studies suggested that penetrating the water from the ground surface to the groundwater can generate the spike-peak signal of CO₂ (g) concentration by filling the volume of pore and pushing out the native air remained at the porous media. Thus, it should be verified whether the precipitation can be a critical factor to reproduce the natural pattern of CO₂ gas concentration in the vadose zone well using other options. The effect of the precipitation on the groundwater can be calculated by using the semi-analytical solution developed by Jeong and Park (2017). Using this model, the influence of rainfall during the gas sampling period was evaluated. The results of this model represented that the precipitation was not affected by the variation of groundwater because the

infiltrated rain was not enough to increase the level of the groundwater. Jeong and Park (2017) also mentioned that the precipitation data during the dry season which is the same season in this study was not influenced by the rising groundwater level. It means that the small amount of rain about 1.2 cm as shown in Figure 4-1 would not be sufficient rainwater to saturate the pore volume from the monitoring depth of CO₂ gas concentration to the ground surface.

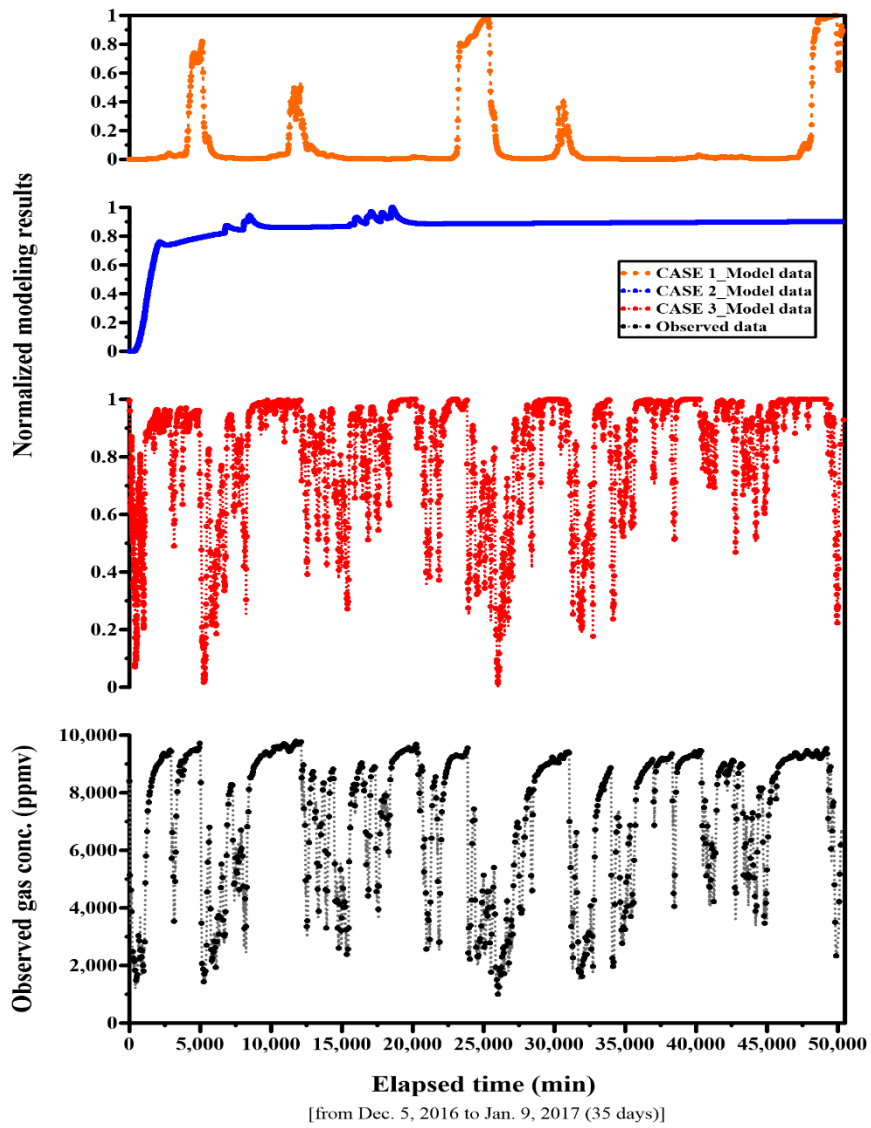


Figure 4-8 The results of numerical simulations for each case and the observed CO₂(g) monitoring data.

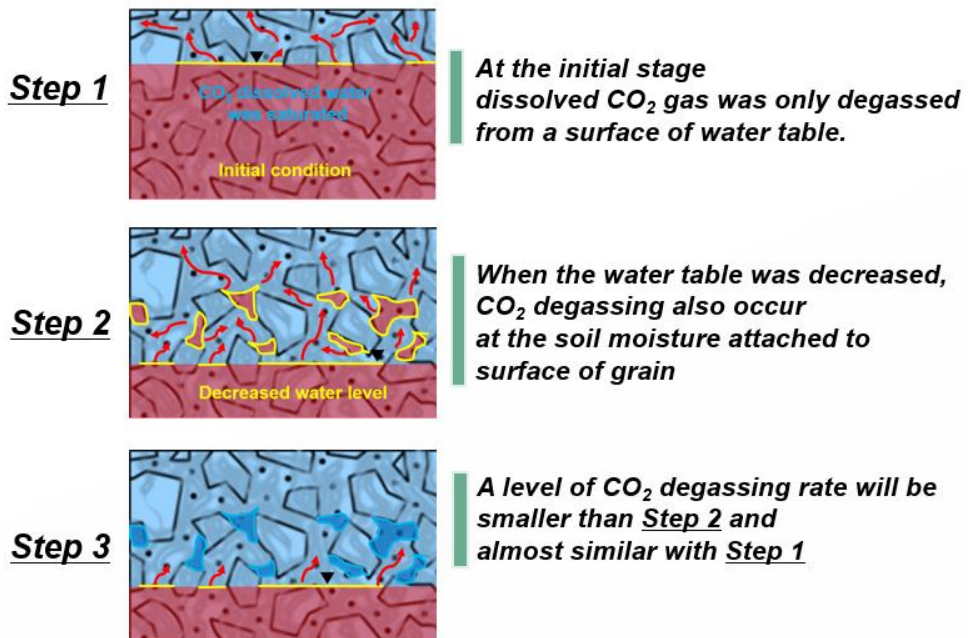


Figure 4-9 Conceptual model of multi-phase CO₂ and water behavior depending on water table fluctuation (Joun *et al.*, 2017).

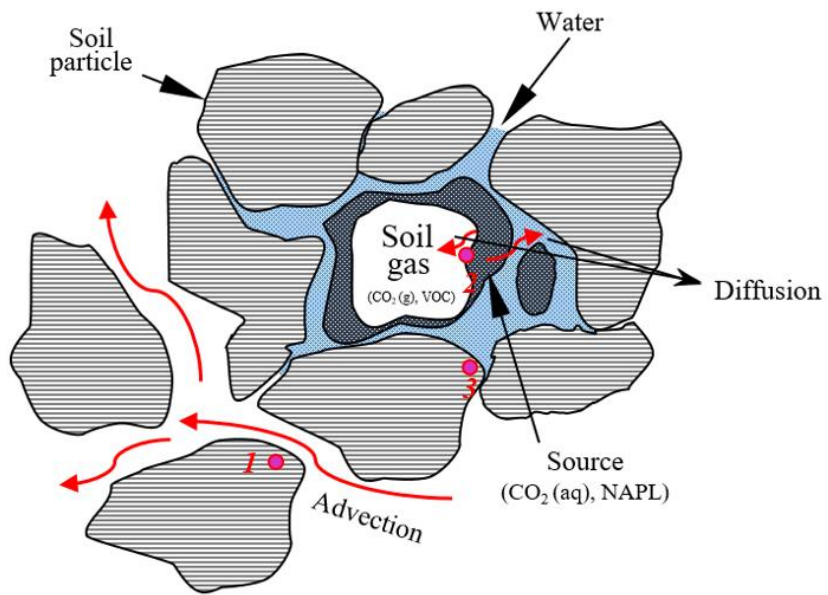


Figure 4 -10 Schematic diagram for a possible flow pathway of gas fluid through the porous media.

4.5 Verification

Although Case 3 was similar to the observed data as shown in Figure 4-8, the extra steps were necessary to evaluate the results of Case 3 had representative values by comparing the naturally varied gas concentration at the subsurface environment installed a gas monitoring well. The verifying methods are listed as follows:

$$\text{RMSE} = \sqrt{\frac{\sum_{i=1}^n (M_i - O_i)^2}{n}} \quad (1)$$

$$\text{RI} = \exp \sqrt{\frac{\sum_{i=1}^n \left(\log_{10} \frac{O_i}{M_i} \right)^2}{n}} \quad (2)$$

$$\text{IA} = 1 - \frac{\sum_{i=1}^n (|M_i - O_i|)^2}{\sum_{i=1}^n (|M_i - O_{\text{avg}}| + |O_i - O_{\text{avg}}|)^2} \quad (3)$$

$$\text{CF} = \frac{\sum_{i=1}^n \left(\frac{|M_i - O_i|}{\sigma} \right)}{n} \quad (4)$$

$$\text{CRM} = \frac{\sum_{i=1}^n O_i - \sum_{i=1}^n S_i}{\sum_{i=1}^n O_i} \quad (5)$$

where M_i is the numerical model value for time i , O_i is the observed values with for time i , n is the number of total measurements, O_{avg} is the average of the observed data, and σ is the standard deviation of the observed data.

The root means square error (RMSE) (Eq. 1) is one of the principal quantitative evaluation methods. The qualitative methods comprise reliability index (RI) (Eq. 2), index of agreement (IA) (Eq. 3), cost function (CF) (Eq. 4), and coefficient of residual mass (CRM) (Eq. 5). RI value represents the confidence of the numerical model. RI always has values greater than one, (Leggett and Williams, 1981). IA is an indicator of how close the results of the numerical model are to those of the observed data (Wilmott, 1982). The CF equation indicates how close the results of the numerical model are to those of the observed values (Gibson et al., 2006). The CRM represents how much the over- or under-estimation of the results derived from the numerical simulation by comparing the observed data (Moreels et al., 2003). The results

for each method were 0.17, 1.19, 0.98, 0.48, and -0.18 respectively (Table 4-4). From these results, we could determine that Case 3 of the numerical simulation recreated the natural pattern of gas concentration well.

Table 4 -4 Results of evaluation for comparing Case 3 with observed data.

Equations	Indexes	Judgments*
RMSE	0.17	acceptable
CC	0.93	close to perfect
RI	1.19	close to perfect
IA	0.89	close to agree
CF	0.48	excellent
CRM	-0.18	a few overestimate

*Criteria: CC=1 (Perfect correlation) and CC<0(no correlation);
RI=1 (perfectly match with measurements);
IA=1 (agree), IA=0(disagree);
CF<1(Excellent), 1<CF<2(Good), 2<CF<3(Average), CF<3(Bad);
CRM>0 (underestimate), CRM<0(overestimate).

4.6 Conclusion

Reproducing the natural variation of CO₂ gas concentration at the vadose zone well is a difficult task because not only there are many influence factors such as wind, precipitation, pressure, humidity, and temperature but also the pattern is varied depending on the certification of monitoring boreholes or monitoring time such as day or night. Thus, this research in chapter 4 is important to understand the leakage signal using the vadose zone well and to separate between the naturally produced CO₂ and the escaped CO₂ from the storage reservoir. In this study, the advanced numerical technique was proposed to recreate the natural pattern of gas concentration at the vadose zone well. This study provided one of the fundamental rules to understand the effect of fluctuating the water table on the gas fate and transport at the shallow aquifer. Also, this study represented a possibility about the influence of small variation of water table on the gas concentration. However, to understand the whole mechanism of natural effect on gas migration through the vadose zone well, more advanced research should be conducted near the future.

This page intentionally left blank

CHAPTER 5 . Simple-application about Predicting CO₂ Short-term Leakage through the Well

5.1 Introduction

The numerical simulation is one of the feasible methods to predict challenging problem what is unrecognized or unexpected phenomena. As represented in the previous chapters, the large-swing variation of gas concentration in the monitoring well is the priority problem to detect the escaped CO₂ from the storage reservoir. Thus, trying to investigate the natural phenomena which effect on the variation of gas concentrations and to recreate these pattern based on the research about the characterization of the gas

concentration patterns. From those researches, in this chapter, predicting the pattern of gas concentration when the pulse-leakage occurs through the monitoring well will be attempted as shown in Figure 5-1. This simple application will be a good example for not only understanding the real-time monitoring data at the GCS site and but also providing a possible rule to solve the complex-mixing CO₂ (g) including the leaking CO₂ (g) and the naturally produced CO₂ (g).

◆ A figure in chapter 5 was cited from the published article, Joun and Lee (2020).

5.2 Materials and methods

The general input values for predicting the pulse-leak simulation followed the Case 3 condition in chapter 4. The same model domain was also used and the distribution of background CO₂ in this simulation was the same as the previous Ch. 4 study as shown in Figure 4-7. The assumption of leaking CO₂

which is an additional source through the monitoring well was applied on the left boundary of the model domain where the virtual monitoring well is installed. The leaking period was set from 10,000 min to 25,000 min (10.4 d). The other initial and boundary condition was also the same as Case 3 including pressure fluctuation on the top and the bottom of the model domain, physical parameters, etc.

5.3 Results and remarks

Figure 5-2 shows one observed data and two results of modeling about the gas concentrations. The blue line represents the results of a simple application, the red line shows the results of Case 3 modeling, and the black line is the real observed data at the K-COSEM research site. As stated in Chapter 4, the reproduced natural pattern of gas concentration was almost the same as the observed data. The two graphs from modeling followed the observed data before the gas leaking event commenced (<10,000 min), however, during the leaking period (10,000 min to 25,000 min), the pattern in the blue graph was

different with two other graphs. Instead of following the observed data, the blue graph has flat and constant value during the leaking period. As showing there three graphs, it could be suggested that the pattern of gas concentration at the vadose zone well will be completely different from the variation which is affected by the natural phenomena if the leakage event occurs around the monitoring well. In addition, these results could be utilized in separating a possible leaking signal or the natural signal from the total mixed CO₂ (g).

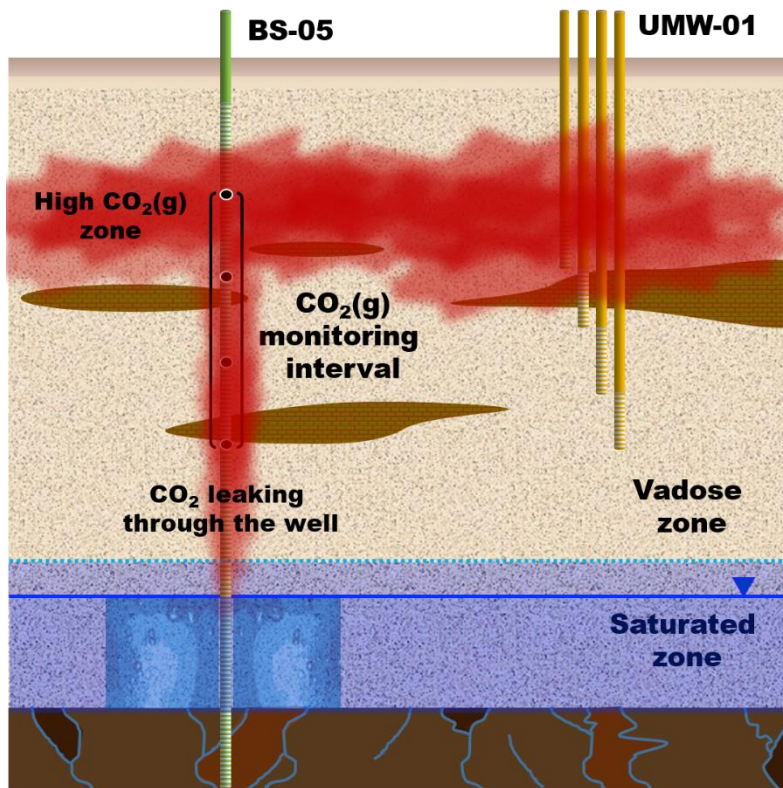


Figure 5-1 Conceptual diagram for representing CO₂ pulse-leakage scenario through the monitoring well

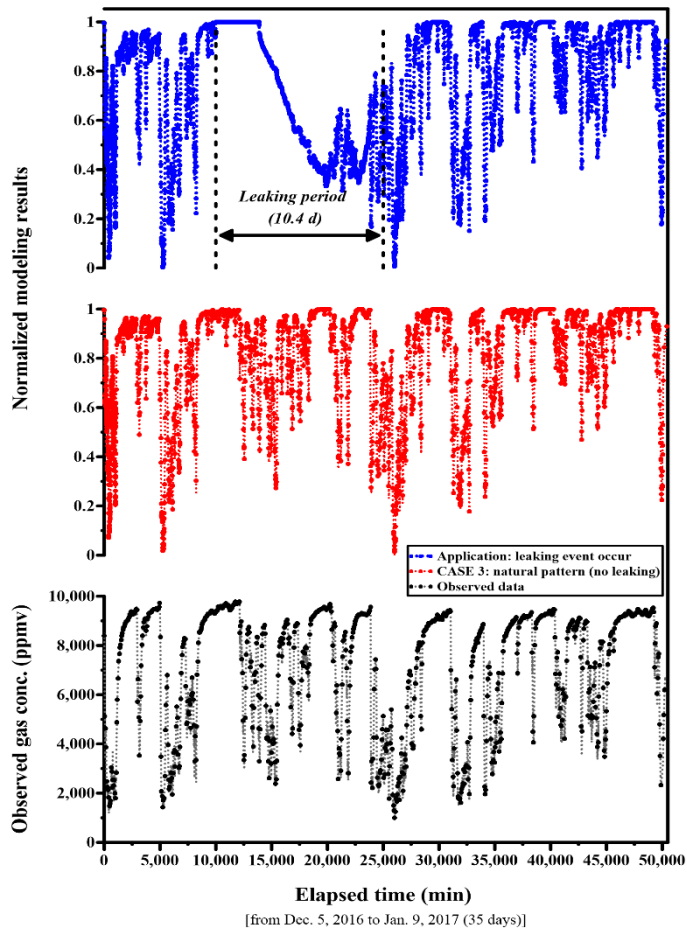


Figure 5-2 Three kinds of results including two modeling and one observed data at the K-COSEM research site.

CHAPTER 6. Conclusion

To mitigate the climate changes or the increasing global warming effects, any possible action should be conducted to find reasonable methods or effective performance. Therefore, many researchers have suggested that CO₂-carbon capture and storage under the deep reservoir and trying to detect the signal of leaking CO₂ which can approach the near-surface to protect the life which lives in the shallow aquifer or the human. However, to understand migrating CO₂ through the preferential pathways such as fracture, abandoned

well, etc. and to develop the monitoring techniques, the CO₂ detection at the real CCS site is not suitable because it will be taken a long time to monitor the CO₂ signal from the deep reservoir (over 10 km) and it will be not enough to determine the potential risks on the shallow aquifer because the purpose of CCS is that CO₂ should not be a leak to the atmosphere. Thus, to understand the impacts on the shallow aquifer by the intrusive CO₂ into the groundwater or the vadose zone, the conceptualized experiments so called “Controlled CO₂ release test” can be one of the good proposes as the alternative methods to clear the effect of leaking CO₂ on the subsurface environments. K-COSEM research site was also one of those experimental sites and field experiments have been conducted at the shallow aquifer by injecting CO₂ infused water or CO₂ gas. From these field experiments, the unexpected large swing CO₂ pattern was detected and we need to understand the reason why this pattern was monitored to identify the artificial leaking signals. Using the real-time monitoring method, we recognized CO₂ concentration can be fluctuated depending on the day or night. Several intensive tests were also conducted to provide the backup evidence to explain the natural phenomena and the results of these test also represented that the fresh air intrusion through the mentoring

well can be a potential problem on the fluctuating CO₂ gas concentration in the vadose zone wells when detecting leaking CO₂ is applied on the shallow subsurface environment (Joun et al., 2019). Reproducing natural variation was also calculated by using the numerical model. From this modeling study, the important rule about the natural mechanism at the vadose zone well was revealed. One is that the natural gas intrusion into the well could be generated by the atmospheric pressures. Thus, several previous studies can calculate the gas flux or the subsurface pressure by only using atmospheric pressure. However, calculating the fate and transport of gas mass is another problem. It means that the transport of gas mass could be not following as much as the magnitude of the gas flow through the vadose zone well vertically and that also would be influenced by the source distributions (Joun et al 2016). Secondary, gas transport is affected by not only the atmospheric pressure but also the groundwater pressure. It means that the flow pathway of gas mass could be hindered by the water contents in the vadose zone. Thus, as mentioned in Chapter 4, the results of Case 3 well-represented the natural variation of gas concentrations in the vadose zone well. The simple application was conducted based on the model results of Case 3 and it will be

useful for understanding the detected signals of CO₂ leakage if the continuous CO₂ gas monitoring is conducted at the shallow aquifer system (Joun and Lee, 2020).

Bibliography

Abbas, T. R. (2011). Effect of water table fluctuation on barometric pumping in soil unsaturated zone. *Jordan Journal of Civil Engineering*, 5(4), 504-509.

ASTM D 1586-11 (2011), *Standard test method for standard penetration test (SPT) and split-barrel sampling of soil*, Annual Book of ASTM Standard, Vol.04.08, American Society for Testing and Materials.

ASTM-D-5314-92, *Standard Guide for Soil Gas Monitoring in the Vadose Zone*, 2006.

Bakk, A., Girard, J. F., Lindeberg, E., Aker, E., Wertz, F., Buddensiek, M., Barrio, M., and Jones, D. (2012). CO₂ field lab at svelvik ridge: site suitability. *Energy Procedia*, 23, 306-312.

Bear, J. (1975). *Dynamics of Fluids in Porous Media*. American Elsevier Publishing Company, Inc., New York.

Beaubien, S. E., Jones, D. G., Gal, F., Barkwith, A. K. A. P., Braibant, G., Baubron, J. C., Ciotoli, G., Graziani, S., Lister, T. R., Lombardi, S., Michel, K., Quattrocchi, F., and Strutt, M. H. (2013). Monitoring of near-surface gas geochemistry at the Weyburn, Canada, CO₂-EOR site, 2001–2011. *International Journal of Greenhouse Gas Control*, 16, S236-S262.

Bereiter, B., Eggleston, S., Schmitt, J., Nehrbass-Ahles, C., Stocker, T. F., Fischer, H., Kipfstuhl, S., and Chappellaz, J. (2015). Revision of the EPICA Dome C CO₂ record from 800 to 600 kyr before present. *Geophysical Research Letters*, 42(2), 542-549.

Berry, H. L., Bowen, K., and Kjellstrom, T. (2010). Climate change and mental health: a causal pathways framework. *International Journal of Public Health*, 55(2), 123-132.

Benson, S. M., and Cole, D. R. (2008). CO₂ sequestration in deep sedimentary formations. *Elements*, 4(5), 325-331.

Boulding, J. R., and Ginn, J. S. (2004). *Practical handbook of soil, vadose zone, and ground-water contamination: assessment, prevention, and remediation*. CRC Press.

Cahill, A. G., and Jakobsen, R. (2013). Hydro-geochemical impact of CO₂ leakage from geological storage on shallow potable aquifers: A field scale pilot experiment. *International Journal of Greenhouse Gas Control*, 19, 678-688.

Cahill, A. G., Marker, P., and Jakobsen, R. (2014). Hydrogeochemical and mineralogical effects of sustained CO₂ contamination in a shallow sandy aquifer: A field-scale controlled release experiment. *Water Resources Research*, 50(2), 1735-1755.

Christophersen, M., and Kjeldsen, P. (2001). Lateral gas transport in soil adjacent to an old landfill: factors governing gas migration. *Waste Management and Research*, 19(6), 579-594.

Clark, I. D., and Fritz, P. (1997). *Environmental Isotopes in Hydrogeology*. CRC press.

DOE (2011). *Report of the Interagency Task Force on Carbon Capture and Storage*. United States.

Duncombe, J. (2020), Climate change will make us sicker and lose work hours, *Eos*, 101(1), page 11.

Epstein, P. R. (2002). Climate change and infectious disease: stormy weather ahead?. *Epidemiology*, 13(4), 373-375.

Falta, R. W., Javandel, I., Pruess, K., and Witherspoon, P. A. (1989). Density-driven flow of gas in the unsaturated zone due to the evaporation of volatile organic compounds. *Water Resources Research*, 25(10), 2159-2169.

Farrell, D. A., Greacen, E. L., and Gurr, C. G. (1966). Vapor transfer in soil due to air turbulence. *Soil Science*, 102(5), 305-313.

Fetter, C. W. (2018). *Applied Hydrogeology*. Waveland Press.

Gal, F., Proust, E., Humez, P., Braibant, G., Brach, M., Koch, F., Widory, D., and Girard, J. F. (2013). Inducing a CO₂ leak into a shallow aquifer (CO₂FieldLab EUROGIA+ project): Monitoring the CO₂ plume in groundwaters. *Energy Procedia*, 37, 3583-3593.

Garcia-Anton, E., Cuezva, S., Fernandez-Cortes, A., Benavente, D., and Sanchez-Moral, S. (2014). Main drivers of diffusive and advective processes of CO₂-gas exchange between a shallow vadose zone and the atmosphere. *International Journal of Greenhouse Gas Control*, 21, 113-129.

Gasda, S. E., Bachu, S., and Celia, M. A. (2004). Spatial characterization of the location of potentially leaky wells penetrating a deep saline aquifer in a mature sedimentary basin. *Environmental Geology*, 46(6-7), 707-720.

Gasparini, A., Sainz-García, A., Grandia, F., and Bruno, J. (2016). Atmospheric dispersion modelling of a natural CO₂ degassing pool from Campo de Calatrava (northeast Spain) natural analogue. Implications for carbon storage risk assessment. *International Journal of Greenhouse Gas Control*, 47, 38-47.

Gee, G. W., Oostrom, M., Freshley, M. D., Rockhold, M. L., and Zachara, J. M. (2007). Hanford site vadose zone studies: An overview. *Vadose Zone Journal*, 6(4), 899-905.

Gibson, R.N., Atkinson, R.J.A., and Gordon, J.D.M. (2006). Review of three-dimensional ecological modelling related to the North Sea shelf system. Part II: model validation and data needs. *Oceanography and Marine Biology: Annual Review*, 44, 1–60.

Glückauf, E., and Paneth, F. A. (1946). The helium content of atmospheric air. *Proceedings of the Royal Society of London. Series A. Mathematical and Physical Sciences*, 185(1000), 89-98.

Guo, L., and Lin, H. (2016). Critical zone research and observatories: Current status and future perspectives. *Vadose Zone Journal*, 15(9).

Harvey, O. R., Qafoku, N. P., Cantrell, K. J., Lee, G., Amonette, J. E., and Brown, C. F. (2012). Geochemical implications of gas leakage associated with geologic CO₂ storage — A qualitative review. *Environmental Science and Technology*, 47(1), 23-36.

Humez, P., Négrel, P., Lagneau, V., Lions, J., Kloppmann, W., Gal, F., Millot, R., Guerrot, C., Flehoc, C., Widory, D., and Girard, J. F. (2014). CO₂–

water–mineral reactions during CO₂ leakage: Geochemical and isotopic monitoring of a CO₂ injection field test. *Chemical Geology*, 368, 11-30.

IPCC, 2018: Global Warming of 1.5°C. An IPCC Special Report on the impacts of global warming of 1.5°C above pre-industrial levels and related global greenhouse gas emission pathways, in the context of strengthening the global response to the threat of climate change, sustainable development, and efforts to eradicate poverty. Masson-Delmotte, V., P. Zhai, H.-O. Pörtner, D. Roberts, J. Skea, P.R. Shukla, A. Pirani, W. Moufouma-Okia, C. Péan, R. Pidcock, S. Connors, J.B.R. Matthews, Y. Chen, X. Zhou, M.I. Gomis, E. Lonnoy, T. Maycock, M. Tignor, and T. Waterfield (eds.), In Press.

Jeong, J., and Park, E. (2017). A shallow water table fluctuation model in response to precipitation with consideration of unsaturated gravitational flow. *Water Resources Research*, 53(4), 3505-3512.

Jones, D. G., Beaubien, S. E., Blackford, J. C., Foekema, E. M., Lions, J., De Vittor, C., West, J. M., Widdicombe, S., Hauton, C., and Queirós, A. M.

(2015). Developments since 2005 in understanding potential environmental impacts of CO₂ leakage from geological storage. *International Journal of Greenhouse Gas Control*, 40, 350-377.

Joun, W. T., Lee, S. S., Koh, Y. E., and Lee, K. K. (2016). Impact of water table fluctuations on the concentration of borehole gas from NAPL sources in the vadose zone. *Vadose Zone Journal*, 15(4).

Joun, W. T., Ha, S. W., Kim, H. J., Ju, Y., Lee, S. S., and Lee, K. K. (2017, April). CO₂ leakage monitoring and analysis to understand the variation of CO₂ concentration in vadose zone by natural effects. In EGU General Assembly Conference Abstracts (Vol. 19, p. 11761).

Joun, W. T., Rossabi, J., and Shin, W. J., and Lee, K. K. (2019). Real-time multi-level CO₂ concentration monitoring in vadose zone wells and the implication for detecting leakage events. *Journal of Environmental Management*, 237, 534-544.

Joun, W. T. and Lee, K. K. (2020). Reproducing natural variations in CO₂ concentration in the vadose zone wells with observed atmospheric pressure

and groundwater data. *Journal of Environmental Management*, 266, 110568.

Ju, Y., Beaubien, S. E., Lee, S. S., Kaown, D., Hahm, D., Lee, S., Park, I. W., Park, K., Yun, S. T., and Lee, K. K. (2019). Application of natural and artificial tracers to constrain CO₂ leakage and degassing in the K-COSEM site, South Korea. *International Journal of Greenhouse Gas Control*, 86, 211-225.

Jun, S. C., Cheon, J. Y., Yi, J. H., and Yun, S. T. (2017). Controlled release test facility to develop environmental monitoring techniques for geologically stored CO₂ in Korea. *Energy Procedia*, 114, 3040-3051.

Kharaka, Y. K., Thordsen, J. J., Kakouros, E., Ambats, G., Herkelrath, W. N., Birkolzer, J. T., Apps, J. A., Spycher, N. F., Zhang, L., Trautz, R. C., Rauch, H. W., and Gullickson, K. S. (2010). Changes in the chemistry of shallow groundwater related to the 2008 injection of CO₂ at the ZERT field site, Bozeman, Montana. *Environmental Earth Sciences*, 60(2), 273-284.

- Kim, H. J., Han, S. H., Kim, S., Yun, S. T., Jun, S. C., Oh, Y. Y., and Son, Y. (2018a). Characterizing the spatial distribution of CO₂ leakage from the shallow CO₂ release experiment in South Korea. *International Journal of Greenhouse Gas Control*, 72, 152-162.
- Kim, H. H., Lee, S. S., Ha, S. W., and Lee, K. K. (2018b). Application of single-well push-drift-pull tests using dual tracers (SF₆ and salt) for designing CO₂ leakage monitoring network at the environmental impact test site in Korea. *Geosciences Journal*, 1-12.
- Kharaka, Y. K., Thordsen, J. J., Kakouros, E., Ambats, G., Herkelrath, W. N., Beers, S. R., Birkholzer, J. T., Apps, J. A., Spycher, N. S., Zheng L., Trautz, R. C., Rauch, H. W., and Gullickson, K. S. (2010). Changes in the chemistry of shallow groundwater related to the 2008 injection of CO₂ at the ZERT field site, Bozeman, Montana. *Environmental Earth Sciences*, 60(2), 273-284.
- Khasnis, A. A., and Nettleman, M. D. (2005). Global warming and infectious disease. *Archives of medical research*, 36(6), 689-696.

Klusman, R.W., 1993, *Soil gas and related methods for natural resource exploration*.

New York, John Wiley & Sons.

Kuang, X., Jiao, J. J., and Li, H. (2013). Review on airflow in unsaturated zones induced by natural forcings. *Water Resources Research*, 49(10), 6137-6165.

Lee, J. Y., and Lee, K. K. (2000). Use of hydrologic time series data for identification of recharge mechanism in a fractured bedrock aquifer system. *Journal of Hydrology*, 229(3-4), 190-201.

Lee, K. K., Lee, S. H., Yun, S. T., and Jeon, S. W. (2016). Shallow groundwater system monitoring on controlled CO₂ release sites: a review on field experimental methods and efforts for CO₂ leakage detection. *Geosciences Journal*, 20(4), 569-583.

Lee, S.S., Kim, H.H., Joun, W.T., Lee, K.K. (2017). Design and Construction of Groundwater Monitoring Network at Shallow-depth CO₂ Injection and Leak Test Site, Korea. *Energy Procedia*, 114, 3060-3069.

Leggett, R.W. and Williams, L.R. (1981). A reliability index for models.

Ecological Modeling, 13 (4), 303–312.

Lewicki, J. L., Evans, W. C., Hilley, G. E., Sorey, M. L., Rogie, J. D., and

Brantley, S. L. (2003). Shallow soil CO₂ flow along the San Andreas and

Calaveras faults, California. *Journal of Geophysical Research: Solid Earth*,

108(B4), 2187.

Lewicki, J. L., Oldenburg, C. M., Dobeck, L., and Spangler, L. (2007).

Surface CO₂ leakage during two shallow subsurface CO₂

releases. *Geophysical Research Letters*, 34(24).

Lewicki, J. L., Hilley, G. E., Fischer, M. L., Pan, L., Oldenburg, C. M.,

Dobeck, L., and Spangler, L. (2009). Eddy covariance observations of

surface leakage during shallow subsurface CO₂ releases. *Journal of*

Geophysical Research: Atmospheres, 114(D12).

Lewicki, J. L., Hilley, G. E., Dobeck, L., and Spangler, L. (2010). Dynamics

of CO₂ fluxes and concentrations during a shallow subsurface CO₂ release.

Environmental Earth Sciences, 60(2), 285-297.

- Lobell, D. B., and Gourdji, S. M. (2012). The influence of climate change on global crop productivity. *Plant Physiology*, 160(4), 1686-1697.
- Looney, B. B., and Falta, R. W. (2000a). *Vadose zone science and technology solutions (volume 1)*. Battelle Press.
- Looney, B. B., and Falta, R. W. (2000b). *Vadose zone science and technology solutions (volume 2)*. Battelle Press.
- Lüthi, D., Le Floch, M., Bereiter, B., Blunier, T., Barnola, J. M., Siegenthaler, U., Raynaud, D., Jouzel, J., Fischer, H., Kawamura, K., and Stocker, T. F. (2008). High-resolution carbon dioxide concentration record 650,000–800,000 years before present. *Nature*, 453, 379-382.
- Mackay, D., Shiu, W. Y., and Ma, K. C. (1997). *Illustrated handbook of physical-chemical properties of environmental fate for organic chemicals (Vol. 5)*. CRC press.
- Massman, W. J., and Frank, J. M. (2006). Advective transport of CO₂ in permeable media induced by atmospheric pressure fluctuations: 2.

Observational evidence under snowpacks. *Journal of Geophysical Research: Biogeosciences*, 111(G3).

Metz, B., Davidson, O., and De Coninck, H. (Eds.). (2005). *Carbon dioxide capture and storage: special report of the intergovernmental panel on climate change*. Cambridge University Press.

Mickler, P. J., Yang, C., Scanlon, B. R., Reedy, R., and Lu, J. (2013). Potential impacts of CO₂ leakage on groundwater chemistry from laboratory batch experiments and field push-pull tests. *Environmental Science and Technology*, 47(18), 10694-10702.

MLTMA (Ministry of Land, Transport and Maritime Affairs, Korea) and KWRC (Korea Water Resources Corporation) (2009). Basic survey of groundwater in Eumseong area.

Mora, C., Frazier, A. G., Longman, R. J., Dacks, R. S., Walton, M. M., Tong,, E. J., Sanchez, J. J., Kaiser, L. R., Stender Y. O., Anderson, J. M., Ambrosino C. M., Fernandez-Silva, I., Giuseffi, L. M., and Giambelluca,

- T. W. (2013). The projected timing of climate departure from recent variability. *Nature*, 502, 183–187.
- Moreels, E., De Neve, S., Hofman, G., Van Meirvenne, M. (2003). Simulating nitrate leaching in bare fallow soils: a model comparison. *Nutrient Cycling Agroecosystems*, 67 (2), 137–144.
- Nachshon, U., Dragila, M., and Weisbrod, N. (2012). From atmospheric winds to fracture ventilation: Cause and effect. *Journal of Geophysical Research: Biogeosciences*, 117(G2).
- Neeper, D. A. (2001). A model of oscillatory transport in granular soils, with application to barometric pumping and earth tides. *Journal of Contaminant Hydrology*, 48(3-4), 237-252.
- Neeper, D. A. (2002). Investigation of the vadose zone using barometric pressure cycles. *Journal of Contaminant Hydrology*, 54(1), 59-80.

Neeper, D. A. (2003). Harmonic analysis of flow in open boreholes due to barometric pressure cycles. *Journal of Contaminant Hydrology*, 60(3), 135-162.

Nilson, R. H., Peterson, E. W., Lie, K. H., Burkhard, N. R., and Hearst, J. R. (1991). Atmospheric pumping: A mechanism causing vertical transport of contaminated gases through fractured permeable media. *Journal of Geophysical Research: Solid Earth*, 96(B13), 21933-21948.

Oldenburg, C. M., and Unger, A. J. (2003). On leakage and seepage from geologic carbon sequestration sites. *Vadose Zone Journal*, 2(3), 287-296.

Oostrom, M., Dane, J. H., and Wietsma, T. W. (2005). Removal of carbon tetrachloride from a layered porous medium by means of soil vapor extraction enhanced by desiccation and water table reduction. *Vadose Zone Journal*, 4(4), 1170-1182.

Parker, J. C. (2003). Physical processes affecting natural depletion of volatile chemicals in soil and groundwater. *Vadose Zone Journal*, 2(2), 222-230.

Peter, A., Lamert, H., Beyer, M., Hornbruch, G., Heinrich, B., Schulz, A., Geistlinger, H., Schreiber, B., Dietrich, P., Werban, U., Vogt, C., Richnow, H. H., Großmann, J., and Dahmke, A. (2012). Investigation of the geochemical impact of CO₂ on shallow groundwater: design and implementation of a CO₂ injection test in Northeast Germany. *Environmental Earth Sciences*, 67(2), 335-349.

Pla, C., Cuezva, S., Garcia-Anton, E., Fernandez-Cortes, A., Cañaveras, J. C., Sanchez-Moral, S., and Benavente, D. (2016). Changes in the CO₂ dynamics in near-surface cavities under a future warming scenario: factors and evidence from the field and experimental findings. *Science of The Total Environment*, 565, 1151-1164.

Reid, R. C., Prausnitz, J. M., and Poling, B. E. (1987). *The properties of gases and liquids*. McGraw-Hill Book Company.

Rillard, J., Gombert, P., Toulhoat, P., and Zuddas, P. (2014). Geochemical assessment of CO₂ perturbation in a shallow aquifer evaluated by a push–pull field experiment. *International Journal of Greenhouse Gas Control*, 21, 23-32.

- Risk, D., Kellman, L., and Beltrami, H. (2002). Carbon dioxide in soil profiles: production and temperature dependence. *Geophysical Research Letters*, 29(6), 11-1.
- Rojstaczer, S., and Tunks, J. P. (1995). Field-based determination of air diffusivity using soil air and atmospheric pressure time series. *Water Resources Research*, 31(12), 3337-3343.
- Romanak, K. D., Bennett, P. C., Yang, C., and Hovorka, S. D. (2012). Process-based approach to CO₂ leakage detection by vadose zone gas monitoring at geologic CO₂ storage sites. *Geophysical Research Letters*, 39(15), L15405.
- Romanak, K., Dobeck, L., Dixon, T., and Spangler, L. (2013). Potential for a process-based monitoring method above geologic carbon storage sites using dissolved gases in freshwater aquifers. *Procedia Earth and Planetary Science*, 7, 746-749.
- Romanak, K. D., Wolaver, B., Yang, C., Sherk, G. W., Dale, J., Dobeck, L. M., and Spangler, L. H. (2014a). Process-based soil gas leakage assessment

at the Kerr Farm: Comparison of results to leakage proxies at ZERT and Mt. Etna. *International Journal of Greenhouse Gas Control*, 30, 42-57.

Romanak, K. D., Womack, G. L., and Bomse, D. S. (2014b). Field test of in situ sensor technology for process-based soil gas monitoring. *Energy Procedia*, 63, 4027-4030.

Rossabi, J., and Falta, R. W. (2002). Analytical solution for subsurface gas flow to a well induced by surface pressure fluctuations. *Groundwater*, 40(1), 67-75.

Sánchez-Cañete, E. P., Oyonarte, C., Serrano-Ortiz, P., Curiel Yuste, J., Pérez-Priego, O., Domingo, F., and Kowalski, A. S. (2016). Winds induce CO₂ exchange with the atmosphere and vadose zone transport in a karstic ecosystem. *Journal of Geophysical Research: Biogeosciences*, 121(8), 2049-2063.

Schloemer, S., Furche, M., Dumke, I., Poggenburg, J., Bahr, A., Seeger, C., Vidal, A., and Faber, E. (2013). A review of continuous soil gas monitoring

related to CCS—Technical advances and lessons learned. *Applied Geochemistry*, 30, 148-160.

Sherwood, S. C., and Huber, M. (2010). An adaptability limit to climate change due to heat stress. *Proceedings of the National Academy of Sciences*, 107(21), 9552-9555.

Smith, K. L., Steven, M. D., Jones, D. G., West, J. M., Coombs, P., Green, K. A., Barlow, T. S., Breward, N., Gwosdz, S., Krüger, M., Beaubien, S. E., Annunziatellis, A., Graziani, S., and Lombardi, S. (2013). Environmental impacts of CO₂ leakage: recent results from the ASGARD facility, UK. *Energy Procedia*, 37, 791-799.

Song, J., and Zhang, D. (2012). Comprehensive review of caprock-sealing mechanisms for geologic carbon sequestration. *Environmental Science and Technology*, 47(1), 9-22.

Stephens, D. B. (1996). *Vadose zone hydrology*. CRC press.

- Strazisar, B. R., Wells, A. W., Diehl, J. R., Hammack, R. W., and Veloski, G. A. (2009). Near-surface monitoring for the ZERT shallow CO₂ injection project. *International Journal of Greenhouse Gas Control*, 3(6), 736-744.
- Spangler, L. H., Dobeck, L. M., Repasky, K. S. Nehrir, A. R., Humphries, S. D., Barr, J. L., Keith, C. J., Shaw, J. A., Rouse, J. H., Cunningham, A. B., Benson, S. M., Oldenburg, C. M., Lewicki, J. L., Wells, A. W., Diehl, J. R., Strazisar, B. R., Fessenden, J. E., Rahn, T. A., Amonette, J. E., Barr, J. L., Pickles, W. L., Jacobson, J. D., Silver, E. A., Male, E. J., Rauch, H. W., Gullickson, K. S. Trautz, R., Kharaka, Y., Birkholzer, J., and Wielopolski, L., (2010). A shallow subsurface controlled release facility in Bozeman, Montana, USA, for testing near surface CO₂ detection techniques and transport models. *Environmental Earth Sciences*, 60(2), 227-239.
- Taylor, R. G., Scanlon, B., Döll, P., Rodell, M., Van Beek, R., Wada, Y., Longuevergne, L., Leblanc, M., Famiglietti, J. S., Edmunds, M., Konikow, L., Green, T. R., Chen, J., Taniguchi, M., Bierkens, M. F. P., MacDonald, A., Fan, Y., Maxwell, R. M., Yechieli, Y., Gurdak, J. J., Allen, D. M., Shamsudduha, M., Hiscock, K., Yeh, P. J.-F., Holman, I., and Treidel, H.

(2013). Ground water and climate change. *Nature climate change*, 3(4), 322-329.

Tillman Jr, F. D., and Smith, J. A. (2005). Site characteristics controlling airflow in the shallow unsaturated zone in response to atmospheric pressure changes. *Environmental Engineering Science*, 22(1), 25-37.

Trautz, R. C., Pugh, J. D., Varadharajan, C., Zheng, L., Bianchi, M., Nico, P. S., Spycher, N. F., Newell, D. L., Esposito, R. A., Wu, T., Dafflon, B., Hubbard, S. S., and Birkholzer, J. T. (2013). Effect of dissolved CO₂ on a shallow groundwater system: A controlled release field experiment. *Environmental Science and Technology*, 47(1), 298-305.

van Genuchten, M. T. (1980). A closed-form equation for predicting the hydraulic conductivity of unsaturated soils 1. *Soil Science Society of America Journal*, 44(5), 892-898.

van Genuchten, M. Th., F. J. Leij, and S. R. Yates. (1991). The RETC Code for Quantifying the Hydraulic Functions of Unsaturated Soils, Version 1.0.

EPA Report 600/2-91/065, U.S. Salinity Laboratory, USDA, ARS, Riverside, California.

VDI 3865-2, Measurement of organic soil pollutants – Techniques of active sampling of soil gas, 1998.

Wells, A., Strazisar, B., Diehl, J. R., and Veloski, G. (2010). Atmospheric tracer monitoring and surface plume development at the ZERT pilot test in Bozeman, Montana, USA. *Environmental Earth Sciences*, 60(2), 299-305.

White, M. D., Oostrom, M., and Lenhard, R. J. (1995). Modeling fluid flow and transport in variably saturated porous media with the STOMP simulator. 1. Nonvolatile three-phase model description. *Advances in Water Resources*, 18(6), 353-364.

White, M.D., and M. Oostrom. (2000b). STOMP, Subsurface Transport Over Multiple Phases, Version 2.0. User's guide. Rep. PNNL-12034. Pac. Northw. Natl. Lab., Richland, WA.

- Willmott, C.J., (1982). Some comments on the evaluation of model performance. *Bulletin of American Meteorological Society*, 63 (11), 1309–1313.
- Yabusaki, S. B., Fang, Y., and Waichler, S. R. (2008). Building conceptual models of field-scale uranium reactive transport in a dynamic vadose zone-aquifer-river system. *Water Resources Research*, 44(12).
- Yang, C., Mickler, P. J., Reedy, R., Scanlon, B. R., Romanak, K. D., Nicot, J. P., Hovorka S. D., Trevino R. H., and Larson, T. (2013). Single-well push–pull test for assessing potential impacts of CO₂ leakage on groundwater quality in a shallow Gulf Coast aquifer in Cranfield, Mississippi. *International Journal of Greenhouse Gas Control*, 18, 375–387.
- You, K., Zhan, H., and Li, J. (2010). A new solution and data analysis for gas flow to a barometric pumping well. *Advances in Water Resources*, 33(12), 1444-1455.

- You, K., Zhan, H., and Li, J. (2011). Gas flow to a barometric pumping well in a multilayer unsaturated zone. *Water Resources Research*, 47(5).
- You, K., and Zhan, H. (2012). Can atmospheric pressure and water table fluctuations be neglected in soil vapor extraction?. *Advances in Water Resources*, 35, 41-54.
- You, K., and Zhan, H. (2013). Comparisons of diffusive and advective fluxes of gas phase volatile organic compounds (VOCs) in unsaturated zones under natural conditions. *Advances in Water Resources*, 52, 221-231.
- Zhang, X., and Cai, X. (2013). Climate change impacts on global agricultural water deficit. *Geophysical Research Letters*, 40(6), 1111-1117.
- Zhang, Y., Oldenburg, C. M. and Benson, S. M. (2004), Vadose zone remediation of carbon dioxide leakage from geologic carbon dioxide sequestration sites, *Vadose Zone Journal.*, 3(3), 858–866.
- Zheng, L., Apps, J. A., Spycher, N., Birkholzer, J. T., Kharaka, Y. K., Thordsen, J., Beers, S. R., Herkelrath, W. N., Kakouros, E., and Trautz, R.

C. (2012). Geochemical modeling of changes in shallow groundwater chemistry observed during the MSU-ZERT CO₂ injection experiment. *International Journal of Greenhouse Gas Control*, 7, 202-217.

Research Outcomes

Peer Reviewed Paper

Joun, W. T. and Lee, K. K. (2020). Reproducing natural variations in CO₂ concentration in vadose zone wells with observed atmospheric pressure and groundwater data. *Journal of Environmental Management*, 266, 110568.

Kim, H., Kawon, D., Kim, J., Park, I. W., **Joun, W. T.**, and Lee, K. K. (2020). Impact of earthquake on the communities of bacteria and archaea in groundwater ecosystems. *Journal of Hydrology*, 583, 124563.

Joun, W. T., Rossabi, J., and Shin, W. J., and Lee, K. K. (2019). Real-time multi-level CO₂ concentration monitoring in vadose zone wells and the implication for detecting leakage events. *Journal of Environmental Management*, 237, 534-544.

Lee, S. S., Kim, H. H., **Joun, W. T.**, and Lee, K. K. (2017). Design and construction of groundwater monitoring network at shallow-depth CO₂ injection and leak test site, Korea. *Energy Procedia*, 114, 3060-3069.

Joun, W. T., Lee, S. S., Koh, Y. E., and Lee, K. K. (2016). Impact of water table fluctuations on the concentration of borehole gas from NAPL sources in the vadose zone. *Vadose Zone Journal*, 15(4).

Park, B. H., **Joun, W. T.**, Lee, B. H., and Lee, K. K. (2015). A study on Significant Parameters for Efficient Design of Open-loop Groundwater Heat Pump (GWHP) systems. *Journal of Soil Groundwater Environment*, 20(4), 41-50.

Kim, H., Lee, S., Park, J., **Joun, W. T.**, Kim, J., Kim, H., and Lee, K. K. (2016). Genetic Prokaryotic Diversity in boring Slime from the Development of a Groundwater Heat Pump System. *Microbiology and Biotechnology Letters*, 44(4), 550-556.

Oral Presentations

Joun, W. T., Ha, S. S., Lee, S., Park, I. W., and Lee, K. K. (2019). Characterizing and reproducing the natural pattern of CO₂ gas concentration in the vadose zone well before CO₂ injecting in K-COSEM research site, Korea. *2019 AOGS 16th Annual Meeting* in Singapore, Singapore

Joun, W. T., Rossabi, J., Ha, S. W., Lee, S., and Lee, S. S. (2019). Comparing analytical and numerical model for calculating the gas flux through the vadose zone well. *2019 Joint Conference of the Geological Science and Technology of Korea* in Jeju, South Korea

Joun, W. T., Shin, W. J., Ha, S. W., Lee, S., and Lee, K. K. (2018). Dynamical changes of CO₂ gas concentration in borehole applying continuous multi-level monitoring system. *2018 IAH 45th Annual General Meeting* in Daejeon, South Korea

Joun, W. T., Ha, S. W., Lee, S. S., and Lee, K. K. (2017). Visualization experiment to understand transport of dissolved CO₂ in shallow aquifer. *KoSSGE Spring Meeting and International Conference of Geo-Environmental Engineering* in Seoul, South Korea

Joun, W. T., Ha, S. W., Lee, S. S., and Lee, K. K. (2017). Experimental and numerical simulation for CO₂ infused water transport affected by density and hydraulic gradients: monitoring aspect. *International Symposium Commemorating the 70th Anniversary of the Geological Society of Korea and 2017 Annual Fall Joint Geology Meeting* in Jeju, South Korea

Joun, W. T., Kim, H., Ha, S., W., Lee, S. Y., and Lee, K. K. (2016). Visualization experiment of dissolved CO₂ plume transport in shallow-depth groundwater condition. *2016 Goldschmidt 26th Annual Meeting* in Yokohama, Japan

Joun, W. T., Lee, S., S., and Lee, K. K. (2015). VOCs concentration change in borehole under water table fluctuation condition: consideration for CO₂ monitoring. *2015 KoSSGE Fall Meeting* in Gwangju, South Korea

This page intentionally left blank

Abstract in Korean

<국문 초록>

불포화 관정에서 관찰된 지하 환경 내 가스 농도의 자연 변동 : CO₂ 누출 탐지와 예측에의 적용성 분석

전원탁

수리지질학 전공

서울대학교 대학원 지구환경과학부

지하 환경 내 오염원을 확인하거나, 저장된 이산화탄소의 누출 확인 및 추적을 하기 위해 가스 모니터링은 매우 중요한 방법 중 하나이다. 가스 모니터링에서 얻은 결과는 그 특성상 주변 환경 변화에 민감하게 반응하며, 주요 반응에 대한 검증과 분석이 동시에 필요하다. 본연구에서는 불포화 지역 관정 내 가스모니터링과 대기에서 기상학적 요소들을 동시에 모니터링하였다. 이를 통해모니터링 관정 내 가스 흐름의 특성을 파악하고,

추후 직접적인 시험을 통한 결과들에 대한 분석을 위한 기초 자료를 확보하고자 하였다.

토양 환경에는 많은 이산화탄소 가스가 만들어지며, 이는 화학적인 것뿐만 아니라 생물학적 발생이 모두 포함된다. 연구지역에서 연간 이산화탄소 변화는 온도변화에 민감하게 반응하며, 깊이 별로 지연 또는 작은 폭의 변화가 관찰되었다. 이러한 변화는 외부요인이 깊이에 따라 다른 영향을 줄 수 있음을 반증한다. 또한, 실시간 관측 자료를 통해 얻은 자료들은 가장 빠르고 정확하게 이산화탄소를 모니터링하여 누출연구에 반영할 수 있으므로 매우 중요하다. 하루 주기로 관찰된 자료를 보면 계절별 자료로 확인할 수 없었던, 큰 폭의 변화를 확인할 수 있었다. 이러한 하루 주기의 큰 변화는 가스 모니터링 결과를 해석하는데 있어서 많은 오차를 발생시킬 수 있으며, 주요 원인과 원리가 어떤 것인지 주의 깊게 파악할 필요가 있다. 농도가 급격히 하락하는 것은 화학적, 생물학적 이산화탄소 가스의 발생이 적어지는 것에 의한 원인보다는 다른 외부요인에 의한 영향으로 판단되었다. 다양한 방법을 통해 관정 내 가스의 흐름이 외기에서 들어오는 공기에 의해 영향을 받은 것으로 확인 되었으며, 이를 기초로 관정 내 공기 흐름을 낮과 밤으로 구분하여 정의할 수 있음을 증명하였다.

불안정한 가스의 흐름을 수치모델로 계산을 시도하였으며, 이를 통해 자연적인 소폭의 변화뿐만 아니라 큰 폭으로 감소 및 증가하는 가스 농도 패턴을 재현할 수 있었다. 많은 연구자들에 의해 선행되었던 가스 flux 계산 연구에서 고정된 경계를 사용한 것과 다르게 본 연구에서는 좀 더 자연의 변화에 맞게 설정한 경계를 통해 실제 농도 변화 패턴을 계산할 수 있었다. 또한 간접적인 변화에 맞춰서 해석하는 것이 아닌 직접적으로 가스 농도를 계산하여 패턴을 파악한 것을 토대로 실제 누출이 예상되는 모니터링 관점에서 CO₂ 농도 크기와 그 패턴을 예측할 수 있었다. 이연구결과는 다양한 조건에서 발생할 수 있는 누출 패턴을 수치 모의하는 연구에 중요한 기초 자료로 활용될 수 있을 것으로 기대된다.

주요 단어

불포화대 CO₂, 자연 변동 CO₂, 자연 변동 재현, 수치 모델링, 그리고 CO₂누출 예측

학번: 2014-31020

This page intentionally left blank

Acknowledgments

I would like to thank my advisor, Professor Kang-Kun Lee for giving me the chance into the field of hydrogeology and guiding me through my Ph. D. study. Prof. Lee was always trust an inside of my potential force and introduces me to numerous chances and show me the excellent ways to approach the good results of Ph. D. study. Pref. Lee, thank you very much for your wonderful endorsement, and thank you very much for the stable research environment conditions.

I would like to thank the Ph.D. reviewers, including Professor Lee Insung, Professor Lee Hyunwoo, Professor Woo Jusun, and Professor Kwon Yikyun, for making insightful and constructive comments on the pervious manuscript.

I sincerely thank the financial support of the “R&D Project on Environmental Management of Geologic CO₂ Storage” from Korea Environmental Industry Technology Institute (KEITI), South Korea (Project Number: 2014001810003 and 2018001810002).

Finally, I greatly thank my wife, Sanghee Maeng, for her love and help in both my life and Ph.D. study, and my 25-months son, Sion Joun, who always gives me sustainable energy and saying me “Daddy, Fighting today”. I also wonderfully thank my mom, dad, and sister for their persistent encouragement and selfless love and mother-in-law, father-in-law, sister-in-law, and brother-in-law for their infinite encouragement and consideration.

